Ministry of Higher Education and Scientific Research
Babylon University
College of Engineering
Department of Materials Engineering

Thermodynamic Stability of Molecular Structure

A Thesis

Submitted to the College of Engineering of the University of Babylon in Partial Fulfillment of the Requirements for the Degree of Master of Science in Materials Engineering

BY

Zaineb Fadhil Kadhim Al-Obaidi

B.SC. ,2001

June-2005

بِسمِ اللهِ الرَّحمَنِ الرَّحِيمِ

الرَّحمَنُ ﴿1﴾ عَلَّمَ القُرءَانَ ﴿2﴾

خَلَقَ الإنسَانَ ﴿3﴾ عَلَّمَهُ البَيَانَ ﴿4﴾

صَدَقَ اللهُ العَلِيُّ العَظِيم

سورة الرحمن ﴿1-4﴾

الاهداء

الى:-

سفينة النجاة....

عين الحياة.....

الحق الجديد.....

العالم الذي علمه لايبيد.....

صاحب العصر والزمان.....

الحجة (عجل الله فرجه و سهل مخرجه)

اهدي ثمرة جهدي المتواضع.

زينب

CERTIFICATION

We certify as an examining committee that we have read this thesis, in title "**Thermodynamic Stability of Molecular Structure**", and as examining the student ***"Zaineb Fadhil Al-Obaidi"*** in its content and what related to it, and found it meets the standard of a thesis for the degree of master of Science in Material Engineering.

Signature:
Name: Asst. Proof.
Dr. Tahseen AL-Hattab
(Supervisor)
Date: / /2005

Sinature:
Name: Asst. Proof.
Dr. Haydar AL-Ithary
(Supervisor)
Date: / /2005

Signature:
Name: Asst. Proof
Dr. Adil A. Al-Moosway
(Member)
Date: / /2005

Signature:
Name:
Dr. Kadhim F. Al-Sultani
(Member)
Date: / /2005

Signature:
Name: Proof.
Kahtan K. Al-Kazraji
(Chairman)
Date: / /2005

Approval of the Material Engineering Department.
Head of the Material Eingineering Department.
Signature:
Name: Proof. Dr. Abd Al-Wahid K. Rajih
Date: / /2005

Approval of the College of Engineering
Dean of the College of Engineering.
Signature:
Name: Proof. Dr. Haroun AK. Shahad
Date: / /2005

ACKNOWLEDGMENTS

"In The Name of ALLAH, The Gracious and Merciful"

First of all, all thanks are do to **ALLAH** who enables me to achieve this research work.

I would like to express my sincere gratitude, great appreciation to my supervisor **Dr. Tahseen AL-Hattab** for his supervision, encouragement and his helpful advice, discussions and suggestions through out my study.

I would like to express my appreciation to my Co-advisor **Dr. Haydar AL-Ithary** for his assistance, advice, discussions and suggestions through out my study.

I would like to thank my parents, who have always encouraged me to pursue my studies and who were the first to interest me in natural sciences.

I am indebted to my sisters especially to my old sister from far away, who did not forget about me for years.

I would like to thank my husband , for his support and encouragement.

Zaineb F. Al-Obaidi

LIST OF CONTENTS

CONTENT **PAGE**

List of Figures

List of Tables

Chapter One

Introduction

1.1 General

The phase diagram is a convenient graphical method of displaying the state of a given system that is stable under a defined set of conditions[1]. The main idea of phase diagrams is based around the latent heat that is evolved when a mixture is cooled, and the phase is changed[2]. Phase diagrams are known as thermal equilibrium diagrams or constitutional diagrams [3].

It shows the mixture of phases present in thermodynamic equilibrium at a given temperature and composition[2] .The equilibrium state is the state of minimum free energy of the binary system at a given temperature and composition at constant pressure. Thus the analysis of a phase diagram is the subject of thermodynamics[4].The equilibrium conditions in phase diagrams can be greatly satisfied by using very slow heating and cooling rates which give sufficient time for phase changing[5].

Phase diagrams enable to predict what phases are in equilibrium for selected alloy compositions at desired temperatures; determine the chemical composition of each phase; and calculate the quantity of each phase present[6]. The important applications of phase diagrams in material science can be abstracted as following:

1-Scientists and engineers have found phase diagrams helpful tools in describing the various forms a certain material can take and anticipate the

stability of specific materials when designing products for service environments [7 and 6]. `

2-Metallurgist have used phase diagrams for many years as an essential to understand the behavior of the systems as a function of temperature and composition[8].

3-Improvement of heat treatment processes and casting processes[9].

4-Phase diagrams help to understand and predict the microstructures[10].

1.2 Types of Binary Phase Diagrams:

1.2.1 Two Metals Completely Soluble in Liquid State:-

A-Two Metals Completely Soluble in Solid State (Isomorphous System): A system consists of two metals have the same crystal structure, and they are chemically and physically very much alike, is called isomorphous system[11]. In one component system melting occurs at a well defined melting temperature. In multi-component systems melting occurs over a range of temperatures between the solidus and liquidus linesas shown in Fig.(1.1). Solid and liquid phases are in equilibrium in this temperature range [10]. Copper- nickel and germanium-silicon are phase diagrams of this type[11].

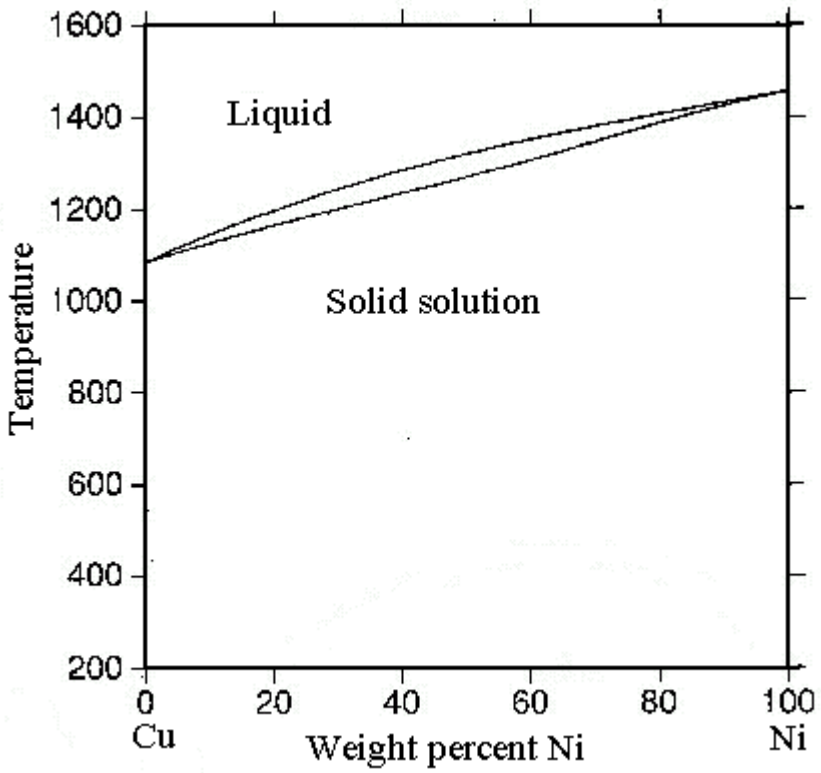

Fig.(1.1): Phase diagram of copper-nickel. Ref.[10]

For phase diagrams of real solution there is the difference between the actual free energy of the solution and the value the free energy would have if the solution were ideal[11], thus at low temperatures, there is a region where the solid solution is most stable as a mixture of two phases because of slow diffusion and difficulty in attaining equilibrium ,this region is called a miscibility gap[10], as shown in Fig.(1.2).

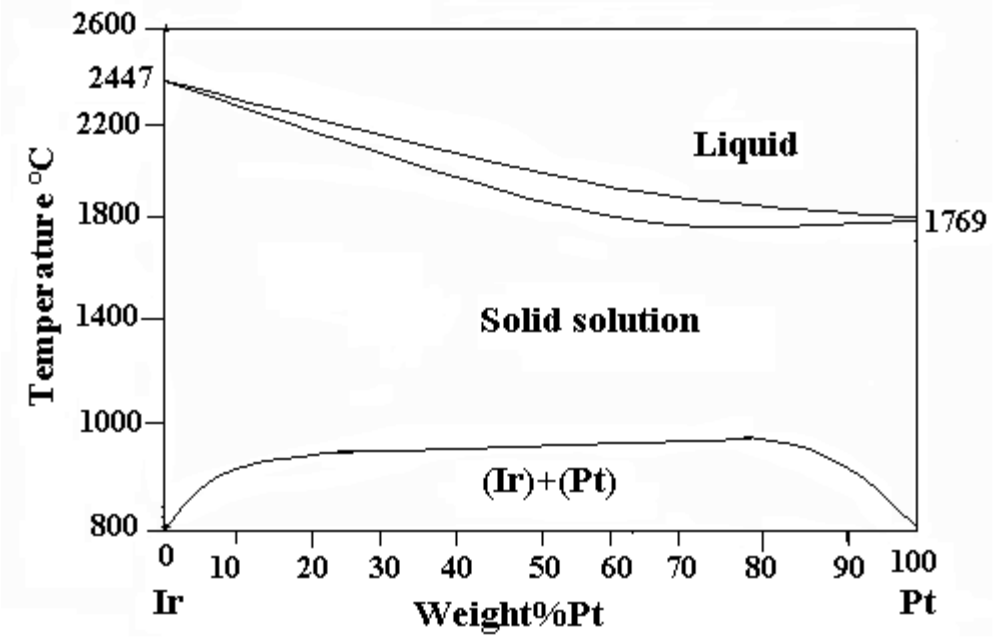

Fig.(1.2):Phase diagram of iridium-platinum. Ref.[12]

B-Two Metals Insoluble in Solid State (Simple Eutectic): A characteristic of this diagram is that the liquidus line consists of two branches falling in temperature from the freezing points of the two metals to a minimum intersection point, known as the eutectic temperature T_E[13].Each component lowers the freezing point of the other based on Raoult's law, which states that the freezing point of a pure substance will be lowered by the addition of a second substance provided the latter is soluble in the pure substance when liquid and insoluble when solidified. The amount of lowering of the freezing point is proportional to the molecular weight of the solute [5] . There must be one temperature at which both freezing points coincide. This point is called the eutectic temperature and it represents the lowest liquid-solid transformation temperature within the system [1]. Bismuth-cadmium is a phase diagram of this type[8].

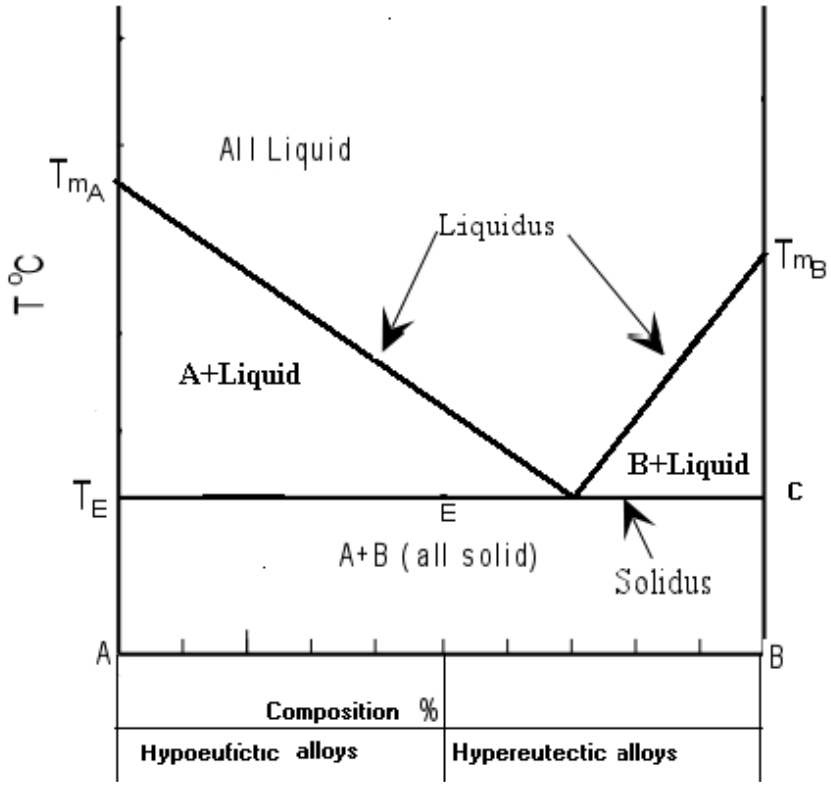

Fig.(1.3): Hypothetical phase diagram of simple eutectic. Ref.[3]

C-Two Metals Partially Soluble in The Solid State:-The equilibrium diagram is formed as intermediate between the two types just discussed, and consists of two parts, one resembling a simple eutectic and the other which may be regarded as a part of a complete solid solution curve, where the two kinds of atoms are very different in size and each metal may be capable of dissolving only a limited percentage of the other [13].

Alloys in this system never solidify crystals coexisting in equilibrium is sufficient to reduce to zero the number of degrees of freedom[11]. The properties of the eutectic can be summarized:-

1. Solidification takes place at a single fixed temperature.
2. The solidification takes place at the lowest temperature in that group of alloys.
3. The eutectic composition is a constant for that range of alloys.

4. The eutectic structure is a mixture of the two solid phases.
5. The solidified eutectic structure is generally a laminar structure of the two solid phases [14] .

Alloy systems coincide this type of phase diagram are: silver-copper, and lead-tin [5].

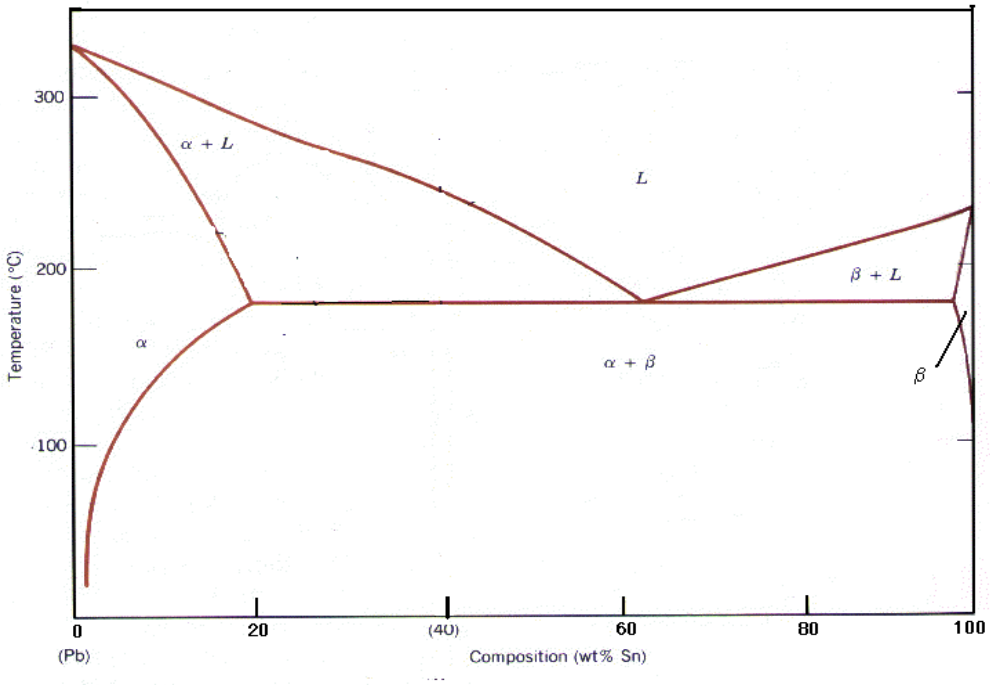

Fig.(1.4): Phase diagram of lead-tin. Ref.[12]

D-The Congruent-melting Intermediate Phase:- When one phase changes into another phase isothermally and without any changing in chemical composition, it is said to be congruent phase change or congruent transformation. All pure metals solidify congruently. If the intermediate phase has a narrow range of composition, as do intermetallic compounds

and interstitial compounds, it is then represented on the diagram as a vertical line divides the diagram into two sections and labeled with the chemical formula of the compound and obey valency law [3 and 15].If the intermediate phase exist over a range of composition , it is usually an electron compound and is labeled with Greek letter and don't obey the valency law [13] . The examples of this type are the phase diagrams of magnesium-tin and copper-phosphorus [13 and 12].

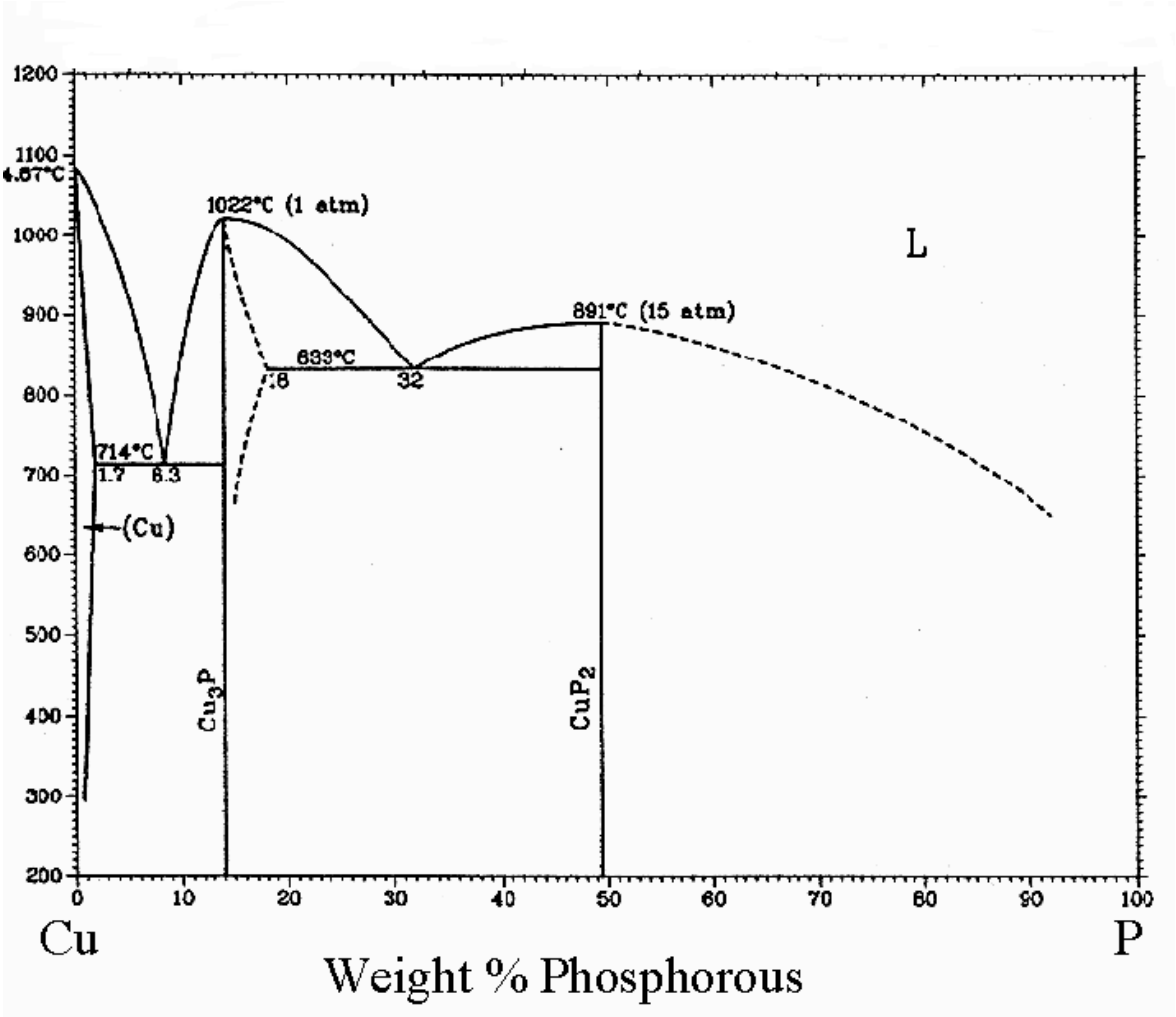

Fig.(1.5): Phase diagram of copper-phosphorus. Ref.[12]

E-The Peritectic Reaction:- In peritectic reaction a liquid and a solid react isothermally to form a new solid on cooling. The new solid formed is usually an intermediate phase, but in some cases it may be a terminal solid solution [3] .The alloy system contains the terminal solid solution as a peritectic reaction is platinum-silver[14]. Each solid particle of α will combine at its periphery with liquid to form a β sheath around the periphery of the α particle. In order for this reaction to continue, atoms of β must diffuse through the β sheath to combine with α particle. Diffusion through solids is relatively slow. Consequently, some α phase is found to exist when the temperature is lowered below the peritectic temperature [1] . The alloy system contain a peritectic reaction are platinum-silver and potassium-sodium [14 and 12] .

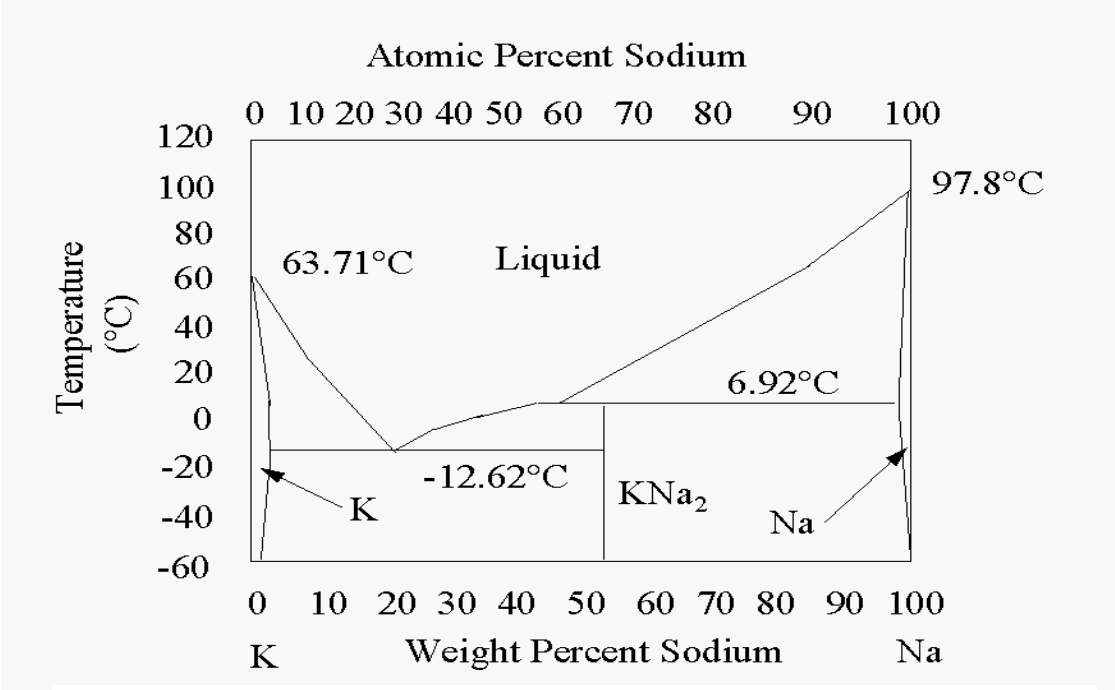

Fig.(1.6): Phase diagram of potassium and sodium. Ref.[12]

1.2.2 Two Liquids Partly soluble in The Liquid State(The Monotectic Reaction):- When one liquid forms another liquid, plus a solid, on cooling, it is known as a monotectic reaction. The monotectic reaction resembles the eutectic reaction, the only difference being that on of the products is a liquid phase instead of a solid phase[3]. The monotectic reaction is found to occur most frequently in systems where the two components are significantly dissimilar electrochemically, as, for example, in metal-nonmetal systems, some nonmetal-nonmetal systems, and even in certain metal-metal systems where the two metals are far apart in the periodic table. Real examples are the copper-phosphorus, iron-oxygen, and silica-manganese oxide [11].

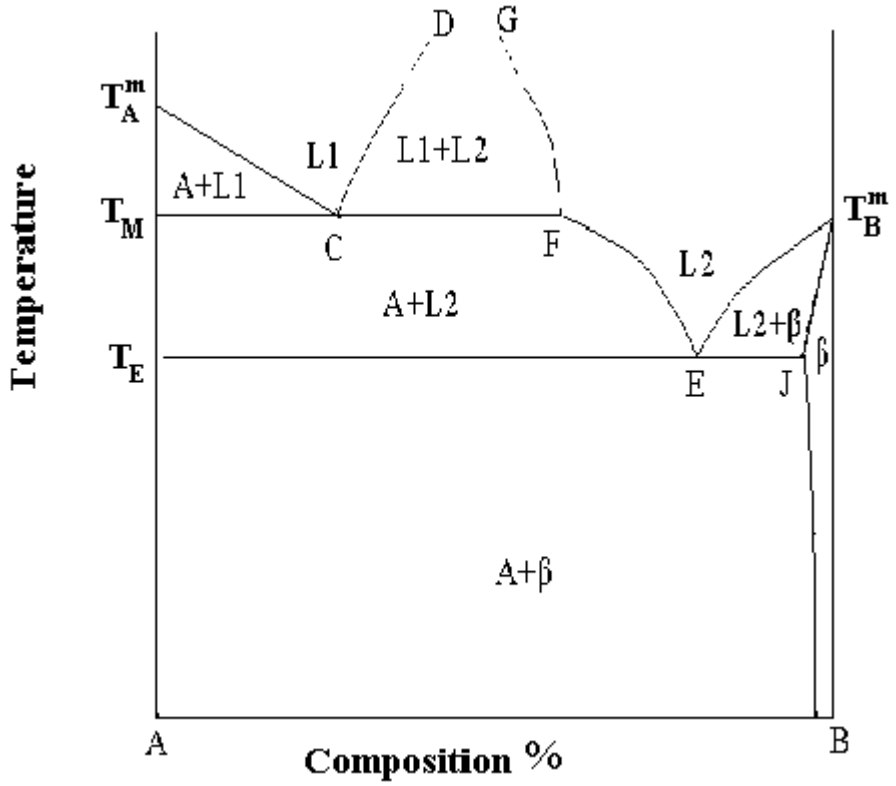

Fig.(1.7): Phase diagram of monotectic reaction. Ref.[3]

1.2.3 Two Metals insoluble in liquid and solid state: An alloy system which comes very close to this type is that between aluminum and lead in Fig.(1.8).The two-phase liquid region extends almost entirely across the diagram. This condition corresponds to a limiting case of the monotectic reaction and the eutectic reaction. The upper of the two horizontal lines represents a monotectic reaction in which the monotectic point is very close to the composition and melting point of pure aluminum. The lower horizontal line represents a eutectic reaction in which the eutectic point is practically coincident with the composition and melting point of lead [3] .

The importance of this type of alloy resides in their ability to produce a dispersion of droplets of one component in another. Such a process is used to make bearing bronze, which consists of lead droplets dispersed throughout copper or zinc. Alloy system coincide this type of phase diagram is lead-zinc[16].

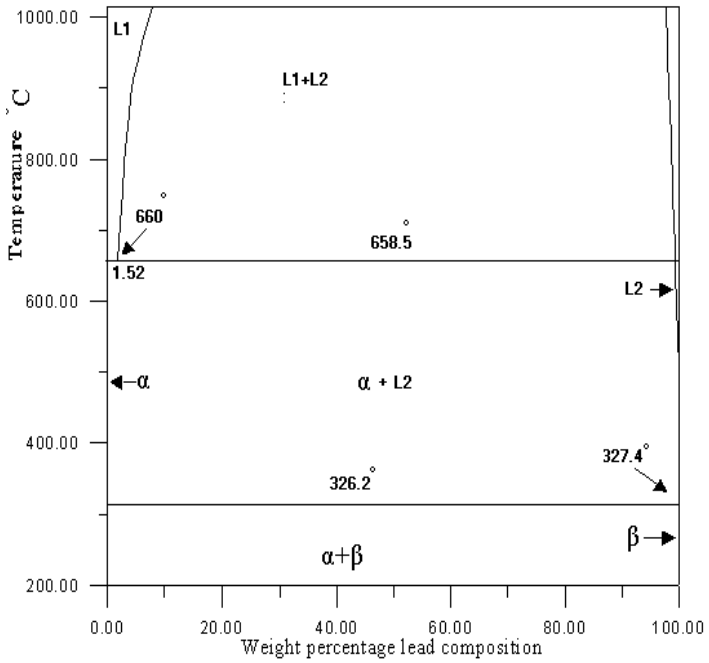

Fig.(1.8): The aluminum-lead alloy system. Ref.[3]

1.2.4 Other Types of Phase Diagrams:- One peritectic-like invariant reaction is known to occur in alloys; this is the syntectic reaction as in Fig.(1.9). This reaction is relatively rare. The best known example occurs in the sodium-zinc system. In general, for normal cooling rates, when the two liquids in the miscibility gap react to form the solid at the syntectic temperature, the layer of solid may be expected to isolate the liquids from each other in subsequent cooling. As a result the final microstructure will tend to be a coarse mixture of the structures characteristic of the lower temperature reactions in the system [11].

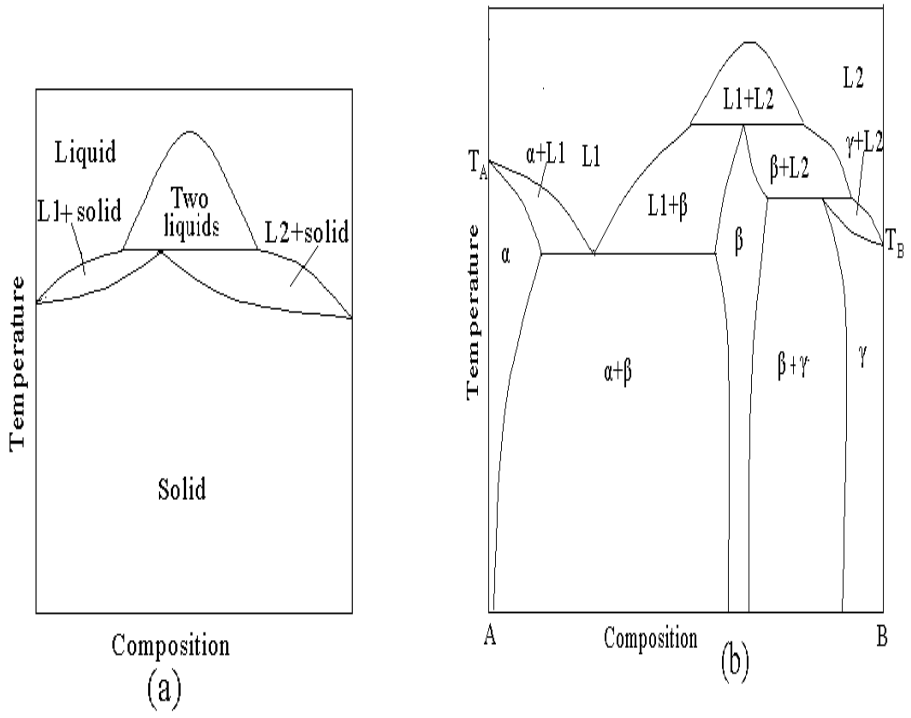

Fig.(1.9): (a) and (b) diagrams containing the syntectic invariant reaction. Ref. [11]

The eutectic-like invariant reaction is known as the metatectic reaction. If the liquid phase and one solid phase in the eutectic are simply interchanged

in position, the invariant shown in Fig.(1.10)results. The metatectic is of relatively rare occurrence; it is , however, somewhat of curiosity in that certain alloys in the system can melt on cooling ! For example , any alloy of composition to the left of the metatectic composition as s in Fig.(1.10) will be completely solidified when cooled to the metatectic temperature but will partially melt again on further cooling into the α-plus-liquid region just below this. Real example of this reaction is the uranium-magazine system [11] .

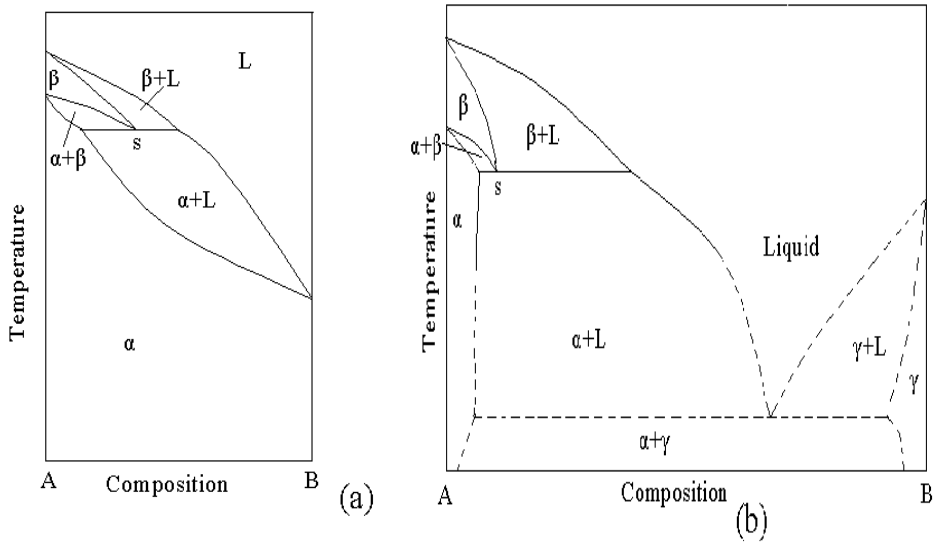

Fig.(1.10):-(a) and (b) diagrams incorporating the metatectic reaction. Ref.[11]

1.3 Transformations in Solid State:

1.3.1 Allotropy, or Polymorphism: - The fundamental difference between liquids and solids is that the former consist of essentially random arrays of particles (atoms or molecules) whereas the latter are made up of particles arranged in regular patterns, solids are crystalline. Since with indistinguishable particles only one type of spatially random array is possible but crystalline arrays may be of many types [11] . Polymorphism means a metal can exist in more than one type of crystal structure. Allotropy means a metal can exist in more than one type of crystal structure repeatedly such as iron [5] .

On an equilibrium diagram, a point or points on the vertical line that represents the pure metal indicate this allotropic change. Many of the equilibrium diagrams involving iron-silicon, iron-molybdenum, and iron-chromium .The metals tin, manganese, and cobalt exhibit allotropy [3] . Allotropy can come about as a result of change in temperature. Some substances exhibit allotropy on heating at ordinary pressures; iron is a typical example. When heated at atmospheric pressure, iron transforms at 912˚C from the α-iron form (BCC) to the γ-iron form (FCC), and at 1304˚C it transforms again to α-iron (BCC) as in Fig.(1.11)[11] .

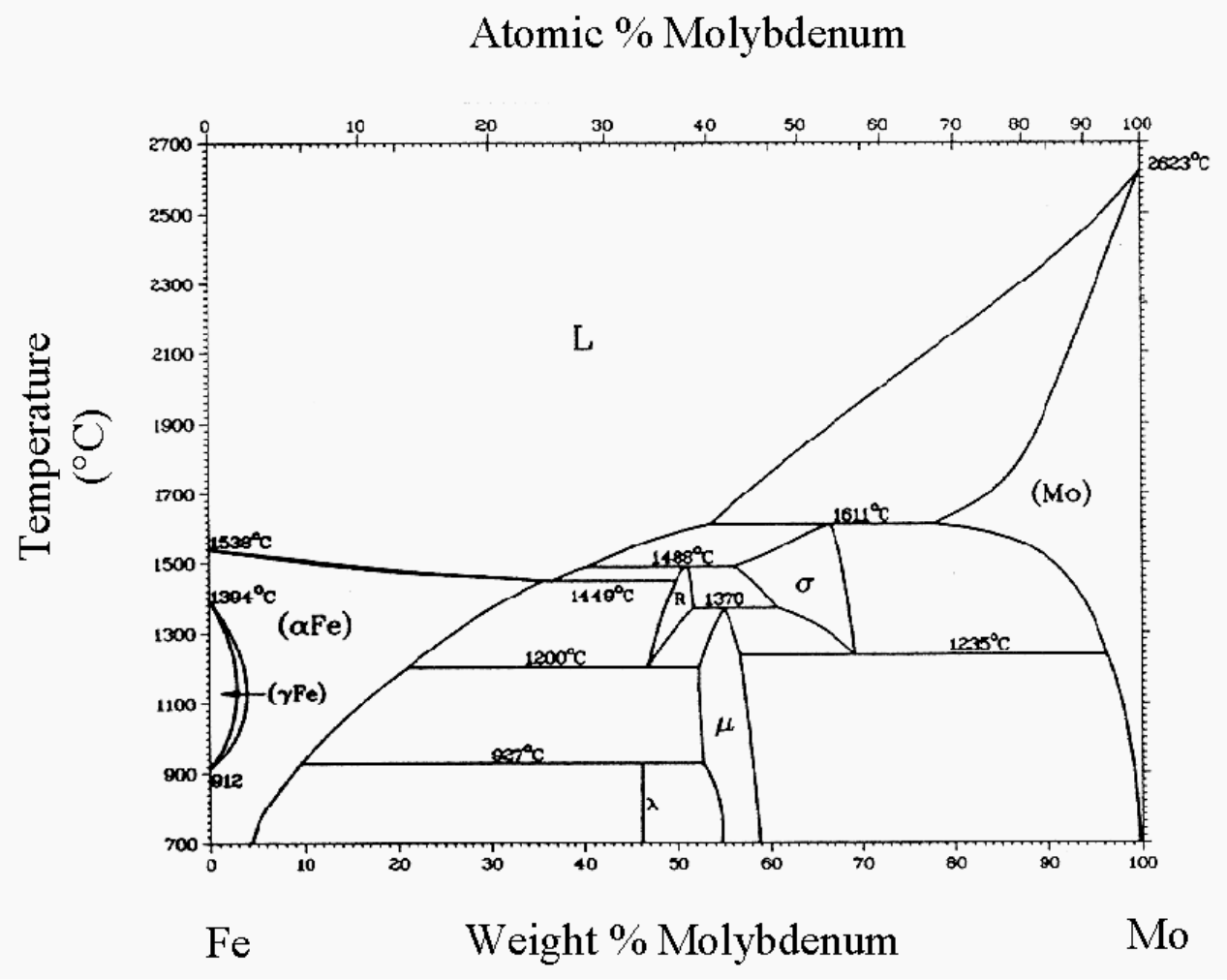

Fig(1.11): Phase diagram of iron-molybdenum. Ref.[12]

1.3.2 Order- disorder Transformation:- Ordinarily in the formation of a substitutional type of solid solution the solute atoms do not occupy any specific position but are distributed at random in the lattice structure of the solvent. The alloy is said to be in a "disordered" condition. Some of these random solid solutions, if cooled slowly, undergo a rearrangement of the atoms where the solute atoms move into definite positions in the lattice. This structure is now known as an ordered solid solution or superlattice as shown in phase diagram of gold-copper[3].

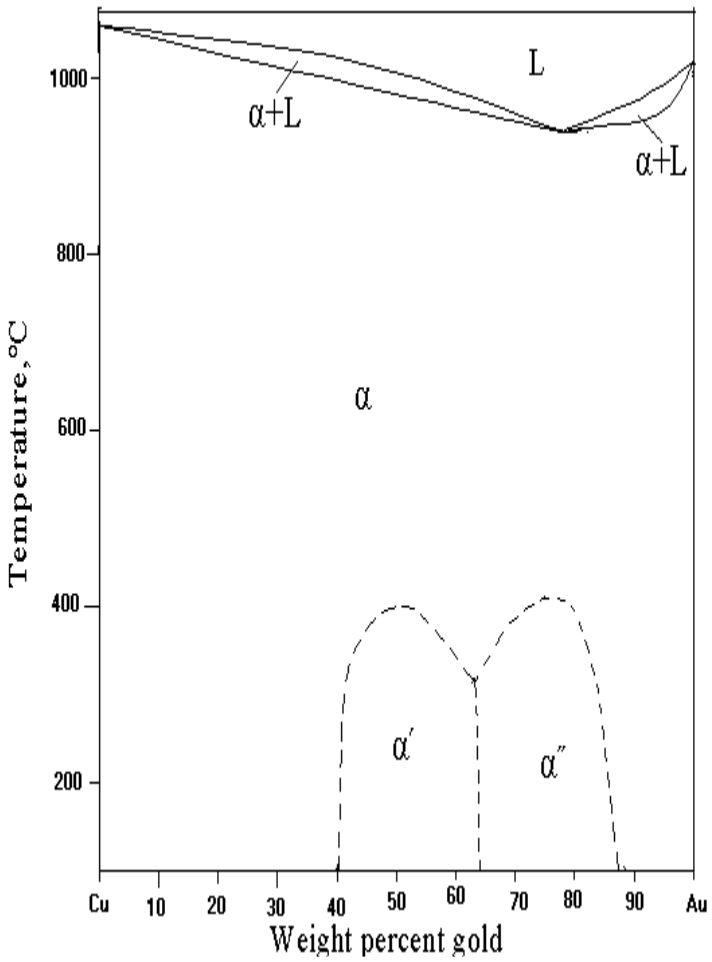

Fig.(1.12): The gold–copper equilibrium diagram. Ref. [3]

1.3.3 The Eutectoid Reaction:-This is a common reaction in the solid state. It is very similar to the eutectic reaction but does not involve the liquid. In this case, a solid phase transforms on cooling into two new solid phases. Under microscope eutectic and eutectoid mixtures generally appear the same, and it is not possible to determine microscopically whether the mixture resulted from a eutectic reaction or a eutectoid reaction[3].The two phases in a eutectoid structure tend to be more regularly arrayed than in a eutectic structure because in the latter the presence of the liquid allows the

growing solids to undergo accidental alterations in growth direction more freely. Real examples of this phase diagrams are the iron-tantalum, iron-carbon, and magnesium oxide-zirconium oxide [11].

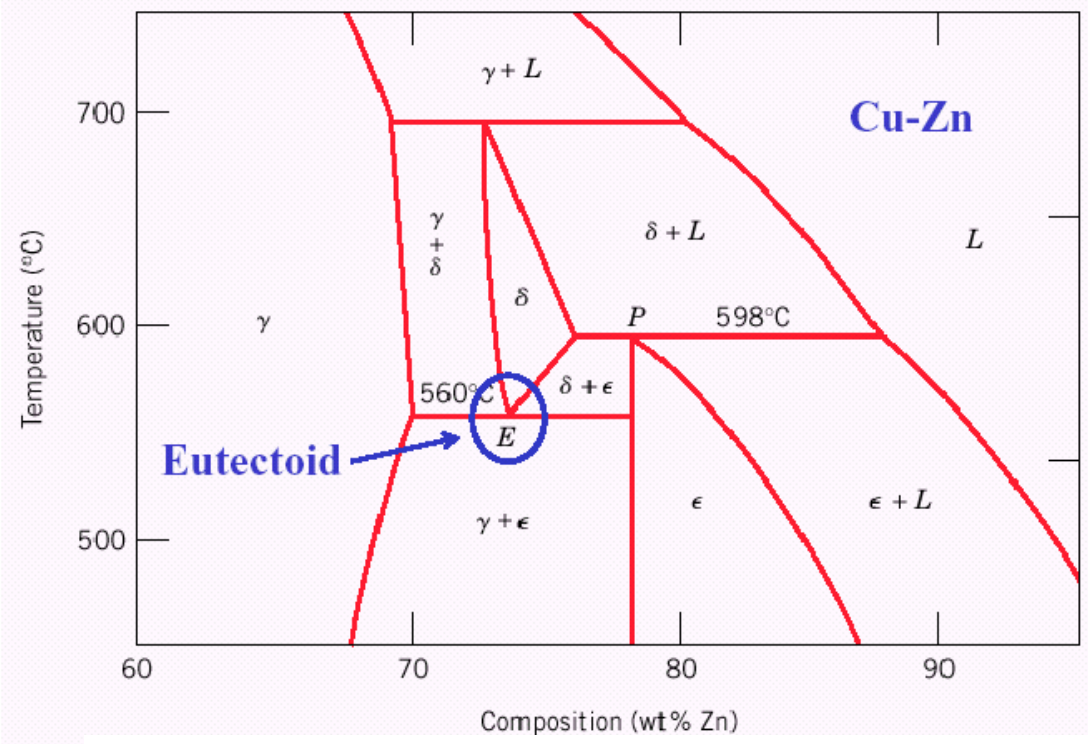

Fig.(1.13): Phase diagram represent the eutectoid reaction. Ref.[10]

1.3.4 The Peritectoid Reaction:- The peritectoid invariant is exactly analogous to the peritectic with the exception that all the phase involved are solid. Peritectoid reactions are more sluggish than peritectic reactions, for they not only involve no liquids, but also they tend to occur at relatively low temperatures, where diffusion rates in the solids involved are extremely slow. Real examples can be seen in the cobalt-tungsten, nickel-molybdenum, and silver-aluminum[11 and 3].

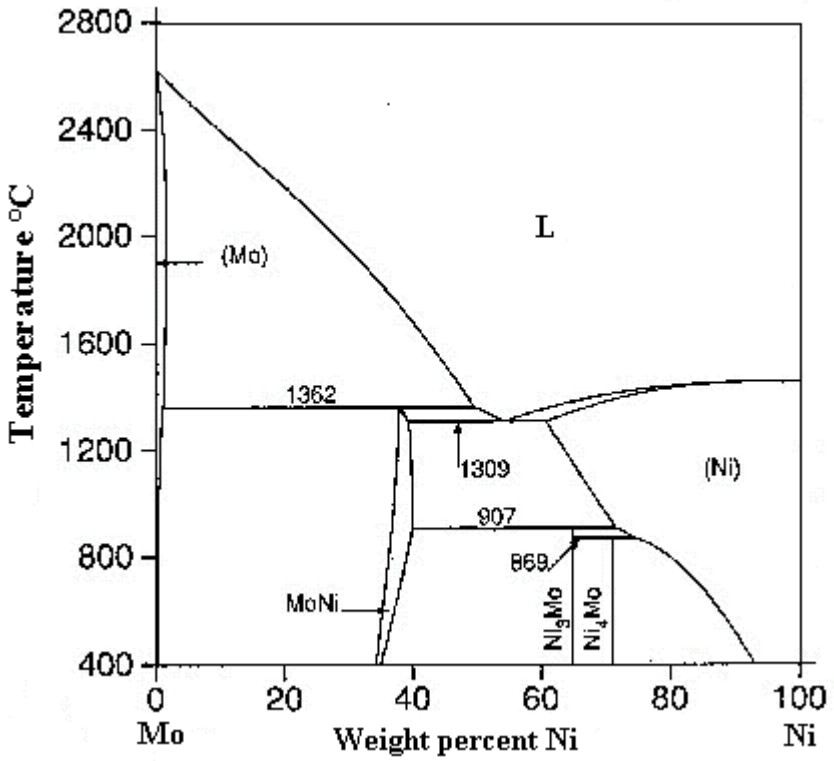

Fig.(1.14): Phase diagram of molybdenum-nickel. Ref.[12]

Name of reaction	Representation on phase diagram	Equation of reaction
Eutectic	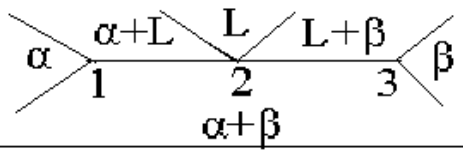	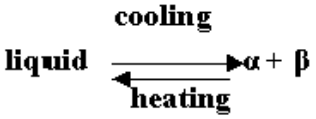
Monotectic	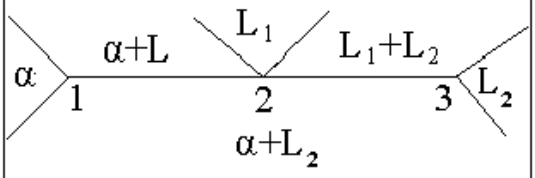	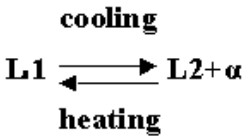
Eutectoid	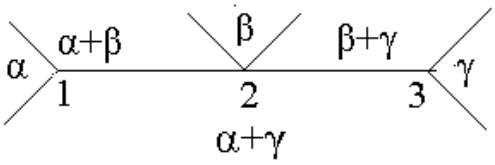	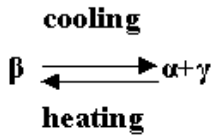
Metatectic	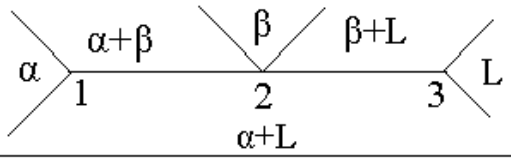	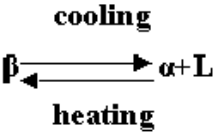
Peritectic	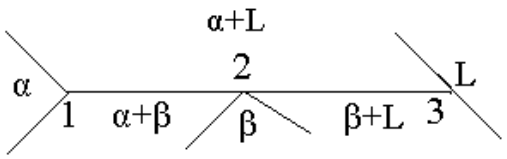	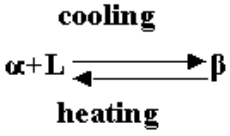
Peritectoid	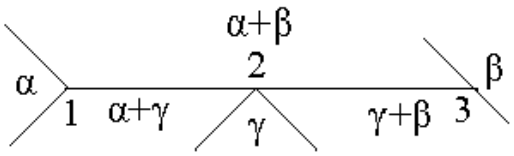	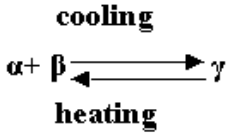
Syntectic	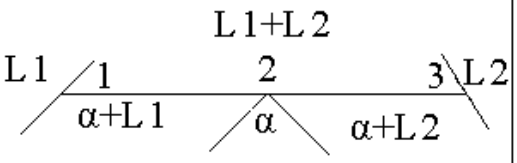	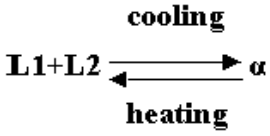

Tab.(1.1): Symbolic representation of equilibirium diagrams reactions. Ref.[11 and 1]

1-4 The Scope of the present work: The objective of the present work is to draw two types of phase diagrams by using thermodynamic properties. Phase diagrams and thermodynamic properties are very important in alloy design and material processing simulation. Theoretical calculation of phase diagrams by using thermodynamic properties is more important than experimental method as:-

-The time is reduced by using the theoretical method.

-Calculations involving solid phases are more manageable than, for instance, those involving liquid phases.

-The determination of the solid state part of a phase diagram in experimental method is most likely to be hindered by sluggish kinetics or characterization problems.

-It enables to predict some features of the system which are not easily measured, as well as to predict phase diagrams of complex multi-component systems.

-It will be easy to draw the phase diagrams of refractory metals.

In this investigation the following types of phase diagrams are studied in detail:-

1- Phase diagrams of two metals completely soluble in liquid and solid state with assuming that diagrams with miscibility gap are considered as diagrams of regular solutions while without miscibility gap are considered as diagrams of ideal solutions.

2-Phase diagrams of two metals completely soluble in liquid and partially soluble in solid state “eutectic systems”.

In this study computer programs of two metals completely soluble in liquid and solid state (TMCSLS), two metals completely soluble in liquid and solid state with regular solution (TMCSLSR),and two metals completely soluble in liquid state and partial soluble in solid state (TMCSLPSS)are designed to achieve the previous objectives. The results are comparing with phase diagrams of experimental method which is represented by thermal analysis by using cooling curves from different references. .

Chapter Two

Literature Review

2.1 General

Phase diagrams provide fundamental processing maps for metals and alloys thus their determination is very important. Theoretical calculation of the equilibrium thermodynamic properties of crystal, over a wide range of temperatures and pressures, has been approached in a number of ways[17].In a crystal, atoms are arranged in a periodic array so that each atom has identical surroundings which is called a lattice structure[18].The energy of a lattice vibration is quantized, where the elastic waves in crystals are made up of phonons[4].

2.2 Literature Review:

In 1968 Gordon, P. [11] discussed the principles of equilibrium phase diagram relationships in one-and two-component materials systems. He developed the thermodynamic foundations of the diagrams on the basis of the free energy criterion, considering temperature, composition, and pressure as the relevant variables.

In 1970 Kaufman and Bernstein[19]summarized the general features of the calculation of phase diagrams and also gave listings of computer programs for the calculation of binary and ternary phase diagrams, thus laying the foundation for the CALPHAD method (Calculation of Phase Diagrams).

The CALPHAD method is based on the minimization of the free energy of the system and is, thus, not only completely general and extensible, but also theoretically meaningful. The experimental determination of phase diagrams is a time consuming and costly task. This becomes even

more pronounced as the number of components increase. The calculation of phase diagrams reduces the effort required to determine equilibrium conditions in a multi-component system.

Phase equilibrium calculations can not only give the phases present and their compositions but also provide numerical values of enthalpy contents, temperature and concentration dependence of phase boundaries for coupling of microscopic and macroscopic modeling[19].

For the calculation of phase equilibria in a multicomponent system, it is necessary to minimize the total Gibbs energy, *G*, of all the phases that take part in this equilibrium:

$$\mathbf{G^t = \sum_{o=1}^{P} NG_o^{\Phi}} \qquad \textbf{(2-1)}$$

A thermodynamic description of a system requires assignment of thermodynamic functions for each phase. The CALPHAD method employs a variety of models to describe the temperature, pressure and concentration dependencies of the free energy functions of the various phases. The contributions to the Gibbs energy of a phase can be written:

$$\mathbf{G^{\Phi} = G_T^{\Phi}(T,X) + G_{pr}^{\Phi}(pr,T,X) + G_m^{\Phi}(T_{cr},\beta_o,T,X)} \qquad \textbf{(2-2)}$$

The temperature dependence of the concentration terms of G_T is usually expressed as a power series of *T*:

$$\mathbf{G = a + b.T + c.T + \sum d_n.T^n} \qquad \textbf{(2-3)}$$

In eq.(2-3) a, b, c, and d are coefficients and n is an integer. Eq.(2-3)is valid for temperatures above the Debye temperature which represent :

$$\theta_D = \frac{h\omega_D}{k_B} \qquad \textbf{(2-4)}$$

For multicomponent systems it has proven useful to distinguish three contributions from the concentration dependence to the Gibbs energy of a phase, G^{Φ}:

$$G^{\Phi} = G^{M} + G^{id} + G^{xs} \quad \textbf{(2-5)}$$

Since Hildebrand introduced the term "regular solution" to describe interactions of different elements in a solution, a series of models have been proposed for phases which deviate from this "regularity", i.e. show a strong compositional variation in their thermodynamic properties, to describe the excess Gibbs energy G^{xs} [19 and 20].

For equilibrium alloys, the calculation of phase diagrams (CALPHAD) approach is a well-established and widely applied method for calculation of thermodynamic functions and phase diagrams. This method uses another analytical expressions to describe the free energy of different phases in an alloy system[21]. In the general formalism, the free energy G of a phase in a binary system is usually expressed as in

$$G = G_A X_A + G_B X_B + k_B T(X_A \ln X_A + X_B \ln X_B) + G^{xs} \quad \textbf{(2-6)}$$

Ref. [21]:

In 1996 Saunders, N. [22]used CALPHAD method to calculate phase diagram and prediction thermodynamic properties for alloys from the following multi-component system: Ni-Al-Co-Cr-Hf-Mo-Nb-Ta-Ti-W-Zr-B-C as super alloys of Ni-base alloy. CALPHAD method is used for calculation phase diagrams of binary and ternary alloys from the system. Results of CALPHAD method are compared with results of experimental method. They are very nearly and identical in some regions.

In 2000 Norgren, S.[23] introduced CALPHAD method (calculation of phase diagrams) to describe the alloy system of Fe-Tb-Dy. In the CALPHAD method the individual phases in a system are assigned Gibbs energy expressions. This work was aimed at the phase relationships and thermodynamic properties of rare earth –iron alloys being the basis of many novel functional materials. The binary data can be combined to calculate phase diagram or thermodynamic properties in binary and possibly in higher-order systems. She concluded the binary systems Fe-Tb, Fe-Dy, Ho-Er, Ho-Tb, Ho-Dy, Er-Tb, Er-Dy, Sc-Nd, Sc-Gd, and Sc-y. She calculated the ternary Fe-Tb-Dy liquidus surface diagram.

In 2002 Zi-Kui Liu ;*et al.* [24] concerned on thermodynamics of the magnesium and boron system with the modeling technique CALPHAD using computerized optimization procedure. They obtained temperature-composition, pressure-composition, and pressure-temperature phase diagrams under different conditions. The results provide helpful insights into appropriate processing conditions for thin films of the superconducting phase. They found that MgB_2 is thermodynamically stable only under fairly high to very high Mg partial pressures at the temperature range.

In 1993 ,Najafabadi, R.; *et al.* [21]calculated the experimental thermodynamic data for the metastable Ag-Cu alloys and for equilibrium phases then compared them with both calculation of phase diagrams (CALPHAD) and atomistic simulation predictions. The atomistic simulations were performed using the free energy minimization method (FEMM). They developed the FEMM and used the

embedded atom method (EAM) interatomic potentials in the FEMM simulations have been well established for this system. The FEMM determination of the equilibrium Ag-Cu phase diagram and the enthalpy of formation and lattice parameters of the metastable solid solutions are in good agreement with the experimental measurements but CALPHAD calculations overestimate the enthalpy of formation. The experimental method is the high energy ball milling to form metastable Ag-Cu solid solutions. Thus, the FEMM is a viable alternative approach for the calculation of thermodynamic properties of equilibrium and metastable phases.

The free energy minimization method (FEMM) ,which is based upon the minimization of an approximate free energy functional with respect to positions of all atoms and the spatial distribution of solutes. In addition to provide thermodynamic functions such as the free energy and entropy of equilibrium alloys, the FEMM also allows determination of thermodynamic functions of metastable alloys.

The Gibbs free energy of an alloy system may be written as:-

$$G=E_{bond}+E_{vib}+E_{conf} \qquad (2\text{-}7)$$

The bonding energy within the embedded atom method (EAM) framework is given as :-

$$E_{bond}(r_1,.....,r_{na})=\sum_{k=1}^{na}\{E_k[\rho(r_k)]+\frac{1}{2}\sum_{k=1}^{na}\psi(r_{kl})\} \qquad (2\text{-}8)$$

The electron density at site of atom k is assumed to be a superposition of the electron densities due to the neighboring atoms:-

$$\rho(r_k)=\sum_{l=1}^{na}\rho_l(r_{kl}) \qquad (2\text{-}9)$$

The vibrational contribution to the free energy is determined that each atom is assumed to vibrate within a potential well which may be characterized by three independent frequencies.. The classical vibrational contribution to the free energy is:

$$E_{vib} = k_B T \sum_{k=1}^{na} \sum_{o=1}^{3} \ln(h\omega_{ko} / k_B T) \qquad \textbf{(2-10)}$$

The configurational energy contribution E_{conf} to the free energy of a binary alloy, is written using the ideal entropy of mixing as[21]:

$$E_{conf} = -k_B T \sum_{k=1}^{na} \{prob_A(as) \ln[prob_A(as)] + prob_B(as) \ln[prob_B(as)]\} \qquad \textbf{(2-11)}$$

In 1997 Zhang, F.; *et al.* [25] developed thermodynamic description of the Ti-Al system, nine phases were considered in this system. The disordered solution phases are: liquid, α(Ti, Al), β(Ti, Al), (Al); ordered intermetallic phases: α_2Ti_3Al, γTiAl, $TiAl_3$ and stoichiometric compounds: $TiAl_2$, Ti_2Al_5. They developed quasi chemical model to describe the excess Gibbs free energy of the ordered intermetallic phases. The thermodynamic properties obtained from the model parameters as well as the calculated phase diagram are in good agreement with the experimental data.

In 1998 Purton, J. A.; *et al.* [26] showed explicitly how a number of modified Monte Carlo techniques may be used for taking explicit account of relaxation, there by sampling efficiently a large number of different configurations and avoiding any averaging out of local effects. In this way they remove the major limitations of the existing methods

which restrict considerably the contact between experiment and theory and extend the range of applications that can be tacked to include real rather than model systems. Order-disorder in alloys, oxides, and silicates are studied by means of Monte Carlo methods. The authors have investigated both convergent and nonconvergent ordering. Applications was studied: Cu/Au ordering in Cu-Au alloy, Mg/ Mn ordering in olivine $MgMnSiO_4$, and L^{+3}/M^{+2} order- disorder in the quaternary cuprates $La_2MCu_2O_6$ (M=Ca, Sr).

Monte Carlo is presented for the calculation of the thermodynamic properties of solid solution and phase diagrams. Monte Carlo is modified as described below. All calculations are based on an ionic model using two-body potentials to represent short-range forces.

The first approach is a Monte Carlo simulation (MC) in which there are no interchanges. Vibrational effects are taken into account by allowing random moves of randomly selected atoms. Both the atomic coordinates and cell dimensions are allowed to vary during the simulation. During one step of the MC simulation, an atomic coordinate or a lattice parameter is chosen at random and altered by a random amount. The maximum changes in the atomic displacements and the volume are governed by the variables r_{max} and v_{max} respectively.The magnitudes of these parameters adjusted automatically during the equilibration part of the simulation to maintain an acceptance / rejection ratio of approximately 0.3.

In the second approach, Monte Carlo Exchange (MCX), both the atomic configuration and the atomic coordinates of all the atoms are changed. In any step, a random choice is made whether to attempt a random exchange between two atoms, a random displacement of an ion, or a random change in the volume of the simulation box.

The final technique is hybrid Monte Carlo (HMC), local structural relaxation is achieved by means of a short molecular dynamics (MD) run thus combining MonteCarlo and molecular dynamics steps in the same simulation. Related techniques have been widely used in the modeling of polymers and biomolecular. Like MCX, the HMC technique allows the efficient sampling of a large number of different configurations. During one HMC cycle, one of three options is chosen at random, with equal probabilities [27].

The first and second methods are the most popular methods in recent times. These approaches rely on generating a set of system states representative of the equilibrium configuration and forming an average over this set. The computationally expensive part is then generating new configurations, both to approach an equilibrium state from an initial configuration, and in sampling the configuration space near the equilibrium, more samples leading to greater accuracy [17].

In 1997 Taylor, M. B; *et al.* [17] concluded method of the fully quasiharmonic dynamical free-energy first derivatives, and static energy second derivatives, for a periodic crystal with respect to various parameters of its geometry. They showed how these derivatives can be used for efficient structural optimization of such a crystal. They calculated the optimized geometry, equilibrium thermodynamic quantities such as free energy, heat capacity, and thermal expansion. This procedure can be used over a wide range of temperatures and pressures.

Quasiharmonic lattice dynamics(QLD) is a simulation technique complementary to Monte Carlo and molecular dynamics. Quantum effects are readily taken into account, and high precision does not normally require long runs. Vibrational stability is a sensitive test of

interatomic potentials, and details of the vibrational motion reveal mechanisms for phase transitions or for thermal expansion. The major computational task is usually to find the equilibrium geometry at a given temperature and pressure; this calculating free energy, heat capacity, and thermal expansion, is rapid and accurate. Quasiharmonic lattice dynamics (QLD) is a relatively inexpensive technique, which avoids the kinetic barriers and critical slowing-down effects suffered by Monte Carlo (MC) and has the advantage that free energies and derived properties such as entropy and heat capacity can be calculated directly with high precision. The main disadvantage is that QLD is valid only when vibrational amplitudes are fairly small, and so other techniques must be at high temperatures as melting is approached[28].

In 2001 Allan, N. L.; *et al.* [28]concluded the quasiharmonic lattice dynamic (QLD) is an economical and precise tool for not only the bulk ,but also surfaces, defects, and solid solutions. For ionic solids they found that QLD is usually valid up to about one-half to two-thirds of the melting point. They used QLD in several applications such as: MgF_2 including the rutile/fluorite transition; negative thermal expansion in ZrW_2O_8 , anisotropic expansion of polyethylene at very low temperatures; surface free energies for MgO; defect energies and volumes in MgO. They applied a new method for obtaining free energies and phase diagrams of disordered solids and solid solutions such as MnO/MgO and CaO/MgO.

In 2001 Barrera, G. D.; *et al.* [29] developed a highly efficient method for the fully dynamic structure optimization of large unit cells that uses lattice statics and quasiharmonic lattice dynamics (QLD). The authors showed how a configurational lattice dynamics technique in

which the free energy of a number of configurations is determined directly by means of fully dynamic structural minimization that can be used to calculate thermodynamic properties of solid solutions and phase diagrams. The authors illustrated this method by using Mn/MgO. They concluded how the rapid calculation of the free energy via quasiharmonic lattice dynamics can be used to calculate thermodynamic properties of solutions over wide ranges of temperatures including H_{mix} and S_{mix} , and phase diagrams.

In 2000 Walle, A.[30]seek to improve one specific type of phase diagram computations "First-principles" calculations to calculate vibrational entropy differences between phases in an alloy system and vibrational properties. Vibrational entropy change can be attributed to changes in bond stiffness associated with the changes in bond length that take place during a phase transformation. First principles calculations can be enabled to develop controlled approximations that allow the inclusion of vibrational effect in phase diagram calculations at a reasonable computational cost.

A first principles calculation seeks to determine the properties of a material without relying on any experimental input, starting solely from the knowledge of the atomic number of constituents.The calculation of phase diagrams from first principles is a challenging task, because phase transitions are determined by the collective behavior of a large number of atoms. However, the computational requirements of the quantum mechanical calculations needed to describe the energetics of the system are such that they can only be performed on systems with a small number of atoms.

In 2001 Ceder, G. [31]worked on development of first principles methods and on the integration of this new expertise with materials research and engineering. First principles computations make it possible to predict properties of materials before they are synthesized. These methods can be used to investigate materials and pre-screen candidate compositions when designing new materials. Examples of properties that can be predicted includes :phase diagrams, thermodynamic properties , thermal expansion, elastic constants, heat conductivity ,diffusivity, infrared and microwave absorption ,electrochemical potentials, reaction activation energies.

In 2001 Gronsky, R.; *et al.* [32] presented the construction of phase diagrams from cooling curves .They used a thermocouple that exploits the Seebeck Effect, the voltage difference induced in a conductor by a temperature gradient. The thermocouple is made from chromel and alumel. They find the phase diagram of lead-antimony by plotting cooling curves at various temperatures.

Thermal analysis method is the most widely used for developing equilibrium diagrams[15]. In this method, alloys mixed at different compositions are melted and then the temperature of the mixture is measured at a certain time interval while cooling back to room temperature. It relies on the information obtained from the cooling diagrams[33]. Cooling diagram will show a change in slop between initial and final phase change temperatures because of the evolution of heat by the phase change. Then these temperatures are used for the construction of the phase diagrams[33 and 3].

In 2002 Chen, S. L. ; *et al.* [34]discovered a new computer software package for multi component phase diagram calculation is

PANDAT. PANDAT is designed to calculate the most stable phase equilibrium automatically[35]. It uses a global minimization algorithm based on the mathematical and thermodynamic properties between Gibbs energy function and the stable phase equilibrium[35].

Calculation of the heat capacity of a solid element, as a function of temperature, was one of the early triumphs of the quantum theory [20] . Thermodynamic properties such as enthalpy, entropy, and Gibbs free energy can be concluded from this method. The first such calculation is due to Einstein, who considered the properties of a crystal comprising na atoms, each of which , in classical terms, is considered to behave as a harmonic oscillator vibrating independently about its lattice point. As each oscillator is considered to be independent such as its behavior is unaffected by the behavior of its neighbors, then each oscillator vibrates with a single fixed frequency , and a system of such oscillators is known as an Einstein crystal.

Quantum theory gives the energy of the Ith level of a harmonic oscillator as:

$$E_I = (I + 1/2)h\omega \qquad \textbf{(2-12)}$$

As each oscillator has three degree of freedom can vibrate in the x, y, and z regarded as being a system of 3n linear harmonic oscillator)is given as :

$$na_I = \frac{me^{-bE_I}}{\sum e^{-bE_I}} \qquad \textbf{(2-14)}$$

$$E_{sys} = 3\sum n a_I E_I \qquad \textbf{(2-13)}$$

By substituting Eqs.(2-14)and(2-15) in (2-13):-

$$b = \frac{1}{k_B T} \qquad \textbf{(2-15)}$$

$$E_{sys} = 3mh\omega\left[\frac{\sum I e^{-h\omega(I+\frac{1}{2})/k_B T}}{\sum e^{-h\omega(I+\frac{1}{2})/k_B T}} + \frac{\frac{1}{2}\sum e^{-h\omega(I+\frac{1}{2})/k_B T}}{\sum e^{-h\omega(I+\frac{1}{2})/k_B T}}\right]$$

$$= 3mh\omega\left[\frac{\sum I e^{-h\omega I/k_B T}}{\sum e^{-h\omega I/k_B T}} + \frac{1}{2}\right]$$

$$= \frac{3}{2}mh\omega\left[1 + \frac{2\sum I e^{-h\omega I/k_B T}}{\sum e^{-h\omega I/k_B T}}\right] \qquad \textbf{(2-16)}$$

taking $\sum I e^{-h\omega_I/k_B T} = \sum I f^I$

where $f = e^{-h\omega/k_B T}$

gives $f(1 + 2f + 3f^2 + 4f^3 + ...) = \frac{f}{(1-f)^2}$

and $\sum e^{-h\omega_I/k_B T} = \sum f^I = 1 + f^1 + f^2 + f^3 + ... = \frac{1}{(1-f)}$

in which case:

$$E_{sys} = \frac{3}{2} mh\omega \left[1 + \frac{2f}{(1-f)} \right]$$

$$E_{sys} = \frac{3}{2} mh\omega + \frac{3mh\omega}{(e^{h\omega/k_B T} - 1)} \qquad \textbf{(2-17)}$$

Equation(2-17) expresses the relationship between the energy of the system and the temperature. Differentiation of Eq. (2-17)with respect to temperature at constant volume gives the constant –volume heat capacity Cv (as the volume remains constant, the quantization of the energy levels remains constant)[20 and 4],thus:

$$Cv = (\partial E_{sys} / \partial T) = 3mh\omega (e^{h\omega/k_B T} - 1)^{-2} e^{h\omega/k_B T} \frac{h\omega}{k_B T^2}$$

$$= 3mk_B \left[\frac{h\omega}{k_B T} \right]^2 \frac{e^{h\omega/k_B T}}{(e^{h\omega/k_B T} - 1)^2} \qquad \textbf{(2-18)}$$

By using Einstein characteristic temperature, and taking m equal to Avogadro's number gives the constant-volume molar heat capacity of the substance as[20]:

$$Cv = 3R\left(\frac{\theta_{Ei}}{T}\right)^2 \frac{e^{\theta_{Ei}/T}}{(e^{\theta_{Ei}/T}-1)^2} \qquad (2\text{-}19)$$

where $\theta_{Ei} = \frac{h\omega}{k_B}$

The next step in the development of the theory was made by Debye, who assumed that the range, or spectrum, of frequencies available to the oscillators was the same as that available to the elastic vibrations of a continuous solid. With respect to the wavelengths of these vibrations, the lower limit is fixed by the interatomic distances in the solid .If the wavelength was equal to the interatomic distance, then successive atoms would be in the same phase of vibration; hence vibration of one atom with respect to another, as such , would not occur. Theoretically the shortest allowable wavelength is twice the interatomic distance, in which case neighboring atoms vibrate in opposition to each other. Taking this minimum wavelength λmin to be in the order of $5*10^{-8}$ cm and the wave velocity υ in the solid to be $5*10^5$ cm/sec gives the maximum frequency of vibration of an oscillator to be in the order of:

$$\omega_{max}=\upsilon/\lambda min=5*10^5/5*10^{-8}=10^{13}sec^{-1} \qquad (2\text{-}20)$$

Debye assumed the frequency distribution to be one in which the number of vibrations per unit volume per unit frequency range increases parabolically with increasing frequency in the allowed frequency range $0<=\omega<=\omega_{max}$; and by integrating the Einstein expression over this frequency distribution, he obtained the heat capacity of the solid as:-

$$Cv = \frac{9mh^3}{k_B^2\theta_D^3}\int_0^{\omega_D}\omega^2\left(\frac{h\omega}{k_BT}\right)^2\frac{e^{h\omega/k_BT}}{(1-e^{h\omega/k_BT})^2}d\omega$$

$$= 9R\left(\frac{T}{\theta_D}\right)^3\int_0^{\theta_D/T}\frac{f^4e^f}{(1-e^f)^2}df \qquad (2\text{-}21)$$

For very low temperature Eq.(2-21) gives

$$Cv = 464.5\left(\frac{T}{\theta_D}\right)^3 \quad \textbf{(2-22)}$$

Eq.(2-22)is termed the Debye T^3 law for very low temperature heat capacities. This equation is of particular use at temperatureS below those at which the heat capacity has been measured experimentally for a given material [20] .

with $f = h\omega / k_B T$ where $\theta_D = \frac{h\omega}{k_B}$

There is few researches about calculating phase diagrams theoretically. Kuufman and Saunders used CALPHAD method to determine binary and ternary phase diagrams. Norgren used CALPHAD method to determine thermodynamic properties and phase diagrams of rare earth-iron alloys and Zi-Kui determine phase diagram of boron-magnesium.
Monte carlo is used to study the ordering in gold-copper, magnesium-manganes in olivine, and in cuprates by Purton. Allan, *et al.* study transition MgF_2 ,thermal expansion, surface free energy ,and phase diagram of MnO-MgO by using quasiharmonic lattice dynamics QLD.

In present work minimization free energy of the system such as CALPHAD method was used. By using Gibbs free energy at melting temperature for each metal is zero and using the enthalpy and the entropy at melting temperature and calculating the interaction parameters

for eutectic system. Theoretical method is more important than experimental method because the latter is a painstaking task, complicated both by the need for high resolution in(composition, temperature)-space, and phases with a small stability region be missed.

Chapter Three

Theoretical Analysis of Phase Diagrams

3.1General

In this work solid solutions α,β, and ε represent FCC, BCC, and CPH respectively. The phase diagrams of two metals completely soluble in liquid and solid state without miscibility gap will be dealt as ideal solutions and with miscibility gap will be dealt as regular solutions. The eutectic system is calculated by another method.

3.2 Theoretical Calculation of Binary Phase Diagram for Ideal Solution -:

Real systems which behave almost ideally in both the solid and liquid states present the possibility of the relatively simple quantitative calculation of phase diagrams [11].By using Gibbs free energy of the liquid and the solid states to find the equilibrium between two phases. For equilibrium in a system the chemical potential of any component in all phases is the same[18]. The equations for the liquidus and solidus curves in the systems of two metals soluble completely in liquid and solid states will be developed from the relations in Ref.[11]:-

$$G^{L} = G^{M,L} + RT(X_A^L \ln X_A^L + X_B^L \ln X_B^L) \quad (3\text{-}1)$$

$G^{M,L}$ in turn may be written as:

$$G^{M,L} = (X_A^L G_A^L + X_B^L G_B^L) \quad (3\text{-}2)$$

The free energy of the liquid solution as a function of partial molal free energy is:-

$$G^{L} = (\mu_A^L X_A^L + \mu_B^L X_B^L) \quad (3\text{-}3)$$

$$dG^{L} = (\mu_A^L dX_A^L + \mu_B^L dX_B^L) \quad (3\text{-}4)$$

The chemical potential of B in the solution at equilibrium is concluded from the next equations؛ by substituting $X_A=1-X_B$ and $dX_A=-dX_B$, combining equations (3-3)and (3-4), and suitably rearranging as in Ref.[11]:

$$\mu_B^L = G^L + X_A^L \frac{dG^L}{dX_B^L} \quad \textbf{(3-5)}$$

$$\mu_A^L = G^L - X_B^L \frac{dG^L}{dX^L} \quad \textbf{(3-6)}$$

Differentiating Eq.(3-1) as in Ref.[11] get that:

$$\frac{dG^L}{dX_B^L} = G_B^L - G_A^L + RT\ln\frac{X_B^L}{X_A^L} \quad \textbf{(3-7)}$$

$$\mu_B^L = G_B^L + RT\ln X_B^L \quad \textbf{(3-8)}$$

Thus the chemical potential of metal B in the liquid phase is:

At a given temperature the difference in Gibbs free energy for metal B is:

In an analogous manner in the solid solution:

$$\mu_B^S = G_B^S + RT\ln X_B^S \quad \textbf{(3-9)}$$

If the liquid and solid solutions are to be in equilibrium, the chemical potentials of B in each must be identical; equating (3-8) and (3-9):-

$$RT\ln\frac{X_B^S}{X_B^L} = G_B^L - G_B^S = \Delta G_B \quad \textbf{(3-10)}$$

When B melts under equilibrium conditions at constant temperature and pressure. At melting temperature the change in Gibbs free energy is

$$\Delta G_B = \Delta H_B - T\Delta S_B \quad \textbf{(3-11)}$$

zero:

$$\Delta G_B^m = 0 = \Delta H_B^m - T_B^m \Delta S_B^m \quad \text{or} \quad \Delta S_B^m = \frac{\Delta H_B^m}{T_B^m} \tag{3-12}$$

Assuming that neither ΔS_B nor ΔH_B varies with temperature, this is equivalent to assuming that the difference between the heat capacity of the liquid and that of the solid,ΔCp, does not change with temperature, as in Ref. [11]:

$$\Delta S_B = \Delta S_B^m \quad \text{and} \quad \Delta H_B = \Delta H_B^m \tag{3-13}$$

then substitution of Eq.(3-12)into (3-11) gives:-

$$\Delta G_B = \Delta H_B^m - T\frac{\Delta H_B^m}{T_B^m} = \Delta H_B^m (1 - \frac{T}{T_B^m}) \tag{3-14}$$

By combining Eqs.(3-10) and (3-14) it can be found:

$$\ln \frac{X_B^S}{X_B^L} = \frac{\Delta H_B^m}{R}\left(\frac{1}{T} - \frac{1}{T_B^m}\right) \tag{3-15}$$

The same analysis obviously holds for the component A in the two solutions, so that:

$$\ln \frac{1 - X_B^S}{1 - X_B^L} = \frac{\Delta H_A^m}{R}\left(\frac{1}{T} - \frac{1}{T_A^m}\right) \tag{3-16}$$

In this work , by assuming that metals melt and solidify at their melting temperature under equilibrium conditions, that is $\Delta G=0$, and using Eqs. (3-15) and (3-16) to calculate the solidus and liquidus curves for ideal solutions (isomorphous systems). The equilibrium melting temperature and the enthalpy of fusion at constant pressure of the pure components at their melting points are needed to determine this type of phase diagrams. In this work these equations can be used for some phase

diagrams which dealt as ideal solution, such as copper-nickel, germanium-silicon, silver-palladium, and ruthenium-osmium

3.3 Determining the Solidus and Liquidus Curves and Miscibility Gap for Regular Solutions Theoretically:-

Depending on chemical potentials of components at equilibrium of phase diagram, two equations to determine the solidus and liquidus curves of regular solutions concerning on X_B^S and X_B^L.It is assumed that the enthalpy of each component at any temperature is equal to its enthalpy of fusion at its melting temperature; and that is true for the entropy. The regular solution has the excess Gibbs free energy which represent excess enthalpy and excess entropy. The excess entropy is negligibly small. Thus it equals zero. At equilibrium:

$$\mu_B^L = \mu_B^S \quad \text{and} \quad \mu_A^L = \mu_A^S$$

For regular solution: $\Delta S^{xs}=0$; $\Delta G^{xs}=\Delta H^{xs}$

The excess enthalpy as a function to critical temperature .The critical temperature is the beginning of miscibility gap, as reported in Ref.[11]:-

$$\Delta H^{xs}=2RT_cX_AX_B \qquad (3\text{-}17)$$

Thus for determining the mole fractions of metal B in the liquid and in the solid solution by the next method. Gibbs free energy of liquid solution in regular system is:

$$G^L = X_A^L G_A^L + X_B^L G_B^L + 2RT_c X_A^L X_B^L + RT(X_A^L \ln X_A^L + X_B^L \ln X_B^L) \qquad (3\text{-}18)$$

The differentiation of Eq.(3-18) is:-

$$\frac{dG^L}{dX_B^L} = G_B^L - G_A^L + 2RT_c - 4RT_cX_B^L + RT\ln\frac{X_B^L}{X_A^L} \quad \textbf{(3-19)}$$

For metal A:

$$\mu_A^L = G^L - X_B^L\frac{dG^L}{dX_B^L}$$

$$= G_A^LX_A^L + G_B^LX_B^L + 2RT_cX_B^LX_A^L + RT(X_A^L\ln X_A^L + X_B^L\ln X_B^L)$$

$$- X_B^L(G_B^L - G_A^L + 2RT_c - 4RT_cX_B^L + RT\ln\frac{X_B^L}{X_A^L})$$

$$= G_A^L + 2RT_c(X_B^L)^2 + RT\ln(X_A^L) \quad \textbf{(3-20)}$$

For solid solution:

$$G^S = X_A^SG_A^S + X_B^SG_B^S + 2RT_cX_A^SX_B^S + RT(X_A^S\ln X_A^S + X_B^S\ln X_B^S) \quad \textbf{(3-21)}$$

$$\mu_A^S = G^S - X_B^S\frac{dG^S}{dX_B^S}$$

$$= G_A^SX_A^S + G_B^SX_B^S + 2RT_cX_B^SX_A^S + RT(X_A^S\ln X_A^S + X_B^S\ln X_B^S)$$

$$- X_B^S(G_B^S - G_A^S + 2RT_c - 4RT_cX_B^S + RT\ln\frac{X_B^S}{X_A^S})$$

$$= G_A^S + 2RT_c(X_B^S)^2 + RT\ln(X_A^S) \quad \textbf{(3-23)}$$

Where: $\Delta G_A = G_A^L - G_A^S$

ΔG_A is Gibbs free

$$\frac{dG^S}{dX_B^S} = G_B^S - G_A^S + 2RT_c - 4RT_c X_B^S + RT\ln\frac{X_B^S}{X_B^L} \quad \textbf{(3-22)}$$

From Eqs.(3-21)and(3-22)the chemical potential of metal A is in solid solution is:

$$\Delta G_A = \Delta H_A^m - T\frac{\Delta}{T_A^m}$$

energy in terms of the quantity ΔH_A^m ,assuming that pure metal melts under equilibrium conditions at constant temperature and pressure, thus:

For metal B,by the same way, in liquid solution:

Chemical potential of metal B in solid solution is:

$$\mu_B^L = G^L + X_A^L\frac{dG^L}{dX_B^L}$$

At equilibrium $\mu_A^L = \mu_A^S$,then $\mu_A^L - \mu_A^S = 0$,from Eqs.(3-20)and(3-23)

$$= G_B^L + 2RTc(X_B^L)^2 - 4RTcX_B^L + 2RTc + RT\ln X_B^L \quad \textbf{(3-25)}$$

$$RT\ln\frac{X_A^S}{X_A^L} = \Delta G_A + 2RTc((X_B^L)^2 - (X_A^L)^2) \quad \textbf{(3-24)}$$

$$\mu_B^S = G^S + X_A^S\frac{dG^S}{dX_B^S}$$

$$= G_B^L + 2RTc(X_B^S)^2 - 4RTcX_B^S + 2RTc + RT\ln X_B^S \quad \textbf{(3-26)}$$

At equilibrium $\mu_B{}^L=\mu_B{}^S$,then $\mu_B{}^L-\mu_B{}^S=0$,from Eq.(4-25)and(4-26)

$$RT\ln\frac{X_B^S}{X_B^L} = \Delta G_B + 2Tc((X_B^L)^2 - (X_B^S)^2 + 2(X_B^S - X_B^L)) \quad \textbf{(3-27)}$$

$$\Delta G_B = \Delta H_B^m - T\frac{\Delta H_B^m}{T_B^m}$$

The miscibility gap can be calculated by knowing its critical temperature and using Eq.(3-28) as in Ref.[11] :-

$$T = \frac{2(1-2X_B^S)Tc}{\ln[(1-X_B^S)/X_B^S]} \qquad (3\text{-}28)$$

Thus the enthalpy of fusion of each component and its melting temperature, and the critical temperature which represent the beginning of the miscibility gap of the system are required. Primary values of X_B^S and X_B^L must be known and these variables are independent. In this work these equations can be used for some phase diagrams which dealt as regular solution, such as gold-platinum, iridium-palladium, niobium-tungsten and rhodium-palladium

3.4 Phase Diagrams for Eutectic Systems:- To determine phase diagrams of eutectic system by calculating mole fractions of liquid and solid phases. Gibbs free energy of liquid phase in the A-B system is given as in Ref.[36]:-

$$G^L = X_A^L G_A^L + X_B^L G_B^L + RT[X_A^L \ln X_A^L + X_B^L \ln X_B^L] + G^{xs,L} \qquad (3\text{-}29)$$

In the regular solution approximation , $G^{xs,L}$ is given by:-

$$G^{xs,L} = inp^L X_A^L X_B^L \qquad (3\text{-}30)$$

Differentiating Eq.(3-29)is:

$$\frac{dG^L}{dX_B^L} = G_B^L - G_A^L + RT\ln\frac{X_B^L}{X_A^L} + inp^L - 2inp^L X_B^L \qquad (3\text{-}31)$$

By using Eqs.(3-5) and (3-6) to calculate chemical potentials of two

$$\mu_B^L = G_B^L + RT\ln(X_B^L) + inp^L (X_A^L)^2 \qquad (3\text{-}32)$$

$$\mu_A^L = G_A^L + RT\ln(X_A^L) + inp^L (X_B^L)^2 \qquad (3\text{-}33)$$

metals in the liquid phase, the resulting Eqs. are:-

The Gibbs free energy for the solid solution which represent β phase is:-

$$G^\beta = X_A^\beta G_A^\beta + X_B^\beta G_B^\beta + RT(X_A^\beta \ln X_A^\beta + X_B^\beta \ln X_B^\beta + G^{xs,\beta} \qquad (3\text{-}34)$$

The excess Gibbs free energy for β phase is given by as reported in Ref.[36]:-

$$G^{xs,\beta} = inp^{\beta} X_A^{\beta} X_B^{\beta} \qquad \textbf{(3-35)}$$

Differentiating Eq.(3-33)is:

$$\frac{dG^{\beta}}{dX_B^L} = G_B^{\beta} - G_A^{\beta} + RT\ln\frac{X_B^{\beta}}{X_A^{\beta}} + inp^{\beta} - 2inp^{\beta} X_B^{\beta} \qquad \textbf{(3-36)}$$

The chemical potentials of two metals in the solid solution β are calculated as in the liquid phase by using Eqs.(3-5) and(3-6):-

$$\mu_B^{\beta} = G_B^{\beta} + RT\ln(X_B^{\beta}) + inp^{\beta}(X_A^{\beta})^2 \qquad \textbf{(3-37)}$$

$$\mu_A^{\beta} = G_A^{\beta} + RT\ln(X_A^{\beta}) + inp^{\beta}(X_B^{\beta})^2 \qquad \textbf{(3-38)}$$

Two-phase equilibria between the β and liquid phases at a fixed temperature require that:

$$\mu_A^{\beta} = \mu_A^L \quad : \quad \mu_B^{\beta} = \mu_B^L$$

it could be concluded that:

$$\Delta G_B^{\beta \longrightarrow L} + RT\ln[(X_B^L / X_B^{\beta})] = (X_A^{\beta})^2 inp^{\beta} - (X_A^L)^2 inp^L \qquad \textbf{(3-39)}$$

$$\Delta G_A^{\beta \longrightarrow L} + RT\ln[(X_A^L / X_A^{\beta})] = (X_B^{\beta})^2 inp^{\beta} - (X_B^L)^2 inp^L \qquad \textbf{(3-40)}$$

Where:

$$\Delta G_A^{\beta \longrightarrow L} = G_A^L - G_A^{\beta} \quad : \quad \Delta G_B^{\beta \longrightarrow L} = G_B^L - G_B^{\beta}$$

Solving Eqs.(3-39) and (3-40) to determine phase diagram of this type. Data of Gibbs free energy of two metals can be found by using free

energy at melting temperature as in Eq. (3-14), and by knowing the enthalpy of melting of each metal and its melting temperature then the entropy can be calculated as Eq.(3-12).

There are two methods to calculate the interaction parameters of liquid and solid phases. In the first method, calculating interaction parameters of liquid and solid phases as reported in Ref.[36]:-

$$\mathbf{inp^{L} = P_{int} + e^{L}} \qquad \textbf{(3-41)}$$

The first term pr_{int} is described in terms of the "solubility parameter" for the binary partners. These solubility parameters δ_A and δ_B are :

$$\delta_A = (H_A^{vap} / v_A^a)^{1/2} \qquad : \delta_B = (H_B^{vap} / v_B^a)^{1/2} \qquad \textbf{(3-42)}$$

The internal pressure term pr_{int}^{*} is evaluated by squaring the difference between solubility parameters and multiplying by the average volume and it is always positive. The present definition of the internal pressure term is :

$$P_{int} = 0.3(v_A^a + v_B^a)[(-H_A^{vap} / v_A^a)^{1/2} - (-H_B^{vap} / v_B^a)^{1/2}] \qquad \textbf{(3-43)}$$

To describe the electronic component of interaction parameter for liquid phase as a function of group number of metals in periodic table.

$$e^{L} = 2\{H^{vap}[(i+j)/2] - 0.5H_i^{vap} - 0.5H_j^{vap}\} \qquad \textbf{(3-44)}$$

*P_{int} the internal pressure contribution by Brewer. Brewer's procedure of evaluating δ_A or δ_B at 298˚K and this reduced the internal pressure by 40% thus the factor 0.3 reflects the above mentioned 40% reduction [36].

In order to estimate the interaction parameter for β phase which represents BCC quantitatively, by considering that the difference

between the interaction parameter for β phase and that for liquid phase is composed of two terms:

$$inp^{\beta} - inp^{L} = E_s + e^{\beta} \qquad \textbf{(3-45)}$$

The first of term is depending on the size or volume difference between A and B.

$$E_s = -0.5(H_A^{vap} + H_B^{vap})(v_A^a - v_B^a)^2(v_A^a + v_B^a)^{-2} \qquad \textbf{(3-46)}$$

In order to compute second term which represent the "electronic component" for the β phase by this way :-

$$H^{\beta} = (1 - X_B)H_A^{\beta} + X_B H_B^{\beta} + X_B(1 - X_B)inp^{\beta} \qquad \textbf{(3-47)}$$

$$H^{L} = (1 - X_B)H_A^{L} + X_B H_B^{L} + X_B(1 - X_B)inp^{L} \qquad \textbf{(3-48)}$$

Where:

$$H^{\beta} - H^{L} = \Delta H^{L \longrightarrow \beta}$$
$$= (1 - X_B)\Delta H_A^{L \longrightarrow \beta} + X_B H_B^{L \longrightarrow \beta} + X_B(1 - X_B)(inp^{\beta} - inp^{L}) \qquad \textbf{(3-49)}$$

so that where the electronic component of β phase is given by:

$$e^{\beta} = 2\{\Delta H^{L \longrightarrow \beta}[(i + j)/2] - 0.5\Delta H_A^{L \longrightarrow \beta} - 0.5H_B^{L \longrightarrow \beta} \qquad \textbf{(3-50)}$$

The computation of the interaction parameter for the ε phase which represents CPH as reported in Ref.[36]:

$$inp^{\varepsilon}=inp^{\beta}+e^{\varepsilon} \quad (3\text{-}51)$$

Hence

$$e^{\varepsilon} = 2\{\Delta H^{\beta\longrightarrow\varepsilon}[(i+j)/2] - 0.5H_A^{\beta\longrightarrow\varepsilon} - 0.5\Delta H_B^{\beta\longrightarrow\varepsilon} \quad (3\text{-}52)$$

The final step is to compute the interaction parameter for the FCC (α)phase. The parameter is defined by this equation as:

$$inp^{\alpha}=inp^{\varepsilon}+e^{\alpha} \quad (3\text{-}53)$$

Where:

$$e^{\alpha} = 2\{\Delta H^{\varepsilon\longrightarrow\alpha}[(i+j)/2] - 0.5H_A^{\varepsilon\longrightarrow\alpha} - 0.5\Delta H_B^{\varepsilon\longrightarrow\alpha} \quad (3\text{-}54)$$

In the second method using eutectic temperature and mole fractions at eutectic temperature from experimental diagrams to calculate the interaction parameters. By substituting $X_A^L=1-X_B^L$ and $X_A^S=1-X_B^S$ in Eqs.(3-39)and(3-40)and calculate the interaction parameter for β phase from Eq.(3-39):

$$inp^{\beta} = \frac{\Delta G_B^{\beta\longrightarrow L} + RT\ln[(X_B^L)/(X_B^{\beta})] + inp^{L}(1-X_B^L)^2}{(1-X_B^{\beta})^2} \quad (3\text{-}55)$$

From Eq.(3-40)can be calculated inp^L:-

$$inp^{L} = \frac{-(\Delta G_A^{\beta\longrightarrow L} + RT\ln[(1-X_B^L)/(1-X_B^{\beta})] - inp^{\beta}(X_B^{\beta})^2)}{(X_B^L)^2} \quad (3\text{-}56)$$

From two Eqs. before, inp^{β} and inp^{L} can be concluded as following:-

$$inp^{\beta} = \frac{-(X_B^L)^2[RT\ln(X_B^L/X_B^S)+\Delta G_B^{\beta\longrightarrow L}]-(1-X_B^L)^2[RT\ln[(1-X_B^L)/(1-X_B^S)]+\Delta G_A^{\beta\longrightarrow L}}{[-(X_B^L)^2(1-X_B^S)^2+(1-X_B^L)^2(X_B^S)^2]} \quad \textbf{(3-57)}$$

$$inp^{L} = \frac{-RT\ln(X_B^L/X_B^S)+inp^{\beta}(1-X_B^S)^2-\Delta G_B^{\beta\longrightarrow L}}{(1-X_B^L)^2} \quad \textbf{(3-58)}$$

$$F_1 = \ln(\frac{X_B^L}{X_B^{\beta}}) - \frac{[inp^{\beta}(1-X_B^{\beta})^2 - inp^{L}(1-X_B^L)^2 - \Delta G_B^{\beta\rightarrow L}]}{RT} \quad \textbf{(3-59)}$$

$$F_2 = \ln(\frac{1-X_B^L}{1-X_B^{\beta}}) - \frac{[inp^{\beta}(X_B^{\beta})^2 - inp^{L}(X_B^L)^2 - \Delta G_A^{\beta\longrightarrow L}]}{RT} \quad \textbf{(3-60)}$$

To determine the intersection point between liquidus and solidus lines which represent eutectic temperature, two functions required are :

The interaction parameters are used to calculate mole fractions as in Eqs.(3-39) and (3-40)at range of temperatures.

When the interaction parameter for the phase β and its equation of the transformation are not defined thus by knowing the interaction parameter for the liquid phase , the method is used as:

$$inp^{\beta} = \frac{\Delta G_A^{\beta\longrightarrow L} + RT\ln[(1-X_B^L)/(1-X_B^{\beta})] + inp^{L}(X_B^L)^2}{(X_B^{\beta})^2} \quad \textbf{(3-61)}$$

Phase diagram of copper –silver can be determined by using the first

$$\Delta G_B^{\beta \longrightarrow L} = inp^{\beta}(1 - X_B^{\beta})^2 - RT\ln(X_B^L / X_B^{\beta}) - inp^{L}(1 - X_B^L)^2 \qquad (3\text{-}62)$$

method of calculating interaction parameters , but phase diagrams of aluminum-silicon, lead-tin, and lead-antimony by using second method.

3.5 Free Energy Differences Between The Solid Forms of The Elemental Components-:

In order to illustrate how to estimate the equations of transformation between liquid and solid phases by using Figs.(3.1)and(3.2) as reported in Ref.[36].

From knowing the enthalpy difference and entropy difference between ε and β phase from Fig.(3.1)can be concluded equation of free energy of transformation between these phases by this equation:

$$\Delta G^{\beta \longrightarrow \varepsilon} = \Delta H^{\beta \longrightarrow \varepsilon} - T\Delta S^{\beta \longrightarrow \varepsilon} \qquad (3\text{-}63)$$

From Fig.(3.2) can be concluded the free energy of transformation between ε and α by this way:

$$\Delta G^{\alpha \longrightarrow \varepsilon} = \Delta H^{\alpha \longrightarrow \varepsilon} - T\Delta S^{\alpha \longrightarrow \varepsilon} \qquad (3\text{-}64)$$

By knowing Gibbs the free energy equation of transformation from solid to liquid phase at the melting point of that metal can be known the free energy of transformation between other solid phase and liquid phase by this manner. By assuming Gibbs free energy of transformation between liquid and α-solid solution is knowing thus:

$$\Delta G^{\varepsilon \longrightarrow L} = \Delta G^{\alpha \longrightarrow L} - \Delta G^{\alpha \longrightarrow \varepsilon} \qquad (3\text{-}65)$$

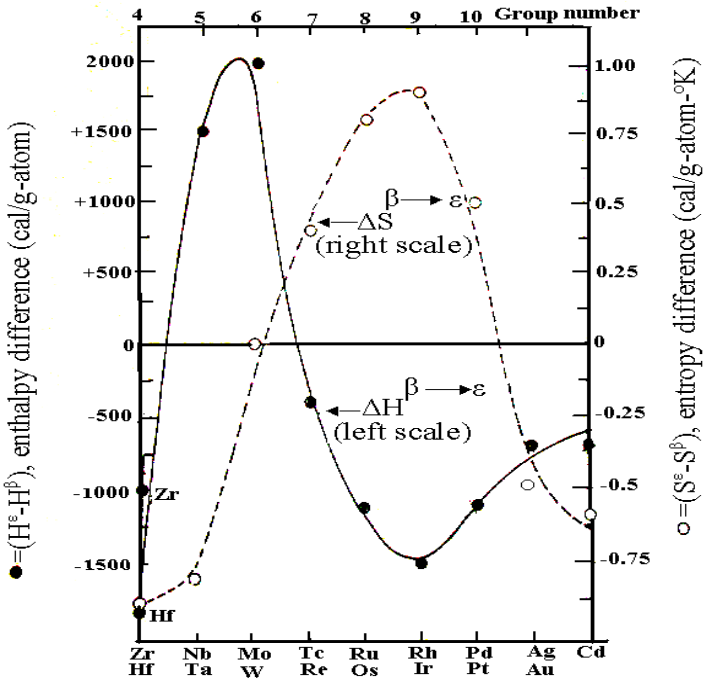

Fig.(3.1):Enthalpy and entropy differences between the CPH(ε) and BCC (β)forms of the transition metals. Ref.[36]

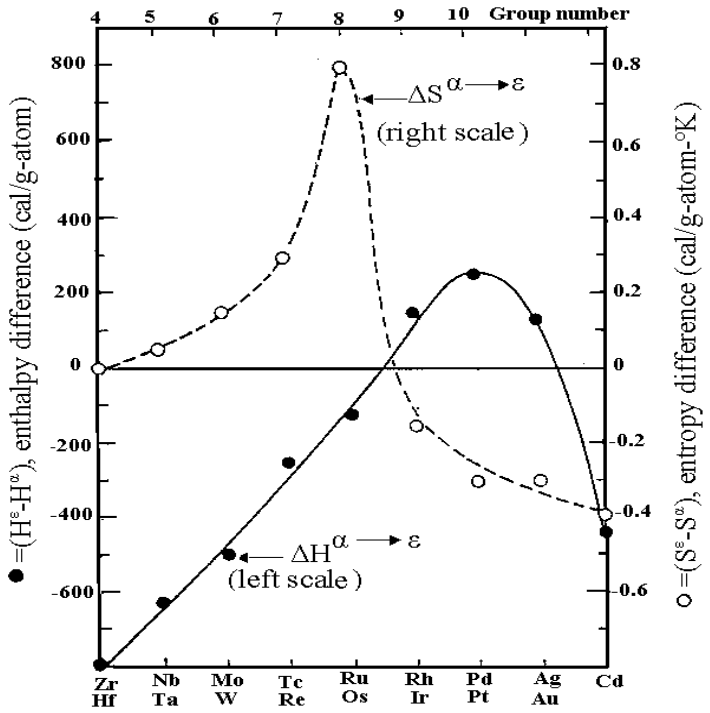

Fig.(3.2)Enthalpy and entropy differences between the CPH (ε) and the FCC (α) forms of the transition metals. Ref.[36]

3.6Computer Programming : Theoretical calculations of phase diagrams involves linear and nonlinear equations. These equations are solved using designed programs in Quick Basic language.

3.6.1 Two Metals Completely Soluble in Liquid and Solid State(TMCSLS):-The designed program is used to solve Eqs.(3-15) and (3-16) by calculating mole fraction in the solid state from the first equation after that calculate mole fraction in the liquid state from the second. To "Run" the "TMCSLS" program; the data of enthalpy of melting and temperature of melting of each metal must be specified. The resulting data can be drawn by subroutine which is called (draw temperature and mole fraction)"DTM1". This subroutine begins from the lower melting temperature to the high melting temperature by drawing mole fractions in the liquid and solid state at each temperature which represent the liquidus and solidus lines.

3.6.2 Two Metals Completely Soluble in Liquid and Solid State with Regular Solution (TMCSLSR) -: This program require the enthalpy of melting and melting temperature for each metal as input , as well as the critical temperature of the system which represent the beginning of miscibility gap .Suppose metal B has the lower melting temperature. The initial values of mole fractions for metal B in the liquid and solid state are 0.01, using in Eqs.(3-24) and (3-27) to obtain the final values of mole fractions. Determining the miscibility gap depending on the critical temperature of the system as in Eq.(3-28). The final values can be drawn by using the subroutine which is called(draw temperature and mole fractions) "DTM2". This subroutine is used to draw liquidus and solidus lines by the values of temperatures and mole fractions at each temperature after that drawing the miscibility gap by uing the

resultiong temperature from Eq.(3-28) with mole fraction of the solid state

3.6.3 Two Metals Completely Soluble in Liquid and Partial Soluble in The Solid State [Eutectic System](TMCSLPSS)-:

This program is represent the main program for this type because there are some of diagrams need another programs ,after that using the main program.This program require equations of transformation for each metal and the melting temperatures and initial values of mole fractions in the liquid and the solid states which represent 0.01. For this program data of interaction parameters determine from Eqs.(3-41),(3-45),(3-51)and(3-53).The subroutine which is called(draw temperature and mole fractions)"DTM3" to draw the liquidus ,solidus and solvus lines for this type by using temperatures and mole fractions at them.

For other phase diagrams which require other programs before using the main program such that:-

"TMCSLPSS1"to calculate interaction parameters for liquid and one of the solid solution depending on data from experimental method as in Eqs.(3-57) and(3-58).To find intersection point between solidus and liquidus lines which represent eutectic temperature by drawing two functions as in eqs.(3-49)and (3-50), and subroutine **"DTM4"** to draw F_1 and F_2 with mole fraction.

"TMCSLPSS2" to calculate interaction parameter for other solid solution and equation of transformation for one of the metals as in Eqs.(3-61) and (3-62).

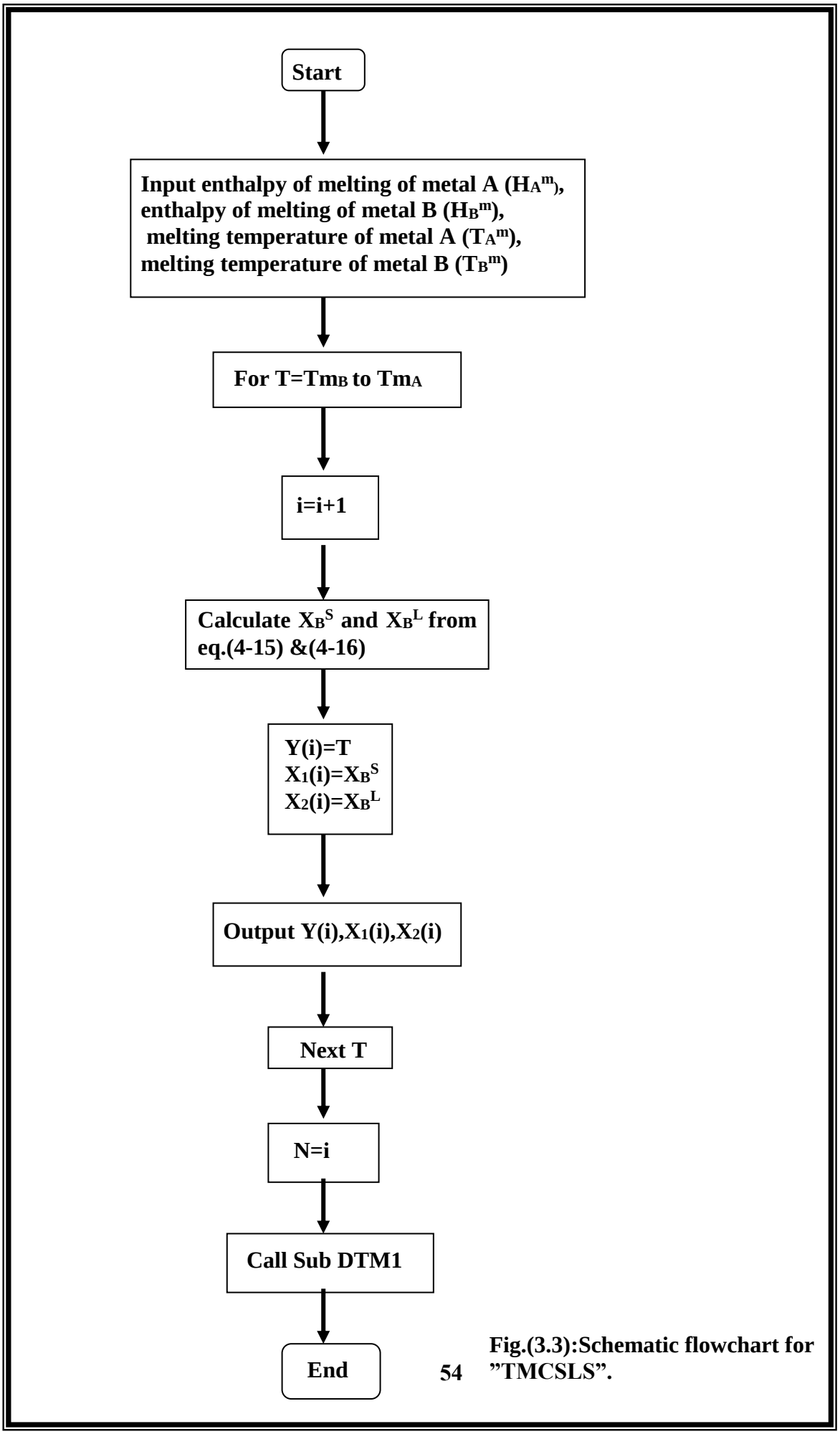

Fig.(3.3):Schematic flowchart for "TMCSLS".

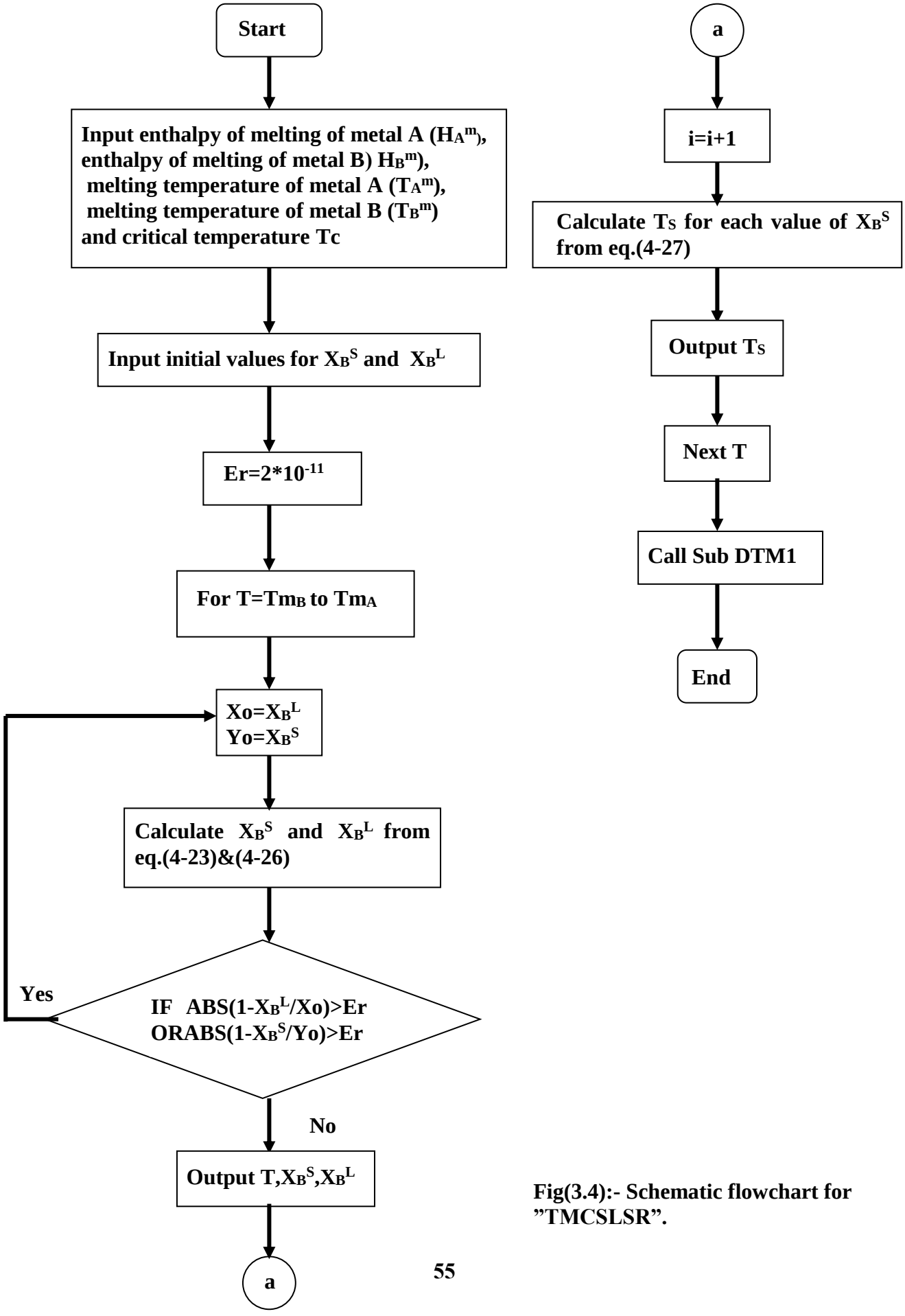

Fig(3.4):- Schematic flowchart for "TMCSLSR".

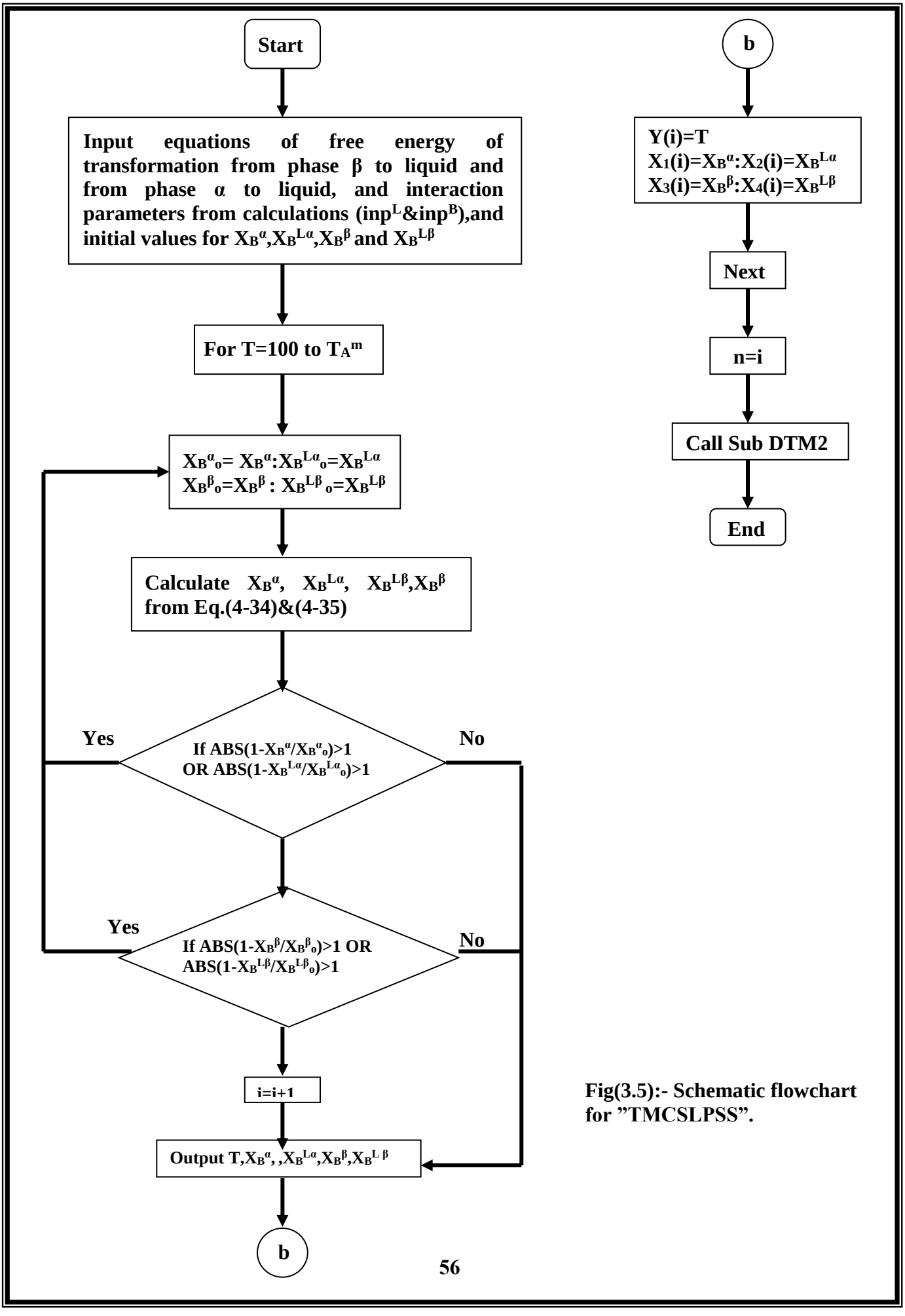

Fig(3.5):- Schematic flowchart for "TMCSLPSS".

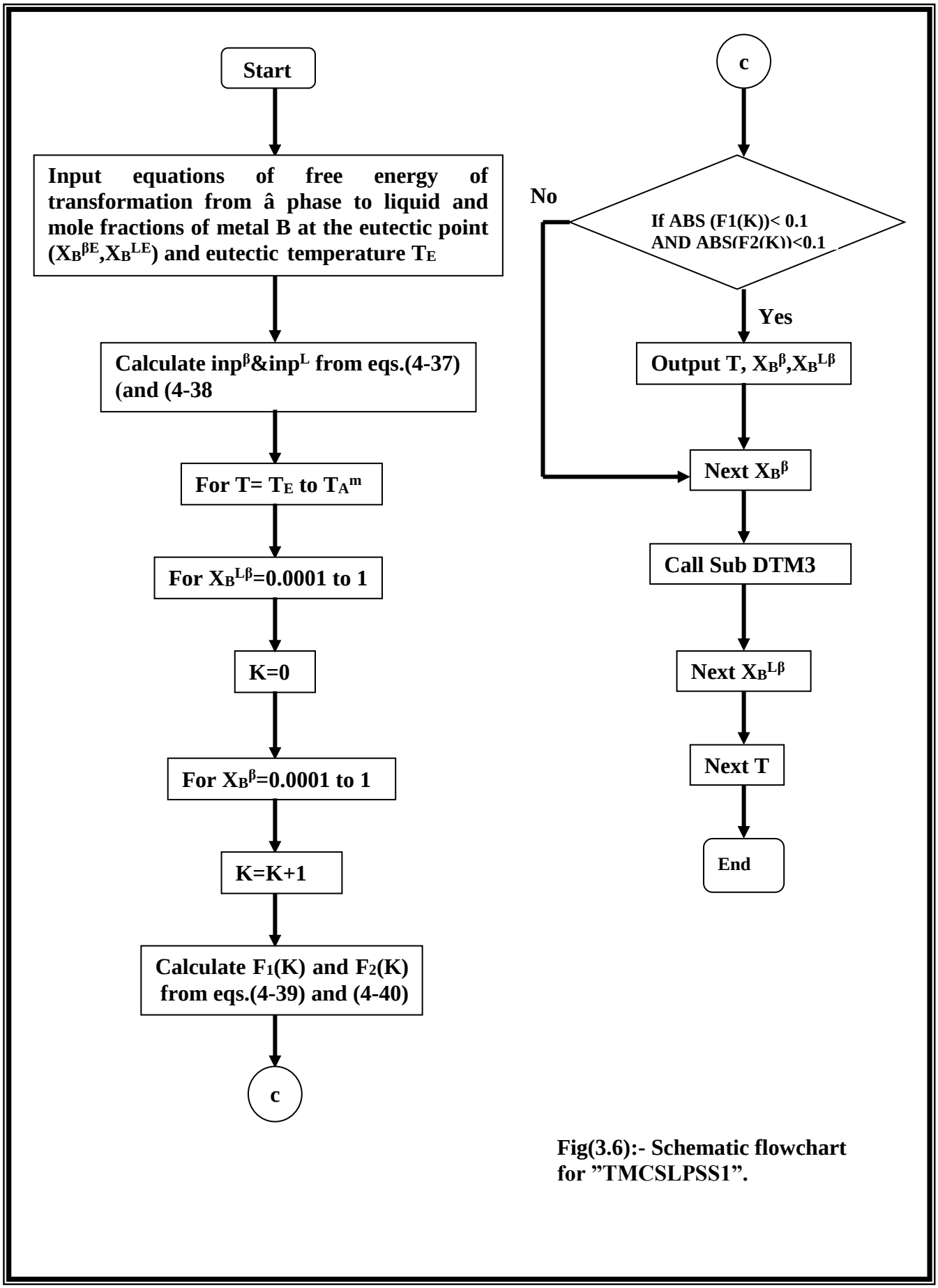

Fig(3.6):- Schematic flowchart for "TMCSLPSS1".

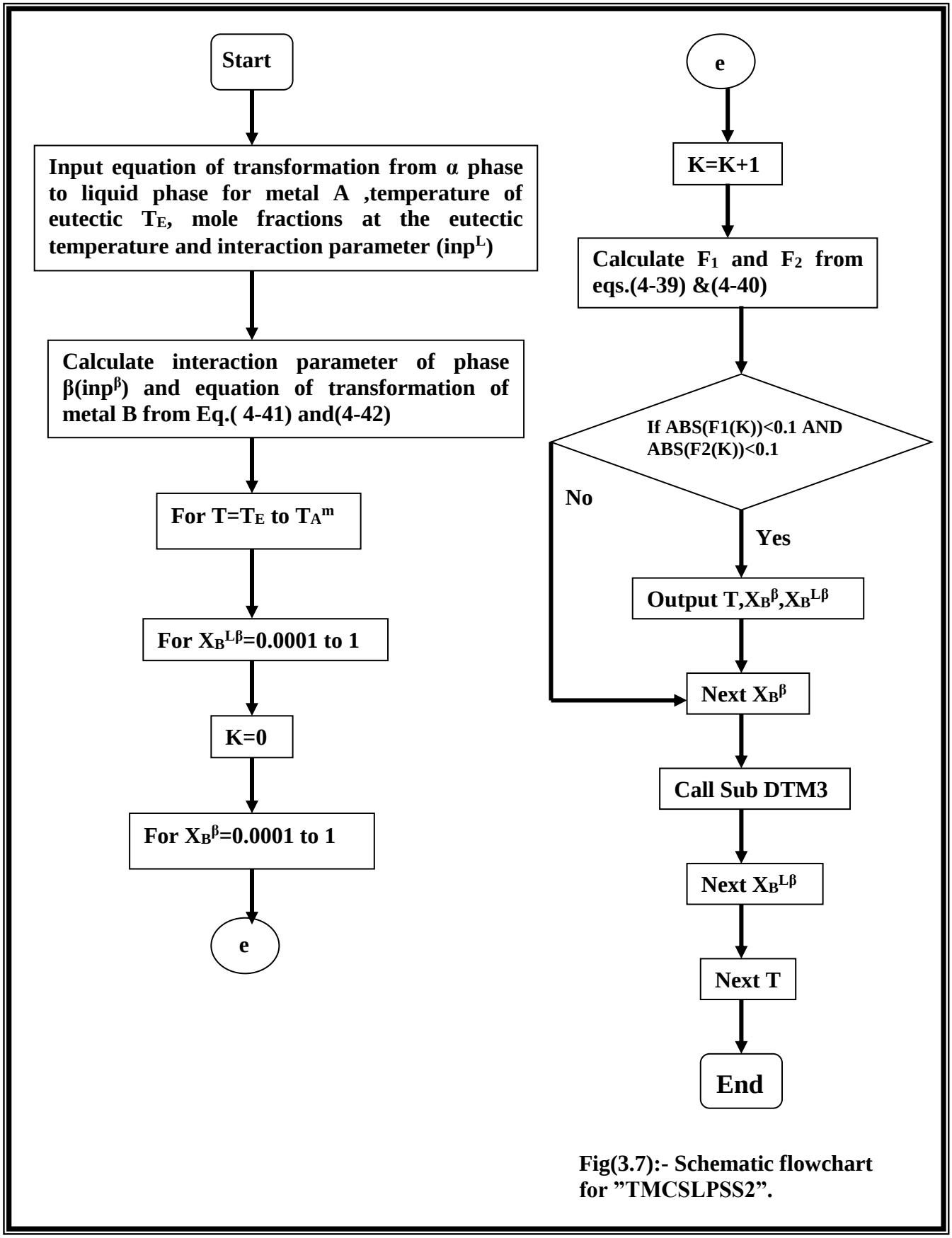

Fig(3.7):- Schematic flowchart for "TMCSLPSS2".

Chapter Four

Results and Discussion

4.1 General

Basing on the theoretical method for calculating phase diagrams and the designed computer programs presented in chapter three, the results of phase diagrams are presented and discussed in this chapter .All the results are compared with that of experimental method from Ref.[11, 12, 36, and 39]; which represent a thermal analysis using cooling curves.

4.2 Phase Diagrams of Two Metals Completely Soluble in Liquid and Solid State with Ideal Solution:-

The results obtained from the computer program (TMCSLS) with eqs.(3-15) and(3-16) are compared well with results of experimental method. The comparison was well done basing on four diagrams of this type : copper-nickel, germanium-silicon, silver-palladium, and ruthenium-osmium. Polynomial fit is used from second degree to make theoretical results more reasonable. The enthalpy of fusion and melting temperature needed are given in Tab.(4.1):-

Metal	ΔH_A^m cal/mol	T_A^m °K	Metal	ΔH_A^m cal/mol	T_A^m °K
Cu	3110	1356*	Ag	2855	1235.9**
Ni	4200	1728*	Pd	4120	1827*
Ge	8300	1232*	Ru	5100	2550**
Si	9470	1700*	Os	6600	3300*

Tab.(4.1):Values of enthalpy of melting and melting temperature.
***Ref.[37]and **Ref.[36]**

4.2.1 Copper-Nickel[Cu-Ni]:- In Fig.(4.1)the solidus and liquidus lines for experimental and theoretical manners started from the same point representing melting temperature of Cu and ended at the melting temperature of Ni. Theoretical solidus line is less than that of experimental solidus line in the region between (0-0.16)mole fraction of Ni with maximum difference of 10ºK at X_{Ni}= 0.08, when $T_{exp.}$=1385ºK and $T_{th.}$ =1375ºK ,while it will be higher in the region between (0.22–0.61) with maximum difference of 10ºK at X_{Ni}=0.5, when $T_{exp.}$=1530ºK and $T_{th.}$=1540ºK. Except these regions, two lines are identical. Experimentally liquidus line for all alloys is higher than theoretical liquidus line with maximum difference of 50ºK at X_{Ni}=0.4, when $T_{exp.}$=1545ºK and $T_{th.}$=1495ºK.

4.2.2 Germanium-Silicon[Ge-Si]:- For this diagram in Fig.(4.2),ending melting temperatures in theoretical method lower than that in experimental method with maximum difference in temperature is 50ºK at $wt._{Si}$=0.27, when $T_{exp.}$=1540ºK and $T_{th.}$=1490ºK. Theoretical and experimental solidus lines are identical in the region between (0.1-0.67) but in other regions theoretical solidus line higher than that that in experimental with max difference in temperature is 15ºK at $wt._{Si}$=0.93 , when $T_{exp.}$=1675ºK and $T_{th.}$=1680ºK

4.2.3 Ruthenium -Osmium [Ru-Os]:- Fig.(4.3) shows that theoretical solidus and liquidus lines are identical to that of experimental in the region between (0-0.12) for the first and (0-0.09)for the second.. In the region between(0.12-0.38) all alloys melt at temperatures lower than that of alloys in experimental manner with maximum difference of 100ºK at X_{Os}=0.23, when $T_{exp.}$=2780ºK and $T_{th.}$=2680ºK. The two lines are identical in the regions between (0.38-0.42).For theoretical method,

all alloys with mole fraction greater than 0.42 start melting at temperatures higher than that for experimental method with maximum difference of 20ºK at X_{Os}=0.46, when $T_{exp.}$=2870ºK and $T_{th.}$=2890ºK. The two lines are identical starting from X_{Os}=0.72 to X_{Os}=1.

The ending melting temperatures for alloys by theoretical method are lower than that of alloys by experimental method with difference of 20ºK at X_{Os}=0.17, when $T_{exp.}$=2710ºK and $T_{th.}$=2680ºK. Theoretical and experimental liquidus lines are identical in the region between (0.28-0.32),but alloys in theoretical method complete their melting at temperatures higher than that of alloys in experimental method with maximum difference of 20ºK at X_{Os}=0.4, when $T_{exp.}$=2860ºK and $T_{th.}$=2880ºK, then the two lines are identical from(0.9-1).

4.2.4 Silver-Palladium[Ag-Pd]:- As shown in Fig.(4.4) the experimental solidus line and theoretical liquidus line are identical in two regions (0-0.06) and(0.47-1), but they are not identical in the region between (0.06-0.47)with maximum difference of 35ºK at X_{Pd}=0.14, when $T_{exp.}$=1370ºK and $T_{th.}$=1335ºK. The maximum difference between theoretical liquidus line and experimental liquidus line is 75ºK at X_{Pd}=0.8, when $T_{exp.}$=1780ºK, and $T_{th.}$=1705ºK but for solidus line is 80ºK at X_{Pd}=0.2, when $T_{exp.}$=1400ºK, and $T_{th.}$=1320ºK .

4.3 Phase Diagrams of Two Metals Completely Soluble in Liquid State and Solid State with Regular Solution and Miscibility Gap:-

The results obtained from computer program (TMCSLSR) by using eqs.(3-24) ,(3-27) and (3-28) are compared with results from thermal analysis method. Polynomial fit is used to approximate results of theoretical analysis. In comparison four phase

diagrams of this type are considered: gold-platinum, iridium-palladium, niobium-tungsten and rhodium-palladium. Values of enthalpy of melting , melting temperature and critical temperature needed are given in Tab.(4.2) :

Metal	**ΔH_A^m cal/mol**	**T_A^m °K**	**Tc °K**
Au	**2955**	**1336**	**1530***
Pt	**4700**	**2042**	
Nb	**5480**	**2740**	**400****
W	**7300**	**3650**	
Pd	**3640**	**1820**	**1190****
Rh	**4480**	**2240**	
Pd	**3640**	**1820**	**1800****
Ir	**5500**	**2750**	

Table(4.2):Values of enthalpy of melting ,melting temperature and critical temperature. *Ref.[11]and **Ref.[36].

4.3.1Gold-Platinum[Au-Pt]:-It can be concluded from Fig.(4.5) that solidus lines by theoretical and experimental manners are identical in the region (0-0.74), while there is 110ºK difference at X_{Pt}=0.9, when $T_{exp.}$=1880ºK and $T_{th.}$=1990ºK. Liquidus lines are identical in the region (0-0.1),while the maximum difference reaches 90ºK at X_{Pt}=0.28, when $T_{exp.}$=1700ºK and $T_{th.}$=1790ºK.

Theoretical miscibility gap starts at X_{Pt}=0.02, when $T_{th.}$=727.4ºK,while experimental miscibility gap starts at X_{Pt}=0.2, when $T_{exp.}$=973ºK. Maximum temperature for the theoretical miscibility gap is $T_{th.}$=1529.8ºK at X_{Pt}=0.51 but that for experimental is $T_{exp.}$=1523ºK at X_{Pt}=0.6. The end point of miscibility gap for theoretical manner is

$T_{th.}$=765.8ºK at X_{Pt}=0.99 but for experimental is $T_{exp.}$.=973ºK at X_{Pt}=0.95 .

4.3.2 Iridium-Palladium[Ir-Pd]:- According to experimental method alloys start to fuse at temperatures less than that analyzed by theoretical method as shown in Fig.(4.6). Maximum difference between them in starting melting temperature is 750˚K at X_{Ir}= 0.6, when $T_{exp.}$=2000˚K and $T_{th.}$=2750˚K Ending melting temperatures for alloys by theoretical method are higher than that alloys by experimental method. There is a maximum difference of 400˚K at X_{Ir}=0.34, when $T_{exp.}$=1960˚K and $T_{th.}$=2360˚K and at X_{Ir}= 0.47, when $T_{exp.}$=2080˚K and $T_{th.}$=2480˚K.

Temperatures for experimental miscibility gap are higher than that temperatures for theoretical in the region (0.05-0.83).Starting temperature and mole fraction of theoretical miscibility gap are: $T_{th.}$=683.3˚K, X_{Ir}=0.014 but for experimental miscibility gap are: $T_{exp.=}$1000˚K.,X_{Ir}=0.05. Ending temperature and mole fraction of theoretical miscibility gap are: $T_{th.}$=683.3˚K, X_{Ir}=0.98 but for experimental miscibility gap are $T_{exp.}$=1000˚K, X_{Ir}=0.9. Top of theoretical and experimental miscibility gap being at X_{Ir}=0.5 but there is 300˚K difference when $T_{th.}$=1500˚K and $T_{exp.}$=1800˚K.

4.3.3 Niobium-Tungsten[Nb-W]:-As shown in Fig.(4.7), in experimental method solidus and liquidus lines are identical in the region between 0 to 0.1, which means that the melting point of alloys in this region alike that of pure metal without difference in temperature to end their melting. By comparing results of theoretical and experimental, it is noted that theoretical and experimental solidus lines are identical in the region (0-0.41) but wherever X_W is more than 0.41 starting of melting of

alloys by theoretical method is lower than that of alloys by experimental method with maximum difference of 60˚K at X_W=0.81, when $T_{exp.}$=3300˚K and $T_{th.}$=3240˚K.Maximum difference for ending temperature in the two methods is 430˚K at X_W=0.4, when $T_{exp.}$=3000˚K and $T_{th.}$=3430˚K.

Theoretical miscibility gap starts at X_W=0.02 when $T_{th.}$=116.52˚K and ends at X_W=0.97 $T_{th.}$=218.51˚K but for experimental miscibility the gap starts at X_W=0.1, when $T_{exp.}$=120˚K and ends at X_W=0.9 $T_{exp.}$=120˚K. There are two points of intersection: X_W=0.22, T=353.5˚K and X_W=0.77,T=356˚K. The highest temperature for experimental method is 550˚K at X_W=0.5, while for theoretical is 398˚K at X_W=0.57.

4.3.4 Palladium-Rhodium[Pd-Rh]:-As shown in Fig.(4.8) starting temperature and ending temperature of fusion for alloys by experimental method is lower than that for alloys by theoretical method with maximum difference of 70˚K at X_{Rh}=0.28, when $T_{exp.}$=1850˚K and $T_{th.}$=1920˚K for starting and 40˚K at X_{Rh}=0.3, when $T_{exp.}$=1990˚K and $T_{th.}$=1950˚K for ending.

Theoretical miscibility gap starts at X_{Rh}=0.063 when $T_{th.}$=582˚K and ends at X_{Rh}=0.95 when $T_{th.}$=548.8˚K but for experimental method it starts at X_{Rh}=0.05 when $T_{exp.}$=550˚K and ends at X_{Rh}=0.93 when $T_{exp.}$=560˚K. Experimental miscibility gap is higher than theoretical miscibility gap with maximum difference of 290˚K at X_{Rh}=0.5 when $T_{exp.}$=1190˚K and $T_{th.}$=900˚K.

4.4 Phase Diagrams of Two Metals Completely Soluble in Liquid State and Partial Soluble in Solid State "Eutectic System":-

The computer program (TMCSLPSS)is used directly for the first example of the eutectic type which represents phase diagram of Ag-Cu. For other diagrams the computer programs TMCSLPSS1 and TMCSLPSS2 are used to calculate the needed values then TMCSLPSS is used. Polynomial fit of two degrees is used for theoretical results to make them more acceptable. Phase diagrams of some metals are studied in this work. These phase diagrams are silver-copper, aluminum-silicon, lead-tin and lead-antimony.

4.4.1 Silver-Copper[Ag-Cu]:- Computer program (TMCSLPSS) is used to draw this phase diagram. Equations of transformation for two phases α and β are stated in Tab.(4.3):-

Metal	ΔG^{α}_{L} cal/mol	Tm^{α} °K	ΔG^{β}_{L} cal/mol	Tm^{β} °K
Ag	**2855-2.3*T**	**1235.9**	**1955-1.36*T**	**1437.5**
Cu	**3120-2.3*T**	**1356**	**2270-2.1*T**	**1080.95**

Table(4.3):Values of equations of transformation and melting temperatures for Ag-Cu. Ref.[36]

To calculate interaction parameters for this diagram as in sec.(3-4) by using eqs.(3-39) and (3-40), where A represents Cu and B represents Ag the values are in Ref.[37]:

H_{Cu}^{vap}=-72810cal/mol: H_{Ag}^{vap}=-60720 cal/mol to calculate v_{Cu}^{a} and v_{Ag}^{a} by using the required vales from Ref.[38]:

ρ_{Cu}=8.954g/cm^3 :M_{wCu} =127.08g/mol

ρ_{Ag}=10.524 g/cm^3 : M_{wAg}=215.74g/mol

$v_{Cu}^{a}= M_{wCu} /\rho_{Cu}=14.2\ cm^3/mol$: $v_{Ag}=: M_{wAg}/\rho_{Ag}=20.5cm^3/mol$

$pr_{int}=3073.4cal/mol$: i=j=11 thus $e^{L}=0$

$inp^{L}=3073.4cal/mol$

$E_s=2200.75cal/mol$: $e^{\beta}=0cal/mol$: $inp^{\beta}=5274.2cal/mol$

$e^{\varepsilon}=e^{\alpha}=0$

thus $inp^{\alpha}=inp^{\beta}$

There are differences between experimental and theoretical results. For solvus line in experimental method maximum amount of Cu dissolve in β-phase is $X_{Cu}=0.09$, when $T_{exp.}=1053^{\circ}K$ but for theoretical it reaches $X_{Cu}=0.275$, $T_{th.}=1125^{\circ}K$. Maximum amount of Ag dissolve in α-phase in experimental method is $X_{Ag}=0.08$ at $T_{exp.}=1053^{\circ}K$ but in theoretical method: $X_{Ag}=0.225$ at $T_{th.}=1125^{\circ}K$. So it can be concluded that in theoretical method a great amount of Cu dissolve in alloys containing a great amount of Ag and vice versa. Theoretical solvus line for β-phase ends at $X_{Cu}=0.01$ when $T_{th.}=273^{\circ}K$ but for experimental method it ends at $X_{Cu}=0.001$ at the same temperature but for α-phase in theoretical method solvus line ends at $X_{Cu}=0.994$ while for experimental at $X_{Cu}=0.98$ when $T=273^{\circ}K$.

There is a difference in temperature for liquidus line between liquid and β-phase between theoretical and experimental methods. Maximum difference is $120^{\circ}K$ at $X_{Cu}=0.21$, when $T_{exp.}=1060^{\circ}K$ and $T_{th.}=1180^{\circ}K$. The difference for liquidus line between liquid and α-phase is $60^{\circ}K$ at $X_{Cu}=0.6$, when $T_{exp.}=1130^{\circ}K$ and $T_{th.}=1190^{\circ}K$.

The difference between solidus lines is measured by difference in mole fraction at constant temperature. Maximum difference for solidus line between theoretical and experimental method for β-phase is 0.255 at $T=1125^{\circ}K$, $X_{Cu(exp.)}=0.02$, $X_{Cu(th.)}=0.275$ but for α-phase is 0.195 at

T=1125˚K, $X_{Cu(exp.)}$=0.94, $X_{Cu(th.)}$=0.745. Theoretical eutectic temperature higher than that for experimental method where $T_{E(th.)}$=1125˚K at X_{Cu}=0.42 and $T_{E(exp.)}$=1053˚K at X_{Cu}=0.28 .

4.4.2 Aluminum-Silicon[Al-Si]:- The computer program (TMCSLPSS1) is used to calculate interaction parameters inp^{L} and inp^{β} by using data in Tab.(4.4) and by knowing eutectic temperature and mole fractions which are substituted in eqs.(3.55)and(3.56)and draw F_1 and F_2 from eqs.(3-59) and (3-60).Computer program (TMCSLPSS2) is applied to calculate equation of transformation of α-phase for silicon and interaction parameter inp^{α} for α-phase using eqs.(3.61) and(3.62).

Metal	**ΔG^{α}_{L} cal/mol**	**Tm^{α} ˚K**	**ΔG^{β}_{L} cal/mol**	**Tm^{β} ˚K**
Al	**2560-2.75*T**	**931****	**150-1.6*T**	**94****
Si	**-14020.39-2.2*T**	**-6372.39[cal.]**	**9470-5.57*T**	**1080.95***

Tab.(4.4):Values of equations of transformation and melting temperatures for Al-Si. *Ref[37] and **Ref.[36]

The required values from Ref.[39]:-

T_E=850˚K :X_{Si}^{L}=0.126 :X_{Si}^{β}=1 :X_{Si}^{α}=0.0165

The results are:-

inp^{L}=-1701.494cal/mol

inp^{β}=9067.947cal/mol : inp^{α}=-14222.07cal/mol

Fig.(4-10) shows that there is a difference between the results of theoretical method and experimental as the theoretical eutectic point is T_E=895˚K at X_{Si}=0.14 while that of experimental method T_E=850˚K at X_{Si}=0.126. Theoretical solvus and solidus lines corresponding experimental solvus and solidus lines for β-phase but experimental

liquidus line is higher than theoretical liquidus line with maximum difference of 100 at X_{Si}=0.73˚K, when $T_{exp.}$=1600˚K and $T_{th.}$=1480˚K.

For α-phase theoretical solidus line corresponds to experimental solidus line but theoretical liquidus line is higher than experimental liquidus line with a difference of 50˚K at X_{Si}=0.126, when $T_{exp.}$=850˚K and $T_{th.}$=900˚K. Maximum amount of Si that dissolve in α-phase is X_{Si}=0.022 at $T_{th.}$=895˚K by theoretical method while by experimental method it is X_{Si}=0.0167 at $T_{exp.}$=850˚K. In theoretical method there is a change in solvus line of α-phase represented by X_{Si}=0.05 at $T_{th.}$=600˚K.

4.4.3 Lead-Tin[Pb-Sn]:-By the same manner used in previous section, the equation of transformation of β-phase for Pb and the equation of transformation of α-phase for Sn are calculated. Equations of transformation and melting temperatures are given in tab.(4.5):-

Metal	**ΔG^{α}_{L} cal/mol**	**Tm^{α} ˚K**	**ΔG^{β}_{L} cal/mol**	**Tm^{β} ˚K**
Pb	**1224-2.039*T**	**600.3***	**-532.77-3.637*T**	**-146.5[cal.]**
Sn	**86.6337-2.2*T**	**39.38[cal.]**	**1720-3.407T**	**504.8***

Tab. (4.5):Values of equations of transformation and melting temperatures for Pb-Sn. *Ref[37]

The required values from Ref.(14)are:-

T_E=456˚K :X_{Sn}^{L}=0.619 :X_{Sn}^{β}=0.975 :X_{Sn}^{α}=0.19 [44]

The results obtained are:-

inp^{L}=1694.638cal/mol

inp^{β}=974.293cal/mol :inp^{α}=720.1848cal/mol

By comparing results of experimental and theoretical methods shown in Fig.(4-11),there is a difference in temperature 4˚K and of 0.282

in mole fraction at the eutectic temperature where $T_{E(exp.)}$=456˚K at $X_{Sn(exp.)}$=0.619 while $T_{E(th.)}$=460˚K at $X_{Sn(th.)}$=0.901. Theoretical solvus line for α-phase starts at $T_{th.}$=460˚K when X_{Sn}=0.198 and ends at $T_{th.}$=273˚K X_{Sn}=0.126 but for experimental method it starts at $T_{exp.}$=456˚K when X_{Sn}=0.192 and ends at $T_{exp.}$=273˚K when X_{Sn}=0.02. Maximum difference between theoretical and experimental solvus lines for α-phase is 0.14 at T=300˚K, when $X_{Sn(exp.)}$=0.02 and $X_{Sn(th.)}$=0.16. For β-phase theoretical solvus line starts at T=460˚K when X_{Sn}=0.81 and ends at T=273˚K when X_{Sn}=0.94 but for experimental it starts at T=456˚K when X_{Sn}=0.975 and ends at T=273˚K when X_{Sn}=1 . Maximum difference between theoretical and experimental solvus lines for β-phase is 0.08 at T=300˚K, when $X_{Sn(exp.)}$=1 and $X_{Sn(th.)}$=0.92.

Theoretical liquidus line for α-phase is higher than experimental liquidus line with maximum difference of 124˚K at X_{Sn}=0.619, when $T_{exp.}$=456˚K and $T_{th.}$=580˚K, but for β-phase the maximum difference is 30˚K at X_{Sn}=0.901 when $T_{exp.}$=490˚K and $T_{th.}$=460˚K. In theoretical method alloys of α-phase start melting at mole fractions greater than that of alloys in experimental method with maximum difference at T=470˚K when $X_{Sn(exp.)}$=0.18 and $X_{Sn(th.)=}$0.29. Solidus lines of experimental and theoretical manner for β-phase are identical.

4.4.4 Lead-Antimony[Pb-Sb]:-Same manner of the previous section is used for this diagram. Melting temperatures and equations of transformation are given in Tab.(4.6)as shown:-

Metal	**$\Delta G^{\alpha}_{\rightarrow L}$ cal/mol**	**Tm^{α} ˚K**	**$\Delta G^{\beta}_{\rightarrow L}$ cal/mol**	**Tm^{β} ˚K**
Pb	**1224-2.039*T**	**600.3***	**-532.77-3.637*T**	**-146.5[cal]**
Sb	**2120-2.2*T**	**964.06[cal.]**	**4770-5.28*T**	**903.4***

Tab.(4.6):Values for equations of transformation and melting temperatures for Pb-Sb. *Ref[37]

The required values in Ref. [14]are:-

T_E=524.7˚K :X_{Sb}^{L}=0.116 :X_{Sb}^{β}=0.96 :X_{Sb}^{α}=0.02

inp^{L}=219.72cal/mol

inp^{β}=851.5cal/mol : inp^{α}=4946.6cal/mol

The phase diagram shown in Fig.(4.12) is drawn without polynomial fitting. Theoretical eutectic temperature and its mole fraction are higher than experimental eutectic temperature and its mole fraction, where $T_{E(th.)}$=530˚K at $X_{Sb(th.)}$=0.12 while $T_{E(exp.)}$=524.7˚K at $X_{Sb(exp.)}$=0.116. Theoretical solvus line of α-phase corresponds on the axis of temperature because small amount of Sb dissolve in α-phase represented by $T_{th.}$=530˚K at X_{Sb}=0.00203 but for experimental method maximum amount of Sb dissolves in α-phase is X_{Sb}=0.02 at $T_{exp.}$=524.7˚K.

Theoretical solidus line for α-phase approximately corresponds on axis of temperature with small amount of Sb. Maximum difference between theoretical and experimental solidus line is 0.0169 in mole fraction at T=530˚K $X_{Sb(exp.)=}$0.019 $X_{Sb(th.)=}$0.00203. Approximately theoretical liquidus line for α-phase corresponds to experimental liquidus line of α-phase.

Theoretical and experimental liquidus lines for β-phase are identical up to X_{Sb}=0.23 at T=610˚K then experimental liquidus line is higher than theoretical liquidus line with maximum difference of 30˚K at X_{Sb}=0.4, when $T_{exp.}$=710˚K and $T_{th.}$=680˚K. Solidus line in theoretical and experimental methods are very nearly with maximum difference in mole fraction of 0.03 at T=840˚K when $X_{Sb(exp.)}$=0.999 and $X_{Sb(th.)}$=0.969. Experimental and theoretical solvus lines for β-phase end at the same temperature T=273˚K when X_{Sb}=0.999 for experimental and X_{Sb}=0.987 for theoretical.

4.5 Discussion of The Results:-For some phase diagrams studied in this thesis there are some differences as comparing with experimental method. The thermodynamic properties and computer programs used with some approximations and assumptions.

4.5.1 Phase diagram of two metals completely soluble in liquid and solid state with ideal solution:-In all phase diagrams of this type starting and ending temperatures of liquidus and solidus lines are identical in theoretical and experimental methods. Approximately theoretical and experimental solidus lines in some regions are identical for Cu-Ni, Ge-Si, and Ru-Os but differ in other regions with percentage 2%,0.086%, and 1% respectively. For Ag-Pd starting melting temperatures in theoretical method less than that in experimental method with maximum percentage is 9%. Ending melting temperatures in experimental method higher than that in theoretical method for Cu-Ni ,Ge-Si, and Ag-Pd with percentage 4%, 6% , and 7% respectively, but for Ru-Os in some regions these temperatures identical but for other theoretical ending temperatures higher than that in experimental with percentage 2%.

The increasing or decreasing values because the assumptions that solution is ideal when the molecules of two metals have similar size and attract one another with the same force, all metals melt and solidify at their melting temperatures under equilibrium conditions that is the difference in Gibbs free energy is zero at the melting temperature, and the difference between the heat capacity of the liquid and that of the solid,ΔC_{pr} does not vary with temperature thus

$$\Delta S_A = \Delta S_A^m \quad \textbf{and} \quad \Delta H_A = \Delta H_A^m$$

Tab.(4.7) will indicate to the difference percentage for solidus and liquidus line of this type

Tab.(4.7):percentages of liquidus and solidus lines.

System	%Liq.	%Sol.
Ag-Pd	7%	9%
Ru-Os	2%	1%
		2%
		0.086%

4.5.2 Phase diagram of two metals completely soluble in liquid and solid state with regular solution and miscibility gap:-

For all diagrams of this type theoretical liquidus line higher than that in experimental method with maximum percentage is 26% for Nb-W. Theoretical and experimental solidus lines for Au-Pt and Nb-W are identical until X_{Au}=0.77 and X_W=0.4 after that differ with percentage of 6% and 2% respectively, but for Pd-Ir and Pd-Rh experimental solidus line lower than that in theoretical method with percentage of 2% and 9.4% respectively. For all diagrams experimental miscibility gap is higher than theoretical miscibility gap but for Au-Pt experimental and theoretical miscibility gaps intersect at X_{Au}=0.6. These differences

between theoretical and experimental methods because: using excess enthalpy which represent deviation from ideality as a function of critical temperature, assuming interaction energy between atoms of metal A is equal to the interaction energy between atoms of metal B, interaction energy between pair of atoms as a function to the critical temperature of miscibility gap, using critical temperature for miscibility gap from experimental diagram, and initial values of mole fractions as input in computer program . Tab.(4.8) will indicate to percentages of liquidus , solidus lines and miscibility gap.

System	%Liq.	%Sol.	%miscibility gap
Au-Pt	8%	6%	16%
Pd-Ir	3%	2%	4%
Nb-W	26%	2%	14%
Pd-Rh	8%	9.4%	33%

Tab.(4.8):percentages of liquidus and solidus lines and miscibility gap.

4.5.3 Phase diagram of two metals completely soluble in liquid and partial solubility in solid state [Eutectic systems]:-

Two different methods are used for phase diagrams of this type. The first method is used for Ag-Cu, by calculating interaction parameters for liquid and solid phases.The results of mole fractions for theoretical solvus line for β-phase higher than that of experimental with 14% percent but for α-phase less than that in experimental method with 11% percent. Theoretical eutectic temperature higher than that for experimental with 72˚K. Theoretical solidus and liquidus lines higher than that in experimental method with maximum percentage is 23%.

In the second method, calculating interaction parameters by knowing the eutectic temperature and mole fractions for liquid and solid phases at eutectic temperature from experimental diagrams after that solving them and drawing two functions and their intersection point in(TMCSLPSS1) also calculating other variables by using (TMCSLPSS2). Theoretical liquidus lines for Pb-Sb and Al-Si lower than that in experimental method with maximum percentage 7.6%, but for α phase of Pb-Sn is higher than that in experimental method maximum percentage of 40%. In these diagrams theoretical eutectic temperature is higher than that in experimental method with difference 4˚K for Pb-Sn and 6˚K for Pb-Sb but 45˚K for Al-Si. Correspondence occurs between solvus and solidus lines for β-phase for Al-Si, and solidus lines for β-phase in Pb-Sn in experimental and theoretical methods. Experimental solvus line for β-phase in Pb-Sb is hidden because the difficulty to conclude it, but in theoretical method it is clear , for solvus line for α-phase there is very small amount of Sb dissolve in Pb-base alloys.

Causes of these differences are:- initial values for mole fractions as input in computer programs, data using from experimental diagrams which concluded from thermal analysis, determining equation of transformations of some metals depending on the group number of metals in periodic table by using Fig.(3-1) and (3-2), using intersection point between two functions as the eutectic temperature, there are some parameters such as free mean path which represent the distance between the electron and the lattice do not calculate in theoretical method, and polynomial fitting used for theoretical values to make them more reasonable.

Tab.(4.9) indicates to percentages for liquidus and solidus and solvus lines for α and β phases.

System	%Liq$^{\alpha}$.	%Sol$^{\alpha}$.	%Solv$^{\alpha}$.	%Liq$^{\beta}$.	%Sol$^{\beta}$.	%Solv$^{\beta}$.
Ag-Cu	**15%**	**15%**	**11%**	**23%**	**22%**	**14%**
Al-Si	**6%**	**0%**	**0.145%**	**7.6%**	**0**	**0%**
Pb-Sn	**40%**	**13%**	**13%**	**12%**	**0%**	**10%**
Pb-Sb	**1%**	**1.7%**	**14%**	**4.3%**	**2%**	**2.8%**

Tab.(4.9):percentages of liquidus , solidus and solvus lines for α and β phases.

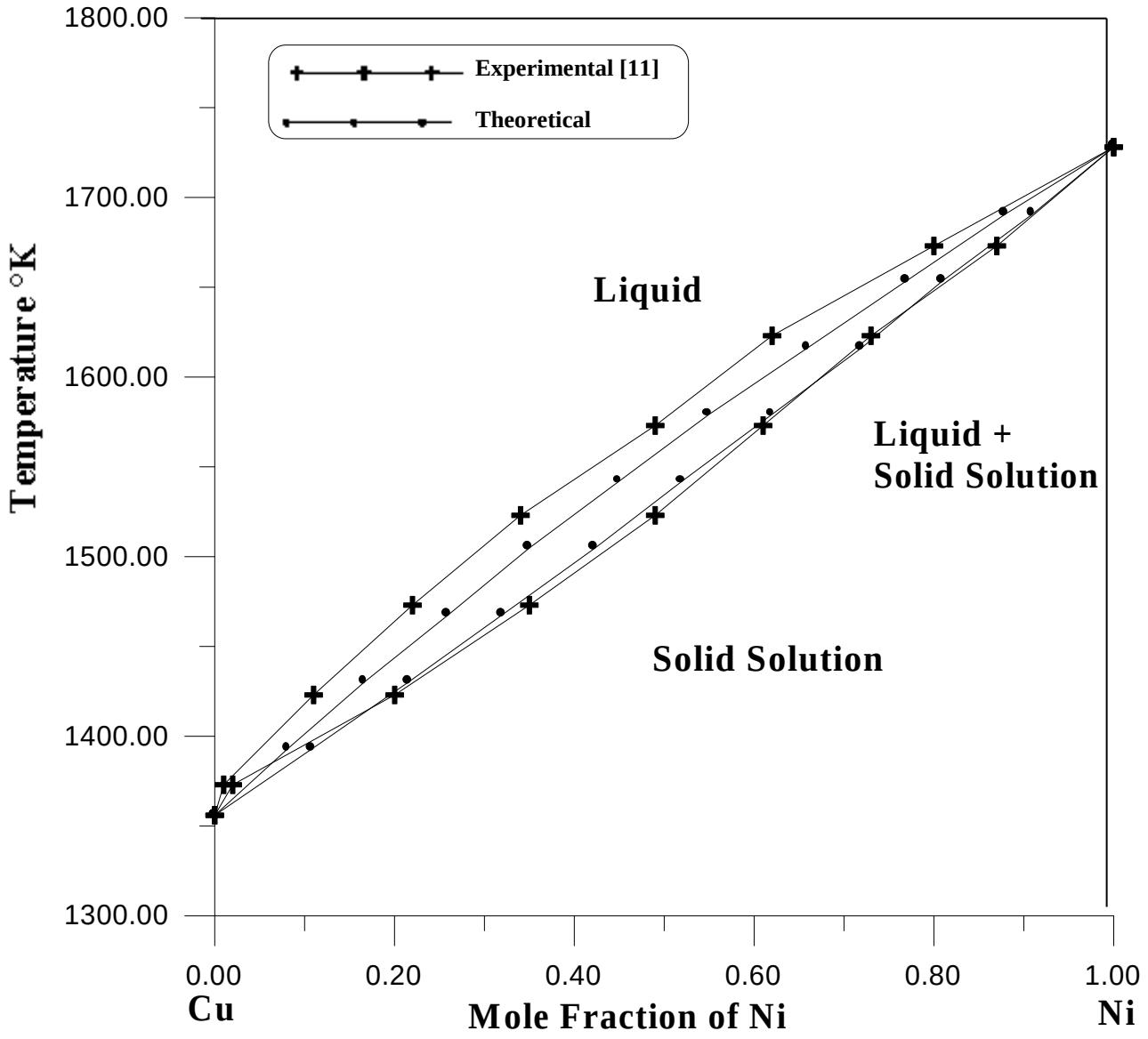

Fig.(4.1): Phase diagram of copper –nickel.

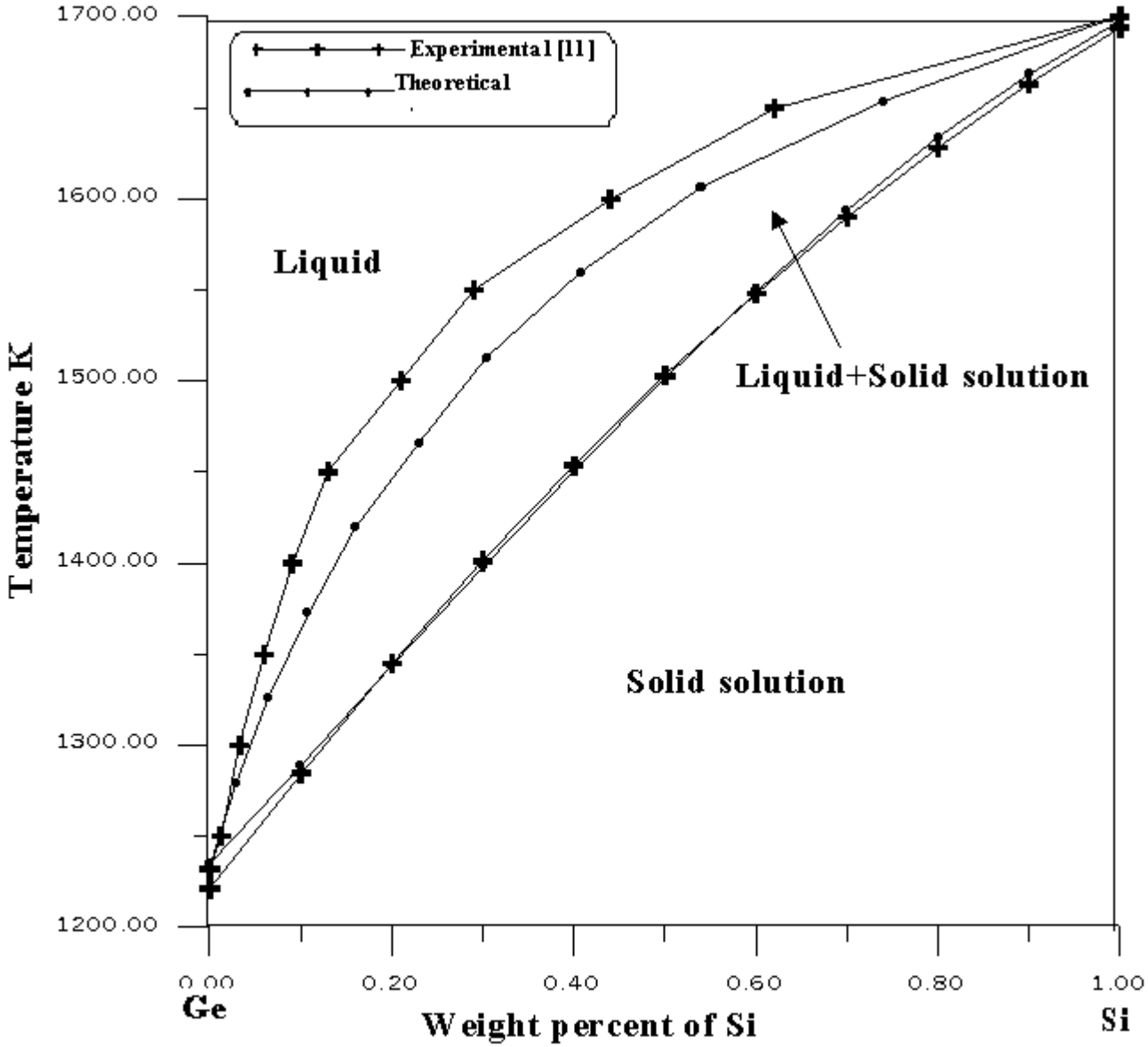

Fig.(4.2): Phase diagram of germanium-silicon.

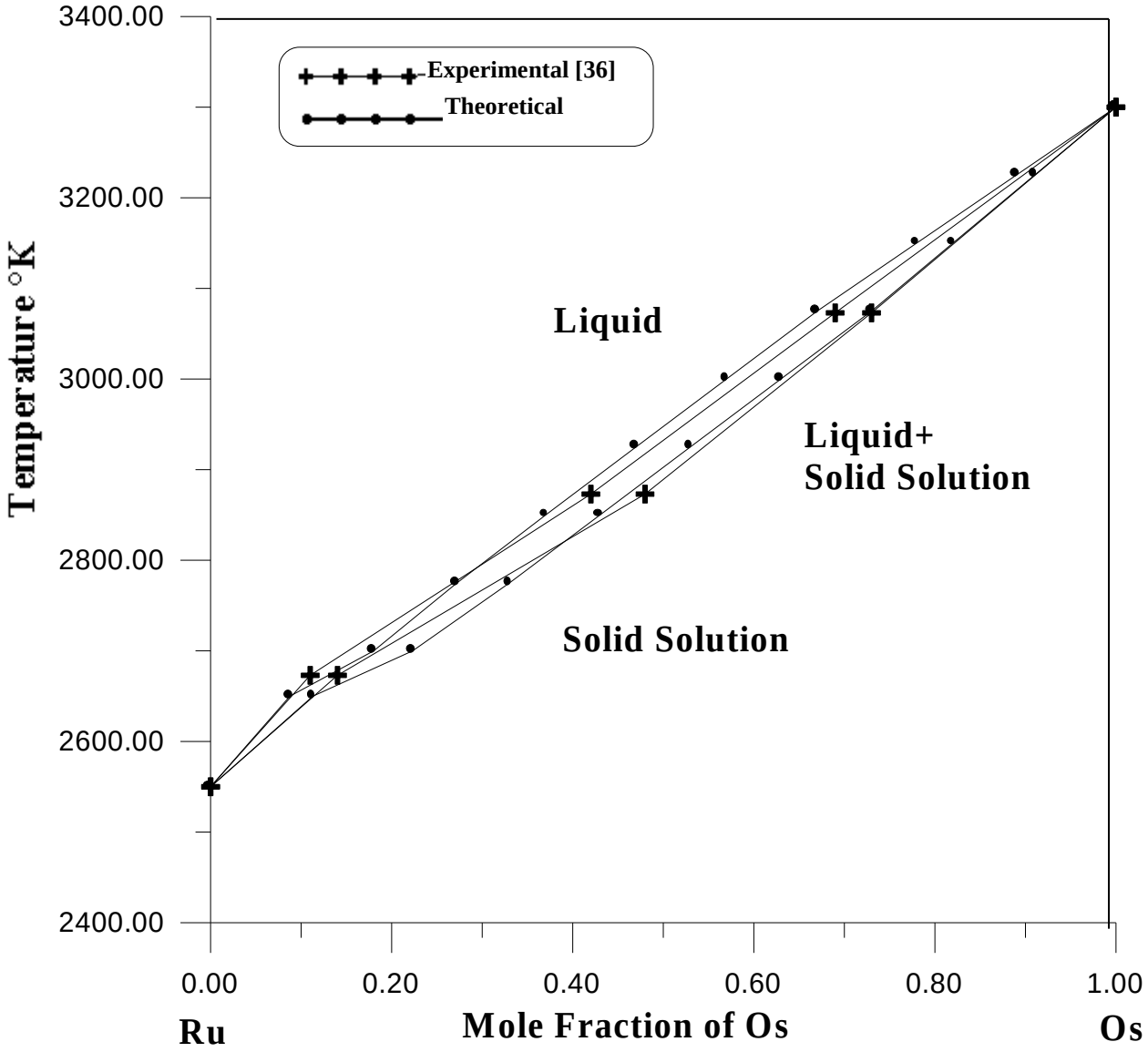

Fig.(4.3): Phase diagram of ruthenium-osmium

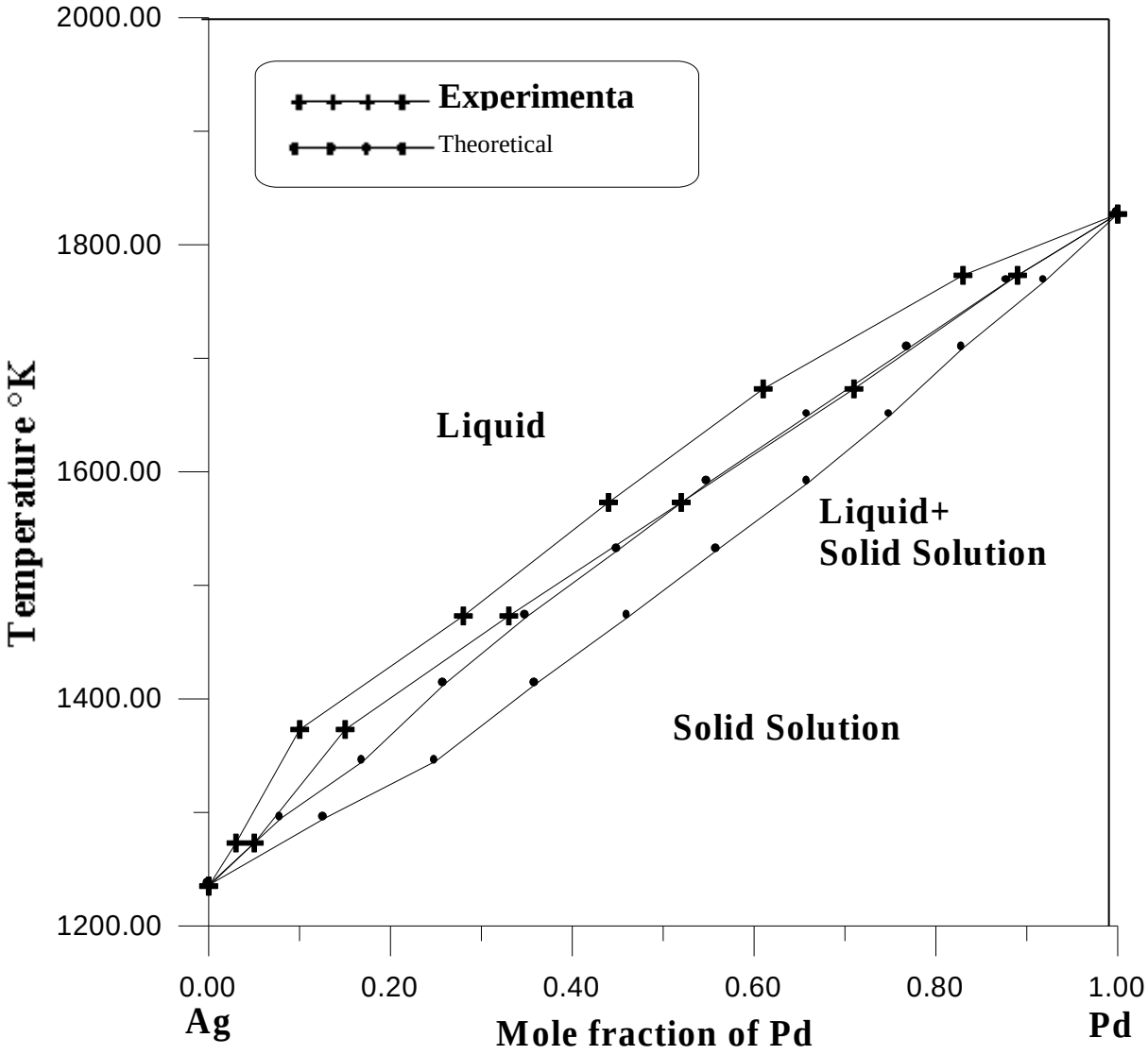

Fig.(4.4): Phase diagram of silver-palladium.

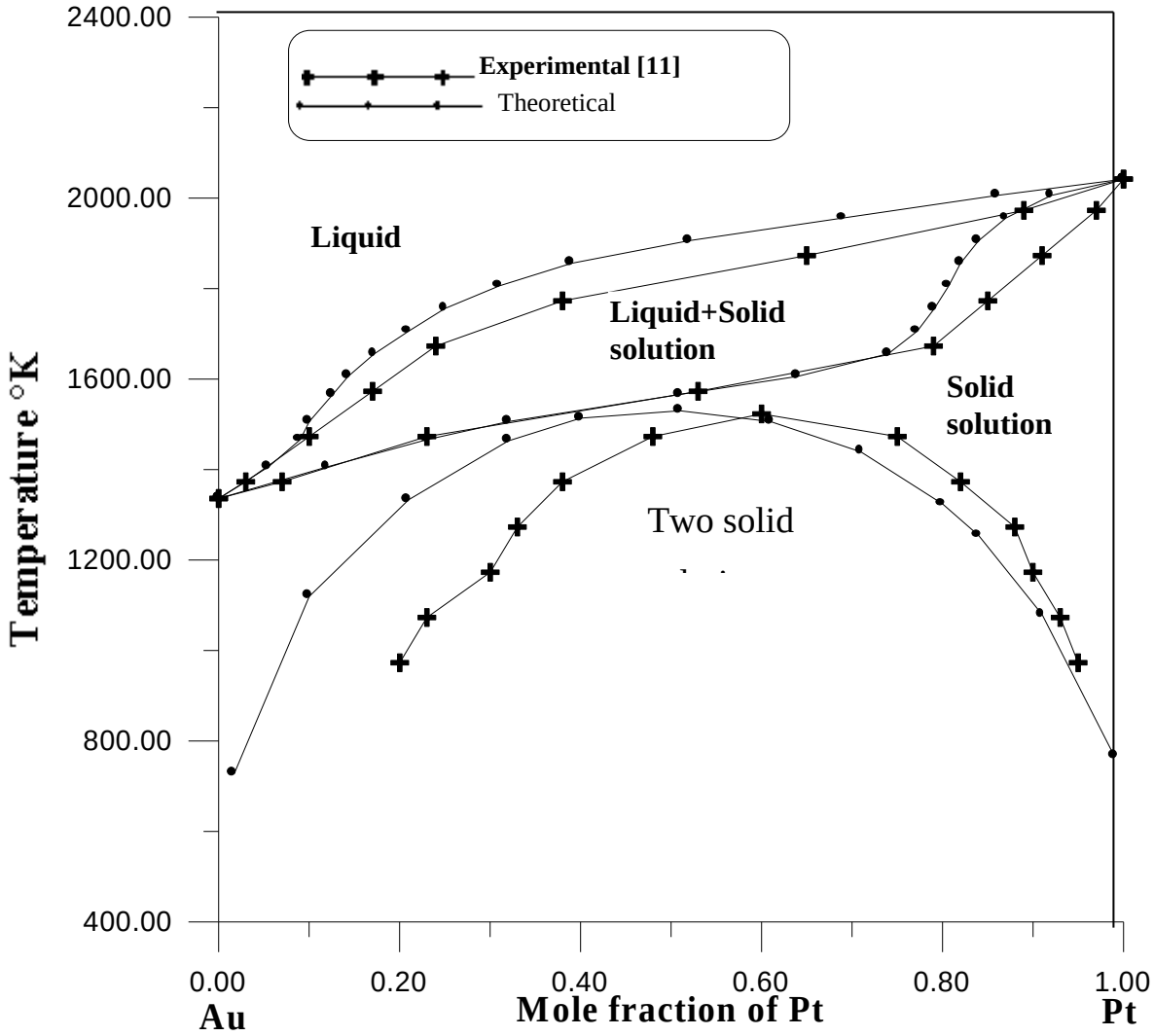

Fig.(4.5): Phase diagram of gold-platinum.

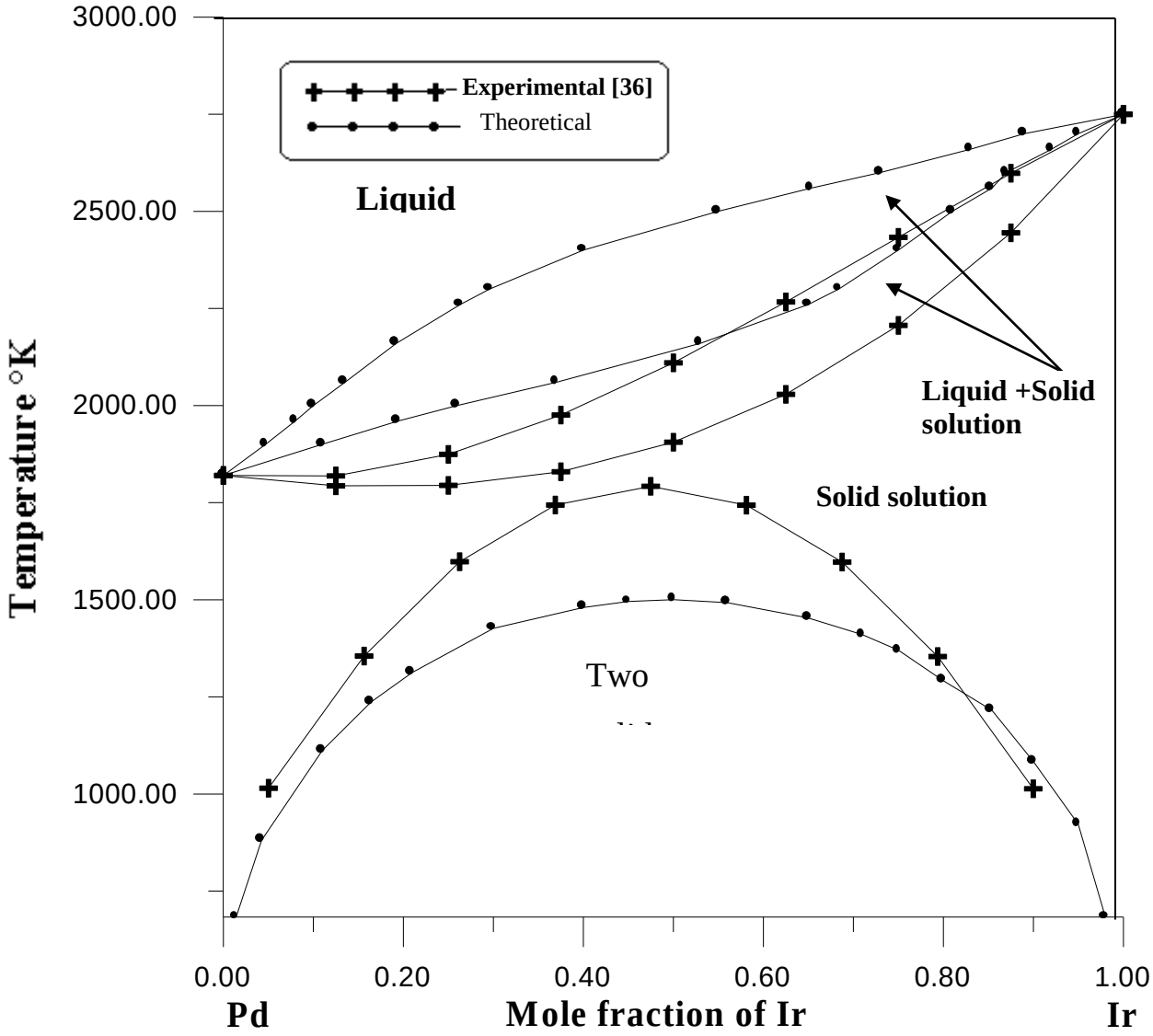

Fig.(4.6): Phase diagram of iridium-palladium.

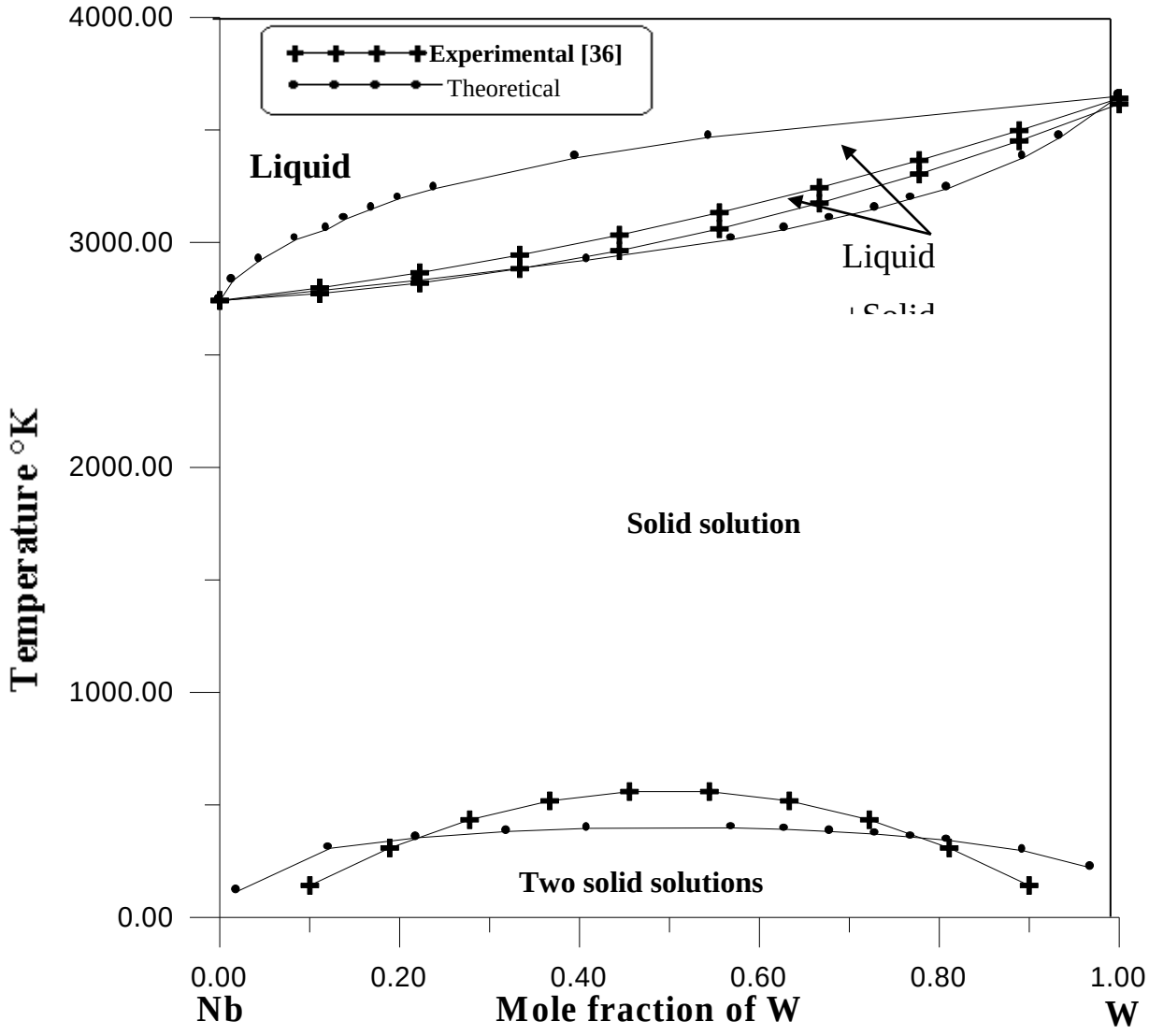

Fig.(4.7): Phase diagram of niobium-tungsten.

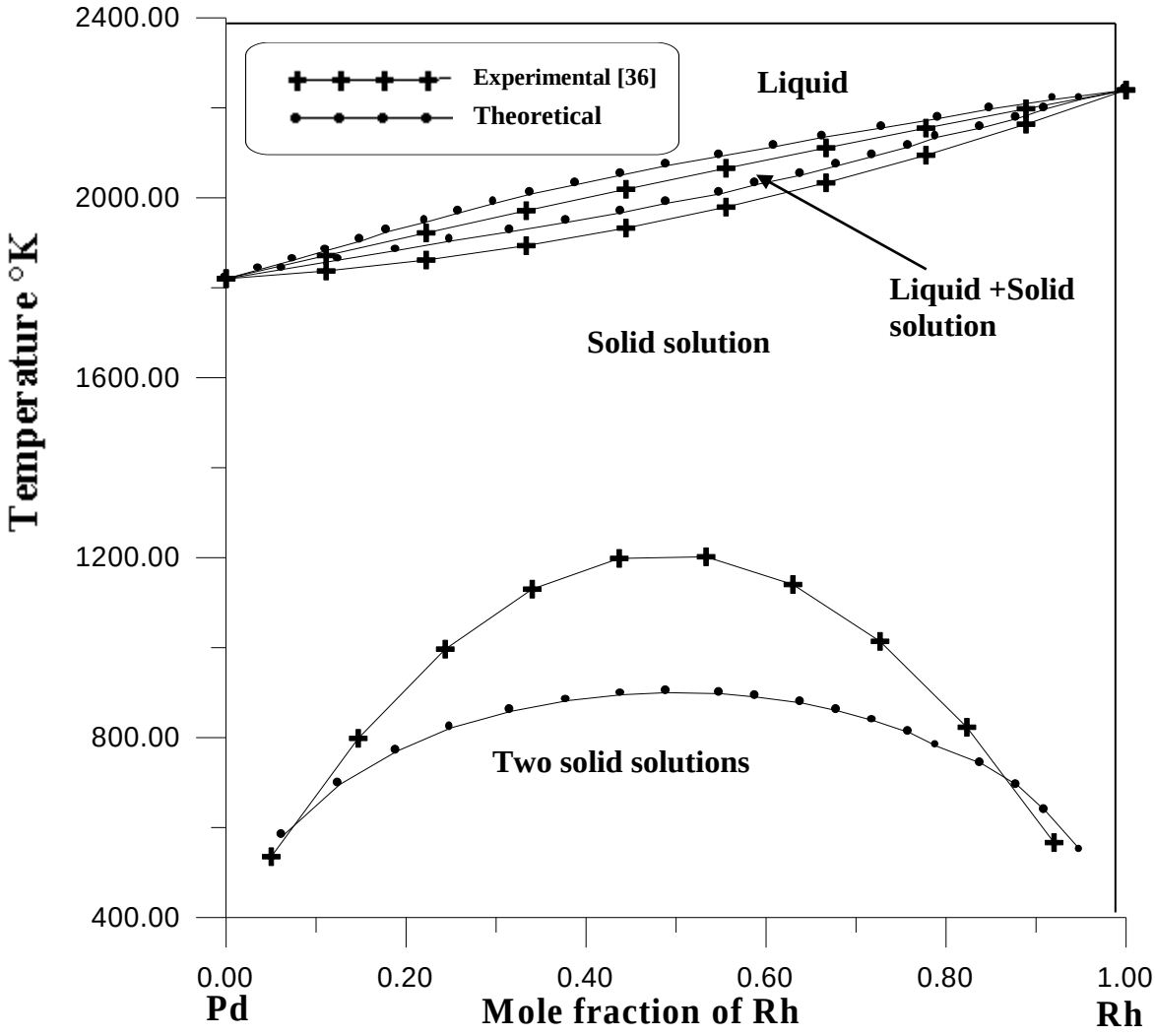

Fig.(4.8): Phase diagram of palladium- rhodium.

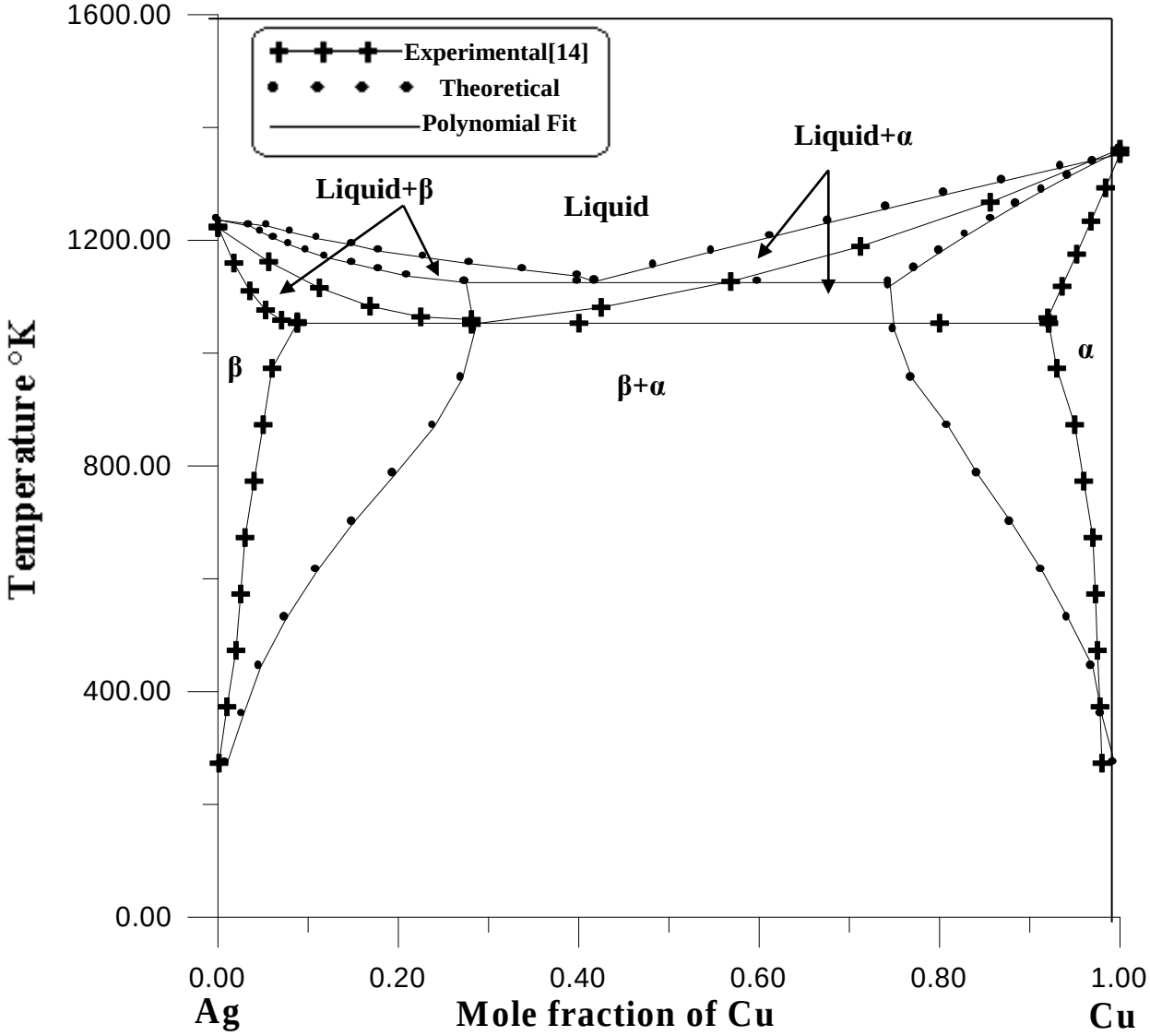

Fig.(4.9): Phase diagram of silver-copper.

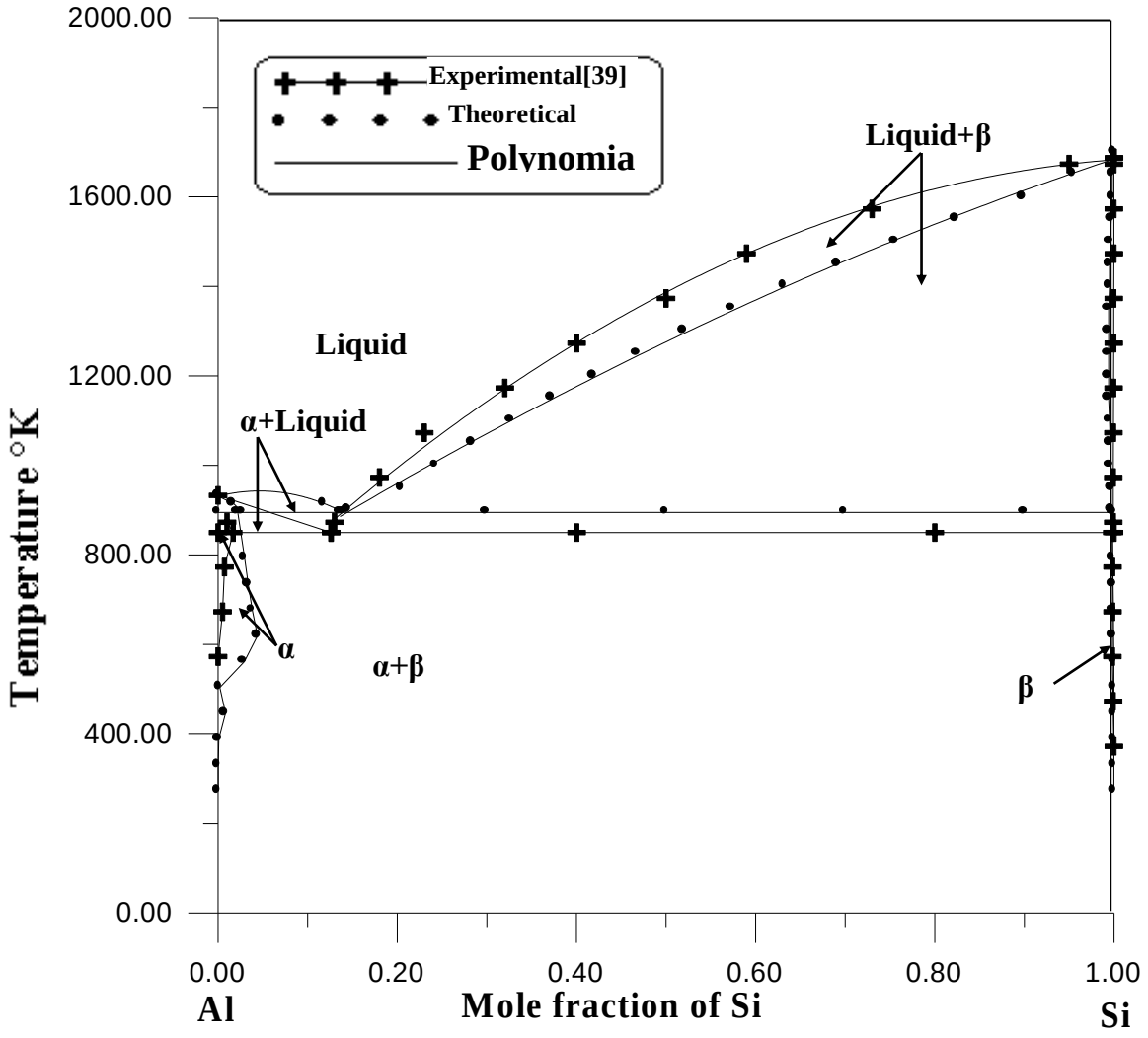

Fig.(4.10): Phase diagram of aluminum-silicon.

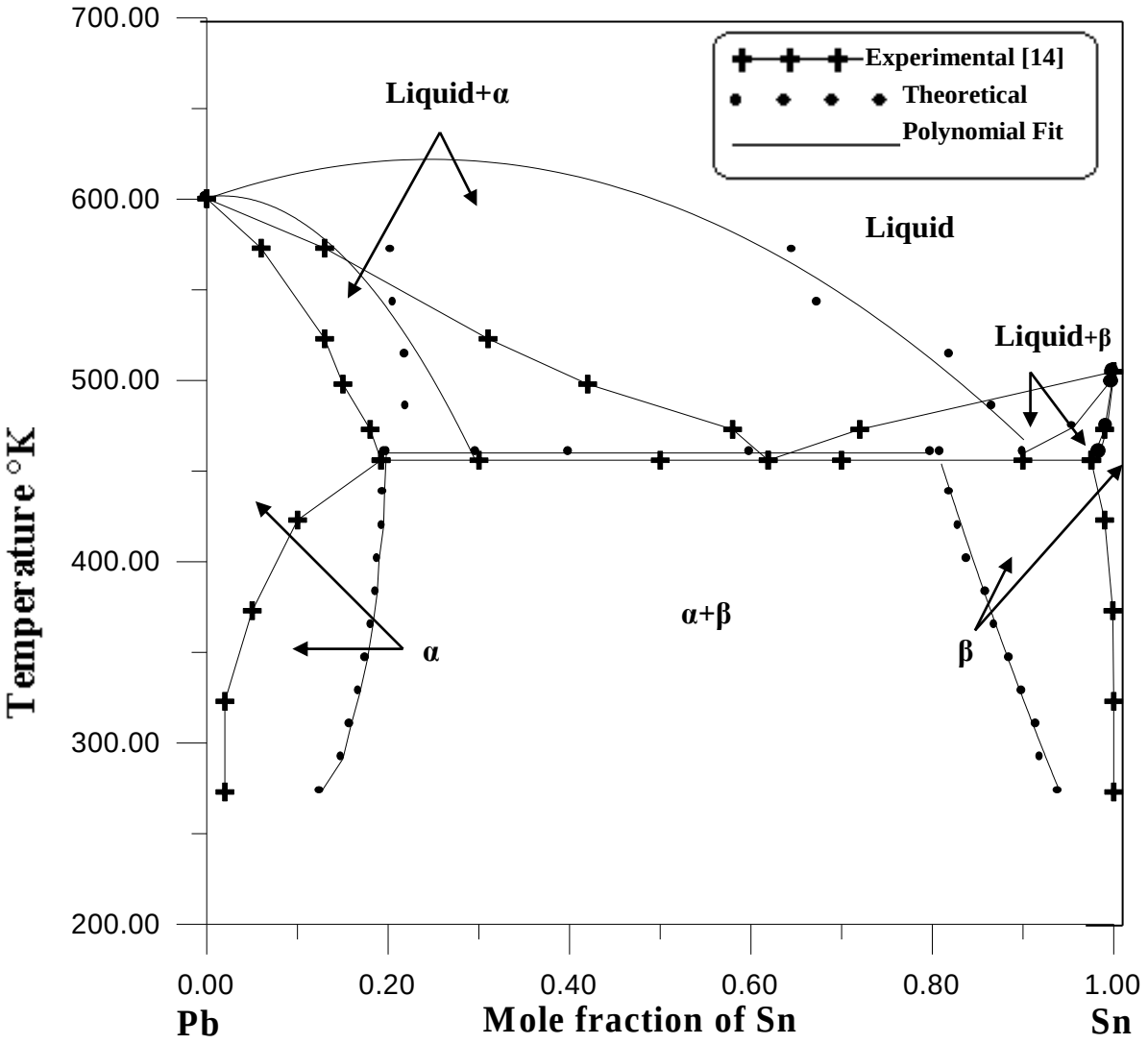

Fig.(4.11): Phase diagram of lead-tin.

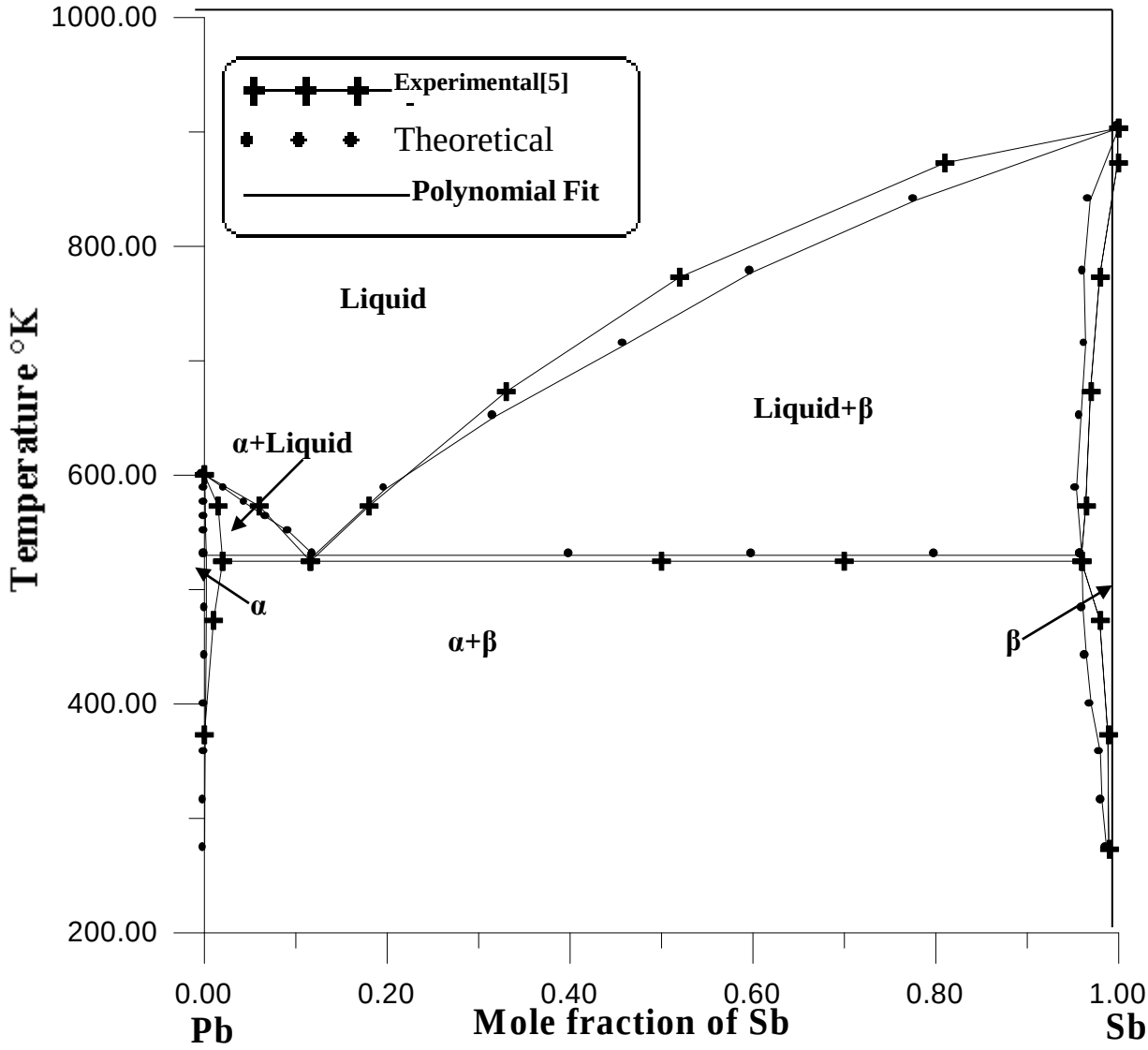

Fig.(4.12): Phase diagram of lead-antimony.

Chapter Five

Conclusions and Suggestions

5.1 Conclusions

Basing on the results of the present investigation, the following conclusions can be stated:-

1-Theoretical method by using mathematically modeling to determine phase diagrams applied in this work, in stead of experimental method which represent the essential method to determine them for many years .

2- The enthalpy and entropy at any temperature equal to the enthalpy and entropy at melting temperature but Gibbs free energy as a function to the temperature.

3-Theoretical method do not take into account a lot of parameters such as the free mean path and compared with experimental method from Refs. [11, 12,36, and 39] .

4-Using enthalpy of melting and melting temperature of two metals to calculate mole fractions in the solid and liquid states for phase diagrams of two metals completely soluble in liquid and solid states with ideal solution.

5-Phase diagrams of two metals completely soluble in liquid and solid states with miscibility gap and regular solution can be determined by using enthalpy of melting and melting temperature for two metals and the excess enthalpy as a function to the critical temperature for the system.

6-Using equations of transformation between different phases and interaction parameters to calculate phase diagrams of eutectic systems.

7-Theoretical phase diagrams of the two metals completely soluble in liquid and solid state (isomorphous systems) differ from that in experimental method with percentage less than 10%.

8-The maximum difference between theoretical phase diagrams of two metals completely soluble in liquid and solid state with regular solution and that in experimental method is 33% for miscibility gap.

9-Theoretical phase diagrams of eutectic systems differ from that in experimental method with maximum percentage is 40%.

5.2 Suggestions for further work:

1- Using Gibbs free energy as a function of temperature.

2- Calculating interaction energy between pair of atoms instead of using it as function to the temperature.

3-Determining other types of phase diagrams.

NOMENCLATURE

The following symbols are used generally throughout the text ,others are defined when there are used.

Symbol	Description	Unit
as	Atomic site	-
Cv	Heat capacity at constant volume	cal/K
e^{L}	Electronic component for the liquid phase	cal/mol
e^{β}	Electronic component for the bcc (β) phase	cal/mol
e^{ε}	Electronic component for the cph (ε) phase	cal/mol
e^{α}	Electronic component for the fcc (α) phase	cal/mol
E_{bond}	The bonding energy	cal
E_I	Energy of the Ith level of harmonic oscillator	cal
E_s	Strain energy	cal/mol
E_{sys}	Energy of the system contains Ith level of harmonic oscillator	cal
E_{vib}	The atomic vibrational energy	cal
$E_k(\rho)$	The energy required to insert atom k into a medium with a uniform electron charge density	cal
G^{t}	Total Gibbs free energy	cal
G^{Φ}	Gibbs free energy of a phase	cal
$G_T^{\Phi}(T,X)$	Gibbs free energy of a phase at specific temperature and composition(mole fraction)	cal
$G_{pr}^{\Phi}(pr,T,X)$	Gibbs free energy of a phase at specific pressure, temperature and composition(mole fraction)	cal
$G_m^{\Phi}(T_{cr},\beta_o,T,X)$	Magnetic Gibbs free energy of a phase at Curie temperature and specific temperature and composition	cal
G^{L}	Gibbs free energy of a liquid phase	cal
G^{M}	Gibbs free energy of a mechanical mixture	cal
G_A^{L}	Gibbs free energy of a pure liquid A	cal
H_A^{vap}	Enthalpy of vaporization for A	cal/mol

I	An integer which can have values in the range zero to infinity	-
m	Constant	-
na_I	Number of atoms in the Ith energy level	-
N	Number of moles	-
$pob_A(as)$	The probability that atomic site (as) is occupied by A atom	-
$pob_B(as)$	The probability that atomic site (as) is occupied by B atom	-
wt.	Weight percent	-
X	Mole fraction	-
r_k	The position of k atom	˚A
r_{kl}	The separation between two atoms k and l	˚A
H^{xs}	Excess enthalpy	cal
S_m	The entropy of mixing	cal/K
S_A^m	The entropy of metal A at melting temperature	cal/K.mol
H_A^β	Enthalpy of metal A in β phase	cal/mol
H_A^m	Enthalpy of melting of metal A	cal/mol
inp^L	Interaction parameter for the liquid phase	cal/mol
inp^β	Interaction parameter for the bcc (β) phase	cal/mol
inp^ε	Interaction parameter for the cph (ε) phase	cal/mol
inp^α	Interaction parameter for the fcc (α) phase	cal/mol
P_{int}	Term of internal pressure	cal/mol
v_A^a	Volume per gram atom of metal A	cm^3/ mol
Tc	The critical temperature for miscibility gap	K
T_{cr}	Curie temperature	K
T_A^m	Melting temperature of metal A	K
T_B^m	Melting temperature of metal B	K
$T_{exp.}$	Experimental temperature	K
$T_{th.}$	Theoretical temperature	K

Greek symbols

Symbol	Description	*Unit*
β_o	Average magnetic moment per atom	$A.mm^2/atom$
ψ	The repulsive pair potential representing the interaction between ion cores of two atoms	cal
ρ_A	Density of metal A	Kg/m^3
ρ	Electron charge density	C/mm^3
ω	Vibrational frequency of the atom	Hz
ω_D	Debye frequency	Hz
υ	Wave velocity	cm/sec
λ	Wave length	$^{\circ}A$
θ_{Ei}	Einstein characteristic temperature	K
θ_D	Debye characteristic temperature	K
μ_A	Chemical potential of metal A	cal/mol
δ_A	Solubility parameter for A	$(cal/cm^3)^{1/2}$

Superscript

Symbol	Description
L	Liquid phase
M	Mechanical mixture
S	Solid solution
β,α,ε	Solid solution phases
ψ	Phase

Subscript

Symbol	Description
A,B	Metals
i,,j	Group number of metals in periodic table
k,l	Atoms

Abbreviations

Abbr.	Description
BCC	Body center cubic
cal.	Calculate
CPH	Closed packed hexagonal
Eq.	Equation
Eqs.	Equations
Fig.	Figure
FCC	Face center cubic

%Liq.	Percentage of liquidus line
%Sol.	Percentage of solidus line
Tab.	Table
TMCSLS	Two metals completely soluble in liquid state and solid state
TMCSLSR	Two metals completely soluble in liquid state and solid state with regular solution
TMCSLPSS	Two metals completely soluble in liquid state and partial solubility in solid state

Constants

Symbol	Description	Value
Av	Avogadro's number	$0.6022 * 10^{24}$/mol
h	Planck's constant of action	$6.6252 * 10^{-27}$erg-sec
k_B	Boltzman's constant	$1.38054 * 10^{-16}$erg/degree
R	Gas constant	1.987 cal/ mol-K

جامعة بابل
كلية الهندسة
قسم هندسة المواد

الأستقرارية الثرموديناميكية

للتركيب الجزيئي

رسالة مقدمة إلى كلية الهندسة في جامعة بابل وهي جزء
من متطلبات نيل درجة ماجستير علوم في
هندسة المواد

من قبل
زينب فاضل كاظم العبيدي

حزيران - 2005

الخلاصة

إن لمعرفة الاستقرارية الثرموديناميكية للتركيب الجزيئي تأثير مهم في فهم التحولات الطورية للمعادن والسبائك التي تتضح في مخططات الأطوار.إن لمخططات الأطوار دور أساسي في إنجاز البحوث العلمية للمواد في عدة مجالات منها:التحول الطوري و الانجماد والنمو البلوري و تفاعلات الحالة الصلبة،حيث تعتبر تلك المخططات كخرائط طرق للحصول على افضل الطرق لتصنيع المواد.أما الثرموديناميك يمكن استخدامه للتعرف على حالة اتزان النظام و القوة الدافعة للتحول من الحالة شبه المستقرة إلى الحالة المستقرة.

لقد تبنى هذا العمل الطريقة النظرية لحساب مخططات الأطوار باستخدام الخواص الثرموديناميكية بديلاً عن الطريقة التجريبية المستهلكة للوقت و المكلفة حيث تم حساب نوعين من مخططات الأطوار خلال هذا العمل:-

الاول :- مخططات الاطوار لمعدنين لهما القابلية على الذوبان بشكل تام في الحالتين السائلة و الصلبة مع افتراض ان المخططات الحاوية على فجوة الامتزاجية تعامل كمخططات للمحاليل المنتظمة والتي لا تمتلك فجوة الامتزاجية تعتبر كمخططات للمحاليل المثالية.

الثاني :- مخططات لمعدنين تاما الذوبانية في الحالة السائلة و بينهما ذوبانية جزئية في الحالة الصلبة (نظام اليوتكتك) .

تم دراسة ثلاث حالات اخترنا لكل منها أربع مخططات كأمثلة مع افتراض انصهار المعادن في جميع المخططات تحت شروط الاتزان بثبوت الضغط و درجة الحرارة . افتراض عدم تغير السعة الحرارية مع درجة الحرارة و كذلك الانثالبي و الانتروبي ولكن تكون الطاقة الحرة لكبس كدالة لدرجة الحرارة للمحاليل المثالية و المنتظمة .افتراض طاقة التفاعل بين ذرات المعدن أ مساوية لطاقة التفاعل بين ذرات المعدن ب و طاقة التفاعل بين زوج من الذرات كدالة

لدرجة الحرارة الحرجة التي تمثل البداية لفجوة الامتزاجية.حساب محددات التفاعل للأطوار الصلبة و السائلة لاستنتاج مخططات اليوتكتك .

بمقارنة النتائج التي تم الحصول عليها من الطريقة النظرية مع المخططات التجريبية من مصادر مختلفة باستخدام التحليل الحراري ،وجد ان اكبر نسبة اختلاف بين المخططات النظرية و العملية هي 40%و اقل نسبة اختلاف فهي 0,086%.

References:-

1- Grante, I. P. E. ,**"MODERN MATERIALS SCIENCE"**, Reston Publishing Company, Inc., U.S.A., 1980.

2-"**DolTPoMS"**, Library of Teaching and Learning Packages for Materials Scince, Department of Materials Science and Metallurgy, University of Cambridge, http://www.msm.cam.ac.uk/doitpoms/ tlplib/CD4/index.

3-Avner, S. H., **"INTRODUCTION TO PHYSICAL METALLURGY"**, 2nd. Edition, McGraw-Hill, New York, 1974.

4- Kittel, C. **"INTRODUCTION TO SOLID STATE PHYSICS"**, John Wiley and Sons, New York, 7th. Edition, 1996.

5- (أ.د قحطان خلف الخزرجي ,**مخططات التوازن الحراري "مخططات الاطوار"**,الجامعة التكنولوجية,قسم هندسة المواد(2002).

-

6-Van Vlack, L. H.**" ELEMENTS OF MATERIALS SCIENCE AND ENGINEERING"**, 4th. Edition, Addison-Wesley Publishing Company, 1982.

7- **"ANALYTICAL AND CONCEPTS OF PHASE DIAGRAMS "** http://www.eng.vt.edu/eng/materials/MSE2094-NoteBook/96Class Proj/analytic/frontan.html.

8-Higgins, R. A. **" ENGINEERING METALLURGY"**, Part 1, The English Universities Press Ltd, 4th Edition, 1973.

9- Baddley, D. F. and Cannon, J. A., **"PROGRESSIVE ENGINEERING MATERIALS"**, Hodder and Stoughton, Great Britain, 1988.

10- Zhigilei, L. V. ,**"MSE 305 PHASE DIAGRAMS AND KINETICS"**, Department of Materials Science and Engineering, University of Virginia, 2002, http:// www .people. virginia. edu/ ~lz2n/ mse 305.

11- Gordon , P. **"PRINCIPLES OF PHASE DIAGRAMS IN MATERIALS SYSTEMS"**, McGraw- Hill, Inc, 1968.

12- "**THE PHASE DIAGRAM WEB",** Georgia Teach ASM/TMS, July 1996, http://cyberbuzz.gateoh.edu/asm-tms/phase-diagrams.

13- Rollason, E. C.**" METALLURGY FOR ENGINEERS"**, 4th. Edition, 1982.

14- Bolton, W. **"ENGINEERING MATERIALS TECHNOLOGY"**, Great Britain Press Ltd., 3rd Edition, 1998.

15-Pollack, H. W. **"MATERIALS SCIENCE AND METALLURGY"**, 3rd Edition, Reston Puplishing Company, 1981.

16- Thornton, P. A. and Colangelo, V. J., "**FUNDAMENTALS OF ENGINEERING MATERIALS**", Prentice- Hall. Inc., U.S.A., 1985.

17- Btaylor, M.; Barrera, G. D.; Allan, N. L. and Barron, T. H. K. **"FREE- ENERGY DERIVATIVES AND STRUCTURE OPTIMIZATION WITHIN QUASIHARMONIC LATTICE DYNAMICS"**, Physical Review , The American Physical Society, Vol. 56, No. 22, 1997.

18- Smallman, R. E.**" MODERN PHYSICAL METALLURGY**", 3rd Edition , Butterworth & Co.(Publishers)Ltd, Great Britain, 1980.

19- Kattner, U. R. **"THERMODYNAMIC MODELING OF MULTICOMPONENT PHASE EQUILIBRIA",** Division National Institute of Standards and Technology Gaithersburg, JOM 49 (12),1997.

20- Gaskell, D. R. **"INTRODUCTION TO METALLURGICAL THERMODYNAMICS"**, McGraw-Hill Kogakush, Pennsylvania University, 1973

21- Najafabadi, R.; Srolovitz, D. J.; Ma, E. and Atzmon, M. **"THERMODYNAMIC PROPERTIES OF METASTABLE AG-CU ALLOYS"**,J. Appl. Phys. 74(5), American Institute of Physics, Sep., 1993.

22- Saunders, N. **" PHASE DIAGRAM CALCULATION FOR NI-BASED SUPERALLOYS"**, Birmingham University, 1996.

23- Norgren, S. **"PHASE EQUILIBRIA AND THERMODYNAMICS OF RARE EARTH-IRON SYSTEMS",** Department of Materials Science and Engineering, Royal Institute of Technology, Stockholm , 2000.

24- Liu Z. and Schlom, D. G. **"THERMODYNAMICS OF THE MG-B SYSTEM: IMPLICATIONS FOR THE DEPOSITION OF MGB_2 THIN FILMS"**, Department of Materials Science and Engineering, The Pennsylvania State University, 2002.

25- Zhang, F.; Chen, S. L. and Chang, Y. A. **"CALCULATION OF THE TI-AL PHASE DIAGRAM"**, Wisconsin University, Madison, 1997, www.tms.org/Meetings/Annual-97/Program/Sessions /WP240A.

26- Purton, J. A.; Barrera, G. D.; Allan, N. L. and Blundy, J. D. **"MONTE CARLO AND HYBRID MONTE CARLO/MOLECULAR DYNAMICS APPROACHES TO ORDER-DISORDER IN ALLOYS, OXIDES, AND SILICATES",** J. Phys. Chem., Vol. 102, P(5202-5207),1998.

27- Allan, N. L. ; Barrera, G. D.; Lavrentiev, M. Yu.; Todrov, I. T. and Purton, A. **"AB INITIO CALCULATION OF PHASE DIAGRAMS**

OF CERAMICS AND MMINERALS", The Royal Society of Chemistry, J. Mater. Chem., Vol. 11,P(63-68),2001.

28- Allan, N. L.; Barrera, G. D.; Barron, T. H. K.; and Taylor, M. B.; "**EVALUATION OF THERMODYNAMIC PROPERTIES OF SOLIDS BY QUASIHARMONIC LATTICE DYNAMICS"**, International Journal of Thermodynamics, Plenum Publishing Corporation, Vol. 22, No. 2, 2001.

29- Allan, N. L.; Barrera ,G. D.; Fracchia, R. M.; Lavrentiev, M. Y.; Taylor, M. B.; Todorov, I. T.; and Purton, J. A. **" FREE ENERGY OF SOLID SOLUTIONS AND PHASE DIAGRAMS VIA QUASIHARMONIC LATTICE DYNAMICS",** Physical Review B, The American Physical Society , Vol. 63, 2001.

30- Walle, A. **"THE EFFECT OF LATTICE VIBRATIONS ON SUBSTITUTIONAL ALLOY THERMODYNAMICS"**, Department of Materials Science and Engineering, Thesis ,Massachusetts Institute of Technology, 2000.

31- Ceder, G. **"COMPUTATIONAL PREDICTION OF MATERIALS PROPERTIES"**, Department of Materials Science and Engineering, Materials Research at MIT, 2002.

32- Gronsky , R.; Arthur, C. and Oppenheimer, P. G. **"ENGINEERING PROPERTIES OF MATERIALS LABORATORY"**, Department of Materials Science & Engineering, University of California ,2001.

33-Elgun, S. Z. **"PHASE DIAGRAMS"**, Part 1, Material Science, MET205,Sep.,1999,info.Iu.farmingdale.edu/depts/met/profiles/elgunsz/elgunsz.html.

34- Chen ,S.-L.; Daniel,S.; Zhang ,F.; Chang ,Y .A .; Yan, X .Y.; Xie ,F. Y .; Schmid-Fetzer , R . and Oates, W .A ."**THE PANDAT**

SOFTWARE PACKAGE AND ITS APPLICATIONS", Clphad ,Vol. 26,P(175-188),2002.

35- Chen, S. L.; Zhang, F.; Daniel, S.; Xie, F. Y.; Yan, X. Y.; Chang, Y. A.; Schmid-Fetzer, R. and Oates, W. A. **"CALCULATING PHASE DIAGRAMS USING (PANDAT)"**, Jom., Dec., 2003.

36- Kaufman, L. and Bernstein, H. , **"COMPUTER CALCULATION OF PHASE DIAGRAMS"**, Academic Press Inc., U.S.A, 1970.

37- Perry, R. H. and Chilton, C. H. **" CHEMICAL ENGINEERING HANDBOOK"**, McGraw-Hill, Inc., 1973.

38- Holman, J. P., **"Heat Transfer**", McGraw-Hill, 4th. Edition, 1976

39-Durbin, T. L., **"MODELING DISSOLUTION IN ALUMINUM ALLOYS"**, Georgia Institute of Technology, Mar., 2005. http:// etd. gatech.edu/theses/available/etd-03252005-102549/unrestricted/durbin_tracie_L_200505_phd.